
2 Molecular Structures and Similarities to Ice

All common natural gas hydrates belong to the three crystal structures, cubic structure I (sI), cubic structure II (sII), or hexagonal structure H (sH) shown in [Figure 1.5](#). This chapter details the structures of these three types of hydrate and compares hydrates with the most common water solid, hexagonal ice Ih. The major contrast is that ice forms as a pure component, while hydrates will not form without guests of the proper size.

Structure I is formed with guest molecules having diameters between 4.2 and 6 Å, such as methane, ethane, carbon dioxide, and hydrogen sulfide. Nitrogen and small molecules including hydrogen ($d < 4.2$ Å) form structure II as single guests. Larger ($6\text{ \AA} < d < 7\text{ \AA}$) single guest molecules such as propane or iso-butane will form structure II. Still larger molecules (typically $7\text{ \AA} < d < 9\text{ \AA}$) such as iso-pentane or neohexane (2,2-dimethylbutane) can form structure H when accompanied by smaller molecules such as methane, hydrogen sulfide, or nitrogen.

Yet, because all three common hydrate structures consist of about 85% water on a molecular basis, many of the hydrate mechanical properties resemble those of ice Ih. Among the exceptions to this heuristic are yield strength, thermal expansivity, and thermal conductivity. The final portion of this chapter examines mechanical, electrical, and transport properties with emphasis on those properties that differ from ice.

Less common clathrate hydrates formed by compounds other than natural gas guests (such as Jeffrey's structures III–VII, structure T, complex layer structures) and high pressure hydrate phases are also briefly described to provide a comprehensive account of clathrate hydrate structural properties.

The purpose of this chapter is also to provide the reader with a source of reference of the structural properties of hydrates. A summary of the key tabulated data given in this chapter is as follows:

[Tables 2.1](#) and [2.2a](#) provide details of the geometry of the hydrate cages (number of cavities per unit cell, average cavity radius) and crystal cell structures (space group, lattice parameters, cell formula, atomic positions), respectively. Table 2.2b lists the atomic coordinates for structures I, II, and H.

[Table 2.3](#) provides an overview of the properties of structures I–VII (cavity types, space group, lattice parameter, cell formula).

[Table 2.4](#) shows the ratio of molecular diameter to cavity diameter for guests in structures I and II. The corresponding data for structure H is given in [Table 2.7](#), and the data for cyclopropane and trimethylene oxide (which form both sI and sII) are also provided.

[Tables 2.5a,b](#) lists the different structure I and II guests, and the structure and properties of the hydrates they form.

[Table 2.6](#) lists the small help guests for structure II, where all the large molecules listed will not stabilize the hydrate without the presence of a help guest.

[Table 2.8](#) summarizes the spectroscopic features, and mechanical and thermal properties for ice and hydrates of structures I and II.

This chapter focuses on the question, “What are hydrates?” and [Chapter 3](#) concerns the question, “How do hydrates form?” Although a few thermodynamic properties are discussed in this chapter, the phase equilibrium conditions are considered in [Chapters 4, 5, and 6](#).

2.1 CRYSTAL STRUCTURES OF ICE IH AND NATURAL GAS HYDRATES

In Section 2.1.1 molecular structures of ice, water, and the hydrogen bond are considered. With these knowledge bases of more common substances, the hydrate cavities are assembled in each hydrate unit crystal in Section 2.1.2. Characteristics of guest molecules in hydrate structures are detailed in Section 2.1.3, before a summary is presented in Section 2.1.4.

2.1.1 Ice, Water, Hydrogen Bonds, and Clusters

In this section, the structures of ice, water, and the hydrogen bond are based on the classical works of Bernal and Fowler (1933), Pauling (1935), and Bjerrum (1952), as well as the reviews of Frank (1970), and Stillinger (1980). These subjects are treated in comprehensive detail in the seven volume series edited by Franks (1972–1982), to which any student of water compounds will wish to refer. A second series of monographs on water, also edited by Franks (1985–1990), was published to update the earlier monograph series. Discussion on computer simulation studies of the structure and dynamics of water is largely based on the work of Debenedetti (1996, 2003).

2.1.1.1 Ice and Bjerrum defects

The most common solid form of water is known as ice Ih (hexagonal ice), with the molecular structure as shown in [Figure 2.1](#) from Durrant and Durrant (1962). In ice each water molecule (shown as a circle) is hydrogen bonded (solid lines) to four others in essentially tetrahedral angles (Lonsdale, 1958). A description of

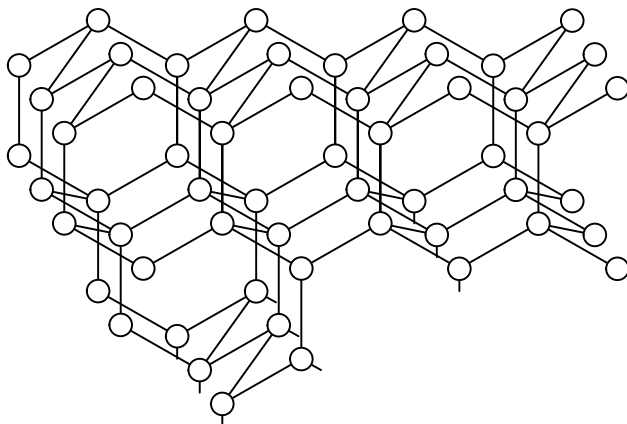


FIGURE 2.1 Basic crystal structure for ice Ih. (Reproduced from Durrant, P.J., Durrant, B., *Introduction to Advanced Inorganic Chemistry*, John Wiley & Sons, Inc., New York (1962). With permission.)

the hydrogen bond is provided in Section 2.1.1.3. The tetrahedral O—O—O angle of 109.5° in the most stable because there is almost no geometrical distortion. Stillinger (1980) suggests that tetrahedral coordination represents the most feasible way of packing molecules to permit fully developed hydrogen bonds.

In ice, the tetrahedrally hydrogen-bonded water molecules form nonplanar “puckered” hexagonal rings, rather than planar sheets. The typical distance between oxygen nuclei is 2.76 Å; covalently bonded protons are about 1 Å from an oxygen nucleus, and the hydrogen-bond length comprises the remaining 1.76 Å. Only one proton lies on each line connecting adjacent oxygen atoms in a hydrogen bond.

The ice crystal structure consists of water molecules hydrogen-bonded in a solid lattice. Since water molecules are similarly bonded in hydrates, both water molecules and hydrogen bonds are considered briefly in the following two sections. Many mechanical properties of ice are similar to hydrates, as detailed in Section 2.2.

Molecular dynamics and material transport in hexagonal ice (ice Ih) are closely related to the occurrence of ice-typical lattice defects. These defects include the Bjerrum defects (orientational defects) and ionic defects that coexist with other solid-state defects (interstitials and vacancies), and originate from distortions in the hydrogen-bond network (Figure 2.2). The Bjerrum crystal defects and their propagation are among the most frequently cited molecular properties. In his classic paper, Bjerrum (1952) considered possible reasons for low temperature disorder in the ice lattice. Normal electrostatic interactions caused by the orientations of the oxygens and the protons are necessary but insufficient to account for the total disorder. In addition, as shown in Figure 2.2, thermally excited water molecules cause two types of proton position faults, or defects, in the ice lattice.

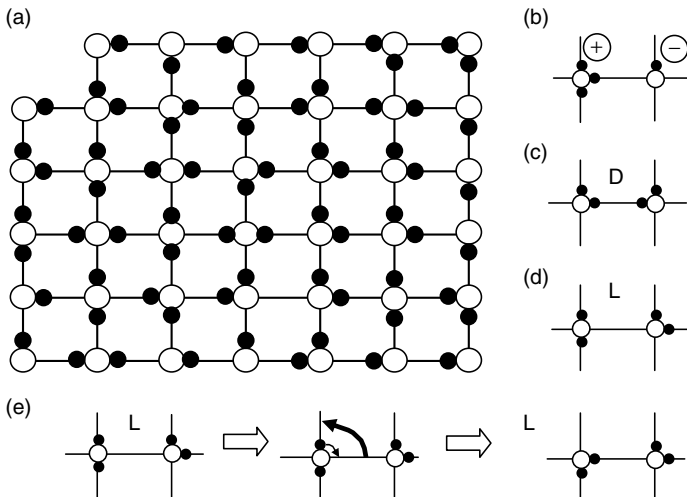


FIGURE 2.2 (a) Two-dimensional proton-disordered ice lattice (Bjerrum defect illustrated between molecules 4–5, in row 5). Open circles: oxygen atoms; closed circles: hydrogen atoms. (b) Ionic (H_3O^+ or OH^-) defects originate from a violation of the Bernal–Fowler (BF) Rule#1 (BF Rule#1: each oxygen atom is covalently bonded to exactly two hydrogen atoms). (c) Bjerrum defects violate the BF Rule#2 (BF Rule#2: there is exactly one hydrogen atom along each O–O vertex, which is covalently bonded to one oxygen and forms a hydrogen bridge to the other oxygen). Bjerrum D-defects (or D-faults), where the O–O vertex is occupied by two hydrogen atoms. (d) Bjerrum L-defects (or L-faults), where there are no hydrogen atoms at the O–O vertex. (e) Displacement (large curved arrow) of a Bjerrum L-defect induced by a tetrahedral (in three dimensions) reorientation of one water molecule (small arrow). (Redrawn from Geil, B., Kirschgen, T.M., Fujara, F., *Phys. Rev. B*, **72**, 014304 (2005). With permission from the American Physical Society.)

Normally, one proton exists between two oxygen nuclei (Figure 2.2a); yet the Bjerrum D-defect has two protons between oxygen nuclei in the ice lattice (Figure 2.2c), while the L-defect has none (Figure 2.2d). These defects cause the surrounding water molecules to pivot about the oxygen atom to provide one hydrogen bond between oxygen atoms thus resolving the unfavorable defect energy strain (Figure 2.2e).

Bjerrum defects act as catalysts to promote dipole turns, with one fault for every 10^6 molecules, corresponding to a turn rate of 10^{-12} s^{-1} at an orientation fault site. Devlin and coworkers (Wooldridge et al., 1987) suggested that Bjerrum defects are essential to the growth of hydrates from the vapor phase.

Molecular reorientations at Bjerrum fault sites are responsible for the dielectric properties of ice. A second type of fault (proton jumps from one molecule to a neighbor) accounts for the electrical conductivity of ice, but cannot account for the high dielectric constant of ice. Further discussion of such ice faults is provided by Franks (1973), Franks and Reid (1973), Onsager and Runnels (1969), and Geil et al. (2005), who note that interstitial migration is a likely self-diffusion mechanism.

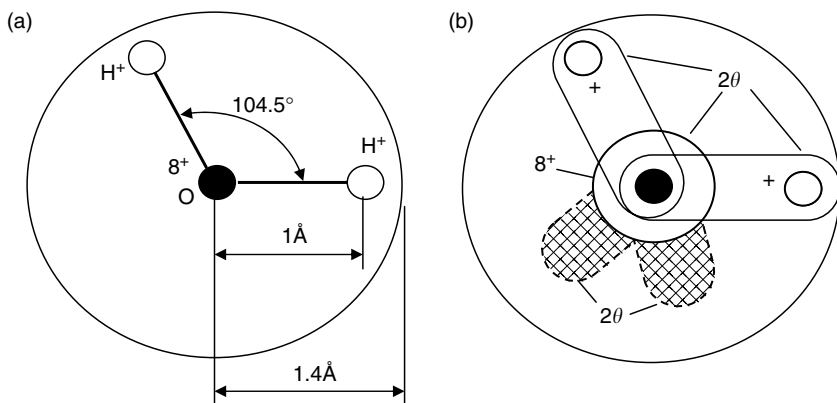


FIGURE 2.3 Water model of Bernal and Fowler (eight electrons on oxygen [8+] and one electron on each hydrogen [+]), indicating (a) the covalent O–H bond length and H–O–H bond angle, (b) the two lone pair orbitals on oxygen—hatched. (Reproduced from Makogon, Y.F., *Hydrates of Natural Gas*, Moscow, Nedra, Izadatelstro, p. 208 (1974 in Russian) Translated by W.J. Cieslesicz, PennWell Books, Tulsa, Oklahoma, pp. 237 (1981 in English). With permission.)

2.1.1.2 The water molecule

Figures 2.3a,b show the model of Bernal and Fowler (1933) for the water molecule. The molecular geometry is well known (Benedict et al., 1956) from rotational and vibrational spectra. The oxygen atom has eight electrons, and has the electronic configuration $1s^2 2s^2 2p^4$. Each hydrogen atom has a $1s^1$ electron; these electrons are shared with two bonding electrons of oxygen, to constitute the water molecule.

In water, four valence electrons form two “lone pair” orbitals that have been determined (Pople, 1951) to point above and below the plane formed by the three nuclei (H–O–H) of the molecule. The shared electrons with the protons give the molecule two positive charges, and the lone pair electrons give the molecule two negative charges. The result is a molecule with four charges and a permanent electric dipole (McCelland, 1963) of 1.84 Debye.

2.1.1.3 Hydrogen bonds

In 1920, two men in G.N. Lewis’ laboratory at Berkeley proposed the hydrogen bond (Latimer and Rodebush, 1920) using a simplified electrostatic point charge model of the water molecule. The work by Kollman (1977) indicated that the simplified model remains acceptable because of a cancellation of two other energy components.

In the preceding section, the water molecule was described as having two positive and two negative poles. The water hydrogen bond, shown in Figure 2.4a, is caused by the attraction of the positive pole on one molecule to a negative pole on a neighboring water molecule. In ice and in hydrates, only one hydrogen (or proton)

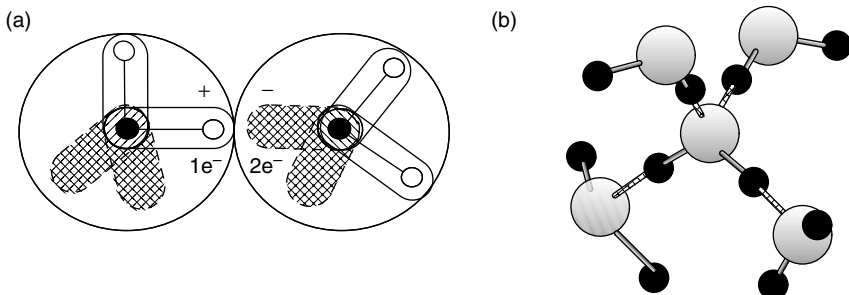


FIGURE 2.4 Hydrogen bonding (hydrogen bonds are crosshatched) (a) between two molecules (Reproduced and modified from Makogon, Y.F., *Hydrates of Natural Gas*, Moscow, Nedra, Izdatelstro, p. 208 (1974 in Russian) Translated by W.J. Cieslesicz, PennWell Books, Tulsa, Oklahoma, p. 237 (1981 in English). With permission), and (b) between four molecules. (Reproduced from Franks, F., Reid, D.S., in *Water: A Comprehensive Treatise* (Franks, F., ed.) Plenum Press, New York, 2, Chap. 5 (1973). With permission.)

lies between two oxygen atoms with a distance between oxygen nuclei of 2.76 \AA . The average O—O—O angle in ice and hydrates only departs a few degrees from the tetrahedral (109.5°) angle (Davidson, 1983).

Through this hydrogen bond, each water molecule is attached to four others, donating two and accepting two hydrogen bonds, as illustrated in Figure 2.4b. Each proton of the molecule is attracted to the negative pole of a neighboring molecule. Also, the two negative poles on the initial molecule attract the positive poles from two other water molecules. The four surrounding molecules are arranged tetrahedrally around the central molecule.

The energy required to break one hydrogen bond (ca. 5 kcal/mol) is more than an order of magnitude greater than a typical van der Waals bond (ca. 0.3 kcal/mol), such as the one that would attract two nonpolar molecules in a fluid. On the other hand, the hydrogen-bond energy is not nearly as large as that of a covalent chemical bond (102 kcal/mol), such as exists between hydrogen and oxygen within a water molecule (Cottrell, 1958).

2.1.1.4 Hydrogen bonds cause unusual water, ice, and hydrate properties

Along with the attraction of the hydrogen bond, the fact that these strong bonds separate the water molecules rigidly causes the solid density to be less than that of the liquid. In ice only 34% of the volume is occupied by water molecules, in contrast to 37% volume occupation in liquid water; this explains the unusual property of a decrease in density on freezing, accounting for the fact that ice floats.

Because the hydrogen bond is significantly weaker than the covalent bond, when hydrates form or dissociate, only hydrogen bonds are considered between neighboring molecules. Van der Waals forces are present, but are insignificant

relative to hydrogen bonds. When hydrates form or dissociate, chemical bonds do not need to be broken between hydrogen and oxygen within a water molecule.

Hydrogen bonds are also present to a large extent in liquid water. In a review, Luck (1973) notes that the hydrogen bonds inhibit the vaporization of liquid water, with the result that the boiling point of water at ambient pressure is 260 K higher than that of methane, a compound with a similar molecular weight. Hydrogen bonds provide a major exception to the heuristic that the vapor pressure of a substance is inversely proportional to molecular weight. Stillinger (1980) indicates that many of the unusual properties of water are caused by the hydrogen bond. These anomalous properties include the density maximum as a function of temperature, the increase in specific heat (C_p) as the temperature is reduced, and an increasing diffusion constant as the density is increased (Speedy and Angell, 1976; Prielmeier et al., 1987; Debenedetti, 2003). The breakdown in tetrahedral order (deviation from tetrahedral geometry) with increasing temperature or density is considered to cause the anomalous properties of liquid water. Molecular dynamics (MD) computer simulations also indicate that several properties of water (e.g., the translational diffusion coefficient and entropy) exhibit anomalous density dependence as a result of the breakdown of local tetrahedrality (Lynden-Bell and Debenedetti, 2005).

Only 15% of hydrogen bonds break when ice melts, as Pauling (1945, p. 304) calculated by comparing the heat of sublimation of ice with the heat of fusion of ice. This estimation supported the Frank and Evans (1945) “iceberg” model of liquid water molecules in a hydrogen-bonded network. The iceberg model comprises an equilibrium mixture of short-lived (10^{-10} s) hydrogen-bonded clusters, together with a nonhydrogen-bonded dense phase. Franks (1975) suggested that the term “iceberg” is often misused, since such short-lived or flickering clusters are not measurable on a macroscopic scale.

Stillinger (1980) suggested that disconnected icebergs should not be present, but that a more likely model is that of a random, three-dimensional network of hydrogen bonds, rather than long-lived clusters of molecules. Such networks of hydrogen-bonded water molecules and clusters are present when hydrates form or dissociate. These clusters are discussed relative to nucleation of hydrates in the following chapter.

The thermodynamic and structural processes that occur when water molecules are in the vicinity of hydrophobic entities (water fearing, insoluble in water) are referred to collectively as “hydrophobic hydration” (Tanford, 1973; Privalov and Gill, 1988; Blokzijl and Engberts, 1993; Chau and Mancera, 1999). Hydrophobic hydration is important in gas hydrate formation, which usually starts with hydrophobic gas molecules (e.g., methane) being introduced into liquid water.

In the Frank and Evans “iceberg” model, ice-like structures form around hydrophobic entities, such as methane. In this model, the hydrophobic molecules enhance the local water structure (greater tetrahedral order) compared with pure water. Ordering of the water hydration shell around hydrophobic molecules has been attributed to clathrate-like behavior, in which the water hydration shell is dominated by pentagons compared to bulk liquid water (Franks and Reid, 1973).

There have been numerous re-examinations of the “iceberg” model, and a considerable amount of controversy still exists. Molecular dynamics’ computer simulations (Head-Gordon, 1995) suggest that although there are larger numbers of pentagons in the hydration shell compared to the bulk, the hydration shell also contains significant numbers of hexagons and larger polygons. Other computer studies indicate that the hydration shell around methane has a higher degree of tetrahedral bond-order than that in bulk water (Chau and Mancera, 1999). Hummer et al. (1996) calculated the potential of mean force between cavities in water and demonstrated that this has the properties expected of hydrophobic interactions. Conversely, Ashbaugh and Paulaitis (2001) presented a thermodynamic theory of hydrophobic hydration that does not invoke the concept of structure enhancement of water near a hydrophobic entity. Hydrophobic hydration has also been examined using neutron scattering (Bowron et al., 2001; Dixit et al., 2002; Buchanan et al., 2005) and surface-specific vibrational spectroscopy (Satana et al., 2001).

2.1.1.5 Pentamers and hexamers

The pentagonal and hexagonal faces are central to hydrate cavities, and therefore, their geometries are considered here. Small clusters, such as pentamers can be studied via geometric considerations, computer simulation, and more recently spectroscopy.

Computer simulation studies by Stillinger and Rahman (1974) suggest that the pentamer is the most likely structure to spontaneously arise in water at many temperatures, followed in frequency by hexamers, and squares. In a review of water, Frank (1970) noted that closed rings of bonds are always more stable than the most stable open chains of the same cluster number, due to the extra energy of the hydrogen bond. Through molecular dynamics studies of many five-molecule clusters, Plummer and Chen (1987) argued that the cyclic pentamer that comprises many hydrate cavities is the only stable five-member cluster above 230 K.

Molecular dynamics studies of liquid water by Ohmine and coworkers have shown that five- and six-membered rings, and even seven-membered rings dominate the topology in the hydrogen-bond network. (Ohmine, 1995; Matsumoto et al., 2002). Stacked pentamer rings have also been shown to be prevalent in the global minima energy structures of larger water clusters (Wales and Hodges, 1998). The global minimum pentamer ring structure was shown to form readily even at 4 K (Burnham et al., 2002).

Recent advances in spectroscopic methods have enabled the water pentamer to be studied experimentally. Infrared cavity ringdown spectroscopy has been used to examine the intramolecular absorption features of the gas-phase water pentamer, which match the spectral features of the pentamer rings in liquid water and amorphous ice (Paul et al., 1999; Burnham et al., 2002). Vibration Rotation Tunnelling (VRT) spectroscopy has been used to provide a more direct probe of the water pentamer intermolecular vibrations and fine structure in liquid water (Liu et al., 1997; Harker et al., 2005). The water pentamer was found to average out

to a symmetric quasiplanar structure on the timescale of the experiments (Harker et al., 2005).

In planar rings, water molecules in solid hydrogen-bonded pentagons have O—O—O angles (108°) only a little different from either the normal water angle (104.5°) or the tetrahedral angle (109.5°). However, the O—O—O angles of square faces (90°) and the hexagonal faces (120°) indicate almost similar strains on the bonds. Such strains may be reflected in thermodynamic properties or kinetic phenomena associated with these faces and cavities. Heptagons (128.6°) and octagons (135°) have still higher strained angles of O—O—O bonds and so occur infrequently in water structures.

2.1.2 Hydrate Crystalline Cavities and Structures

The information on hydrate structures I and II in this section is derived in large part from the excellent reviews of Jeffrey and McMullan (1967), Davidson (1973), and Jeffrey (1984), with the addition of substantial work on molecular motions reviewed by Davidson and Ripmeester (1984). The structure H material was excerpted from Ripmeester et al. (1987, 1988, 1991, 1994), Udachin et al. (1997b, 2002), Mehta (1996), and Mooijer-van den Heuvel et al. (2001, 2002).

Of more than 130 compounds that are known to form clathrate hydrates with water molecules, the majority form either sI, sII, or sH, with exceptions such as (1) bromine (Allen and Jeffrey, 1963; Dyadin et al., 1991), (2) dimethyl ether (Gough et al., 1974, 1975; Udachin et al., 2001a), (3) ethanol (Brownstein et al., 1967; Calvert and Srivastava, 1967), and (4) very high pressure hydrate phases (Dyadin et al., 1997; Loveday et al., 2001b, 2003b; Kursonov et al., 2004). Detailed emphasis is given to sI, sII, and sH hydrates since these are by far the most common natural gas hydrate structures.

The above (1)–(3) exceptions do not involve natural gas compounds and therefore are not described in any detail, but rather just mentioned in passing. The reader is referred to reviews by Davidson (1973), Davidson and Ripmeester (1978), and the papers of Jeffrey (1984), Dyadin et al. (1991), Udachin and Ripmeester (1999) and Udachin et al. (2001a) for further details on the less common hydrate structures of other compounds. The relevance of other compound structures is becoming increasingly of interest in areas of refrigeration, gas storage, and gas separation using clathrate hydrates.

2.1.2.1 The cavities in hydrates

The hydrate structures (Figure 1.5) are composed of five polyhedra formed by hydrogen-bonded water molecules shown in Figure 2.5, with properties tabulated in Table 2.1. Jeffrey (1984) suggested the nomenclature description (n_i^{mi}), for these polyhedra, where n_i is the number of edges in face type “i,” and m_i is the number of faces with n_i edges.

The pentagonal dodecahedron (12-sided cavity) of Figure 2.5 is labeled 5^{12} because it has 12 pentagonal faces ($n_i = 5$, $m_i = 12$) with equal edge lengths and

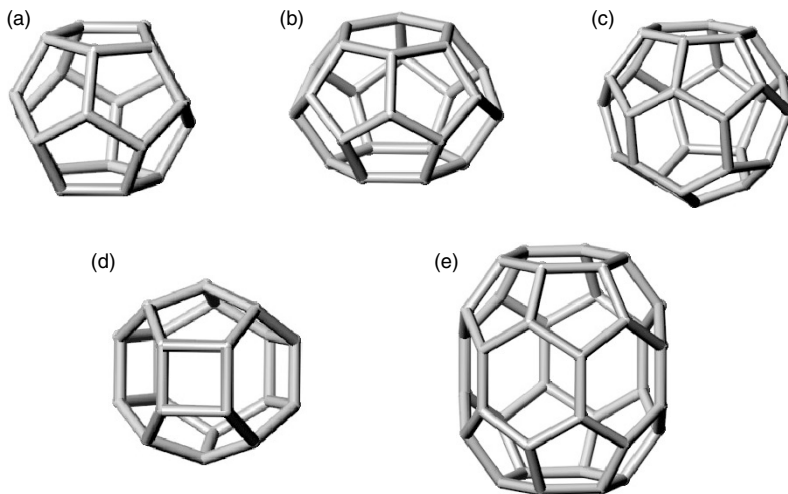


FIGURE 2.5 Three cavities in gas clathrate hydrates: (a) pentagonal dodecahedron (5^{12}), (b) tetrakaidecahedron ($5^{12}6^2$), (c) hexakaidecahedron ($5^{12}6^4$), (d) irregular dodecahedron ($4^35^66^3$), and (e) icosahehedron ($5^{12}6^8$).

equal angles. The 14-sided cavity (tetrakaidecahedron) is called $5^{12}6^2$ because it has 12 pentagonal and 2 hexagonal faces. The 16-hedron (hexakaidecahedral cavity) is denoted $5^{12}6^4$ because in addition to 12 pentagonal faces, it contains 4 hexagonal faces. The irregular dodecahedron cavity ($4^35^66^3$) has three square faces and six pentagonal faces, in addition to three hexagonal faces. The largest icosahehedron cavity ($5^{12}6^8$) has 12 pentagonal faces, as well as a girdle of 6 hexagonal faces and a hexagonal face each at the cavity crown and foot.

Tabushi et al. (1981) suggested that the 15-hedron ($5^{12}6^3$) is absent from Figure 2.5 and in all clathrates except bromine due to an unfavorable strain relative to the other cavities in sI and sII. In their review of simple and combined cavities, Dyadin et al. (1991) suggested that in addition to the cavities found in sI, sII, and sH, there are 4^25^8 and $5^{12}6^3$ cavities. In Jeffrey's (1984) list of a series of seven hydrate crystal structures (Table 2.3), additional cavities to those found in sI, sII, and sH are $5^{12}6^3$, 4^45^4 , $4^35^96^27^3$, 4^66^8 .

Since the cavities are expanded relative to ice, hydrate cavities are prevented from collapse by the repulsive presence of guest molecules, either in the cavity itself or in a large percentage of the neighboring cavities. Rodger (1990a,b) indicates that guest repulsion is more important than attraction to maintain cavity expansion. The mean polyhedral volume of the 12-, 14-, and 16-hedral cavities has been shown to vary with temperature and guest size and shape (Chakoumakos et al., 2003).

Jeffrey noted that the 12-, 14-, and 16-hedra are not stable in a pure water structure. However, some studies have suggested that liquid water is structured as cavities (Sorensen, 1994; Walrafen and Chu, 1995). Pauling (1959) proposed that water was composed of complexes of 5^{12} cavities with a water molecule as

TABLE 2.1
Geometry of Cages

Hydrate crystal structure	I		II		H		
	Small	Large	Small	Large	Small	Medium	Large
Cavity							
Description	5^{12}	$5^{12}6^2$	5^{12}	$5^{12}6^4$	5^{12}	$4^35^66^3$	$5^{12}6^8$
Number of cavities/unit cell	2	6	16	8	3	2	1
Average cavity radius ^a (Å)	3.95	4.33	3.91	4.73	3.94 ^b	4.04 ^b	5.79 ^b
Variation in radius ^c (%)	3.4	14.4	5.5	1.73	4.0*	8.5*	15.1*
No. of water molecules/cavity ^d	20	24	20	28	20	20	36

^a The average cavity radius will vary with temperature, pressure, and guest composition.

^b From the atomic coordinates measured using single crystal x-ray diffraction on 2,2-dimethylpentane·5(Xe,H₂S)-34H₂O at 173 K (from Udachin et al., 1997b). The Rietveld refinement package, GSAS was used to determine the atomic distances for each cage oxygen to the cage center.

^c Variation in distance of oxygen atoms from the center of a cage. A smaller variation in radius reflects a more symmetric cage.

^d Number of oxygen atoms at the periphery of each cavity.

Asterisks represent the variation in radius taken by dividing the difference between the largest and smallest distances by the largest distance.

the guest. On the basis of computer simulations, anomalies observed in the water cluster distributions determined by mass spectrometry were proposed to be due to a pentagonal dodecahedron with a mobile surface proton in the cage structure (Holland and Castleman, 1980).

The first direct experimental evidence for a stable clathrate structure of (H₂O)₂₁H⁺, where the H₃O⁺ ion is encaged inside the clathrate structure of (H₂O)₂₀ came from time-of-flight mass spectrometry (Wei et al., 1991). It is worth noting that evidence for the so-called magic number (21) water clusters found by Castleman and coworkers is restricted to the vapor phase (Holland and Castleman, 1980; Wei et al., 1991). More recently Dec et al. (2006) have used nuclear magnetic resonance (NMR) spectroscopy to obtain direct evidence of long-lived hydration shells around methane in the aqueous phase, which have a hydration number of 20. This corresponds to the magic number of 21, where similar to H₃O⁺, methane is encaged inside a (H₂O)₂₀ hydration shell. Computer simulations indicated that the enhanced stability of the “magic number” (21) water cluster is due to the strong Coulombic interaction between the encaged H₃O⁺ ion and surrounding 20 water molecules that form a deformed pentagonal dodecahedral cage (Nagashima et al., 1986).

Many hydrate cavities have analogs: (1) in the clathrasils in which SiO_2 replaces water as a host molecule (Gerke and Gies, 1984) and (2) in the Buckminsterfullerene (covalently bonded carbon cavities) family (Curl and Smalley, 1991). Even with these analogous structures providing estimates of other cavities, for hydrate unit crystals there is the additional restriction that the cavities must be packed to fill space.

With the exceptions of cavities containing square faces, all hydrate cavities (as well as clathrasil and Buckyball family cavities) follow Euler's theorem (Lyusternik, 1963) for convex polyhedra, stated as ($F + V = E + 2$). The number of faces (F) plus the vertices (V) equals the edges (E) plus 2. Euler's theorem is easily fulfilled in cavities having exactly 12 pentagonal faces and any number of hexagonal faces except one.

Pentagonal Dodecahedra. The basic building block, present as the small cavity in all known natural gas hydrate structures, is the 5^{12} pentagonal dodecahedron of [Figure 2.5a](#). When 12 pentagons are combined, the 5^{12} structure results. All 60 of the molecules in the 12 pentagons are not required for the structure; because pentagons share sides, only 20 molecules are required to make a 5^{12} cavity.

Euclid (fl.c. 300 BC) proved that the 5^{12} structure is the largest of the five strictly regular convex polyhedra. That is, it is the only hydrate cavity, which has planar faces that have both equal edges and O—O—O angles. In the 5^{12} structure there is only 1.5° departure of the O—O—O angles from the tetrahedral angles of ice Ih, and only 3.5° departure from the free water angle; the O—O bond lengths exceed those in ice by only 1%. Angell (1982) suggested that unstrained 5^{12} polyhedra arise naturally within the random hydrogen-bonded network in highly supercooled water.

The 5^{12} cavity geometry (faces, $F = 12$; vertices, $V = 20$; edges, $E = 30$) follows Euler's theorem of $F + V = E + 2$. Chen (1980, p. 109) suggested that the 5^{12} cavity seems geometrically favored by nature because it maximizes the number of bonds (30) to molecules (20) along the surface, when compared to similar cavities. Holland and Castleman (1980) studied a number of clusters and determined that the 5^{12} cluster had a hydrogen bond advantage over ice, and that it was less strained than other clathrate clusters.

Note that Figure 2.5a, for simplicity, does not display the hydrogen atoms that protrude from the 5^{12} cavity. Because there are 20 water molecules with 30 bonds, 10 water molecules have hydrogen atoms pointing away from the cavity, as potential points of attachment to other molecules or cavities. Thus the 5^{12} cavity, with ten protruding hydrogen atoms, has the appearance of a "dandelion" rather than a sphere. Similarly, the other cavities also have protruding hydrogen atoms.

As shown in [Table 2.1](#), the 5^{12} cavity is almost spherical (showing a low percentage variation in radius, that is, a low variation in oxygen atom distances from the cavity center) with a radius of 3.95 and 3.91 Å in structures I and II, respectively. This small dimensional difference determines the size of the occupant. Until recently, it was thought (Davidson, 1973) that the smallest hydrate guest molecules stabilized the 5^{12} cavity of structure I.

Davidson et al. (1984a) crystallographically confirmed the suggestion of Holder and Manganiello (1982) that guest molecules of pure argon (3.83 Å diameter) or krypton (4.04 Å diameter) occupy the 5^{12} cavities of structure II. More recently, Davidson et al. (1986a) and Tse et al. (1986) determined that nitrogen and oxygen, respectively, occupied the 5^{12} cavity of structure II. Methane and hydrogen sulfide, with diameters of 4.36 Å and 4.58 Å, respectively, occupy the 5^{12} cavity of structure I. Helium, hydrogen, and neon, the smallest molecules with diameters less than 3.0 Å were considered too small to stabilize any cage. More recently, these small molecules have been shown to multiply and singly occupy large and small cages, respectively, of structure II at very high pressures (Manakov et al., 2002; Mao et al., 2002; Lokshin et al., 2005a,b). See [Section 2.1.2.2.5](#) on high pressure hydrate phases for more details.

Tetrakaidecahedron. The geometries of the 14-hedra ($5^{12}6^2$) and the 16-hedra ($5^{12}6^4$) are detailed by Allen (1964), who presented Schlegel diagrams of these cavities, to complement the diagrams of [Figures 2.5b,c](#). In these two-dimensional diagrams, shown in [Figures 2.6a,b](#) for the $5^{12}6^2$ and $5^{12}6^4$ cavities, one has the perspective of placing one's eye at a hexagonal face and looking into the cavity interior. The periphery of each figure is hexagonal, and the placement of other hexagonal faces serve to locate the pentagonal faces.

The $5^{12}6^2$ cavity also follows Euler's theorem, with 14 faces plus 24 vertices to give 36 edges plus 2. Figure 2.6a shows the 14-hedra to be formed by 2 facing hexagons, with 12 connecting pentagons. Each hexagon has six pentagons attached to its edges, resulting in two "cups," each formed by a hexagon at the base with six pentagons at the hexagon sides. The two cups join at the periphery to form the $5^{12}6^2$ cavity.

The orthogonal view of the $5^{12}6^2$ cavity, in [Figure 2.5b](#), shows it to be the most nonspherical cavity in sI or sII. The four crystallographically different types of oxygen sites are 4.25, 4.47, 4.06, and 4.64 Å from the 14-hedra cavity center, giving a 14% variation from sphericity ([Table 2.1](#)), resembling an oblate ellipsoid. This cavity also has the largest O—O—O angle variation (5.1°) from the tetrahedral angle preferred by water.

With an average radius of 4.33 Å, the $5^{12}6^2$ cavity is large enough to contain molecules smaller than 6.0 Å in diameter. Ripmeester (Personal Communication, May 2, 1988) indicates that the 14-hedron is the preferred cage for almost all structure I hydrates, in which it plays the main stabilizing role. The oblate nature of the $5^{12}6^2$ cage causes the shape of the guest molecule to play a role in cavity stability.

Hexakaidecahedron. [Figures 2.5c](#) and [2.6b](#) provide the orthogonal view and the Schlegel diagram for the $5^{12}6^4$ structure, respectively. The latter diagram allows Euler's theorem to be verified: 16 faces plus 28 vertices equals 42 edges plus 2. The $5^{12}6^4$ notation for this cavity indicates four hexagonal faces.

The hexagonal faces are symmetrically arranged so that normals to hexagonal face centers form the vertices of a tetrahedron. Each hexagonal face is surrounded entirely by pentagonal faces. No two hexagons share a common edge. The radii from the cavity center to the crystallographically different oxygen sites do not vary

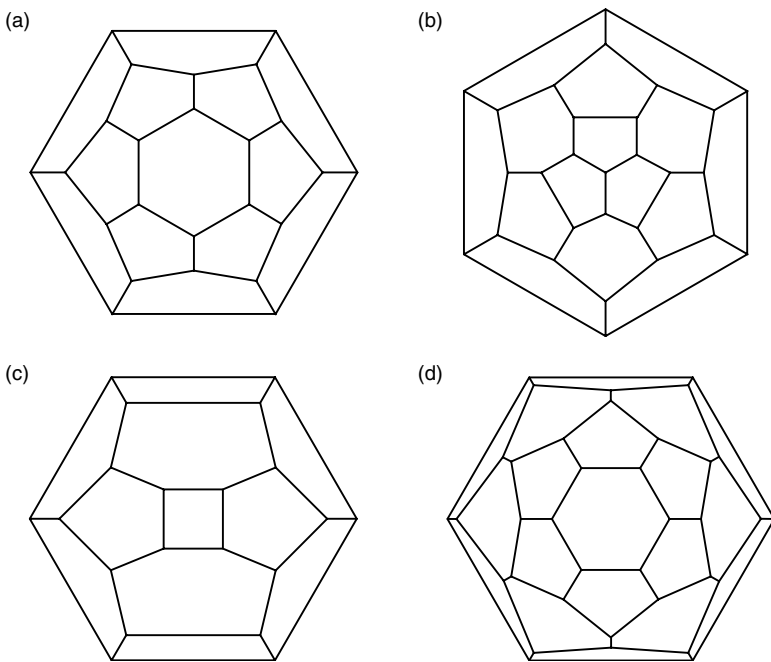


FIGURE 2.6 Schlegel diagrams for (a) tetrakaidecahedron ($5^{12}6^2$), (b) hexakaidecahedron ($5^{12}6^4$), (c) irregular dodecahedron ($4^35^66^3$), (d) icosahedron ($5^{12}6^8$). (Reproduced from Allen, K.W., *J. Chem. Phys.*, **41**, 840 (1964). With permission from the American Institute of Physics.)

more than 1.7% (Table 2.1); therefore, the 16-hedron is the most spherical cavity of the five types.

The $5^{12}6^4$ cavity can contain molecules as large as 6.6 Å. Consequently, when the larger components of natural gas such as propane or iso-butane form simple (single guest) hydrates, they stabilize this cavity alone in structure II but the smaller cavities remain vacant.

Trimethylene oxide (Hawkins and Davidson, 1966), cyclopropane (Hafemann and Miller, 1969; Majid et al., 1969), and ethylene sulfide (Ripmeester, Personal Communication, May 2, 1988) are three molecules that can form in either the 5^{12} of structure I or the $5^{12}6^4$ of structure II as simple hydrates. Raman spectroscopy measurements suggest that a low fraction of 5^{12} cages may also be occupied by cyclopropane at high pressures (Suzuki et al., 2001). Such compounds change structures depending on the temperature and pressure of formation, and guest composition in the aqueous phase as discussed in Section 2.1.3.

The Irregular Dodecahedron ($4^35^66^3$) and the Icosahedron ($5^{12}6^8$). Single crystal diffraction data for sizes of structure H cavities ($4^35^66^3$ and the $5^{12}6^8$ shown in Figures 2.5d,e) have been performed by Udachin and coworkers (Udachin and Lipkowski, 1996; Udachin et al., 1997b; Kirchner et al., 2004). The radii of the $4^35^66^3$ and $5^{12}6^8$ cavities were determined to be 4.04 and 5.79 Å, based on single crystal x-ray diffraction data (Udachin et al., 1997b), as indicated in Table 2.1.

The irregular dodecahedron ($4^35^66^3$) has the unusual property of following Euler's theorem ($F = 12$, $V = 20$, $E = 30$, so that $F + V = E + 2$) without having 12 pentagonal faces. The geometry of the cavity is remarkable due to the three square and three hexagonal faces that contain a considerable amount of bond strain. A Schlegel diagram is shown in [Figure 2.6c](#) for the $4^35^66^3$ cage, with the perspective first discussed for the $5^{12}6^2$ cavity.

The size of the $4^35^66^3$ cavity can be estimated using the correlation of Ripmeester et al. (1988) for the NMR measurements of chemical shift of isotopic ^{129}Xe as a function of the free radius available to the xenon atom inside each cage. Using this correlation and adding the van der Waals radius of water (1.4 Å), the radius of the $4^35^66^3$ cage was estimated as 4.06 Å. This estimated value was verified using single crystal x-ray diffraction.

The $5^{12}6^8$ cavity also follows Euler's theorem ($F = 20$, $V = 36$, $E = 54$), but it has a more usual geometry with 12 pentagonal and 8 hexagonal faces. The girdle of hexagonal faces, plus those at the crown and foot, provide a greatly expanded cage, allowing for occupants over 1 Å larger than those of any other cage. A Schlegel diagram is drawn for the $5^{12}6^8$ cage in [Figure 2.6d](#).

Two points should be noted about both the $4^35^66^3$ and $5^{12}6^8$ cages: (1) the square and hexagonal faces are highly strained and (2) they are significantly less spherical than the 5^{12} cavity. In [Figure 2.5](#), the two free-standing cavities are shown as having approximately planar sides; however, when they are connected in a sH model of the unit structure, both the strains and nonsphericity become apparent. (See discussion of the next section related to sH, [Figures 2.9a,b](#).)

The fraction of strained angles in each of the five cavities may be estimated by considering pentagonal O—O—O angles to be approximately unstrained (3.5°) relative to free water (H—O—H angle of 104.5°) with cubic and hexagonal angles having essentially the same strain (15°). The fraction of strained angles in each cavity increases in order of $5^{12}6^2 < 5^{12}6^4 < 5^{12}6^8 < 4^35^66^3$ (16.7% < 28.6% < 44.4% < 50%, respectively). The two unusual cavity types in sH each have almost half their angles strained. Such strains may be reflected in a slow kinetics of formation.

A visual inspection of the cavities in [Figure 2.5](#) shows b, d, and e to be nonspherical. The $5^{12}6^8$ is the most oblate of all five cavities; consequently, the shape of the occupying molecule is more significant than other cages. Ripmeester and Ratcliffe (1990a) note that, in contrast to the criteria for all other hydrate cages, size alone does not seem to be sufficient for a molecule to be a suitable guest in the $5^{12}6^8$. As indicated in Section 2.1.3.2, efficient space filling of the cage is necessary to optimize the van der Waals contact between the guest and the cage walls.

2.1.2.2 Hydrate crystal cells—structures I, II, and H

Crystal properties of sI, sII, and sH are given in [Table 2.2a](#). [Table 2.2b](#) lists the atomic coordinates for these structures, which will enable the advanced reader to generate computer models of the hydrate crystals. The contrast of sI and sII structures is obtained by linking the basic 5^{12} cavity in two different ways to achieve fourfold hydrogen bonds. All modes of associating pentagonal

TABLE 2.2a
Hydrate Crystal Cell Structures

Structure	I	II	H																																																									
Crystal system	Cubic	Cubic	Hexagonal																																																									
Space group	Pm3n (No. 223) ^c	Fd3m (No. 227) ^c	P6/mmm (No. 191) ^c																																																									
Lattice description	Primitive	Face centered	Hexagonal																																																									
Lattice parameters ^a	$a = 12 \text{ \AA}$ $\alpha = \beta = \gamma = 90^\circ$	$a = 17.3 \text{ \AA}$ $\alpha = \beta = \gamma = 90^\circ$	$a = 12.2 \text{ \AA}$ $c = 10.1 \text{ \AA}$ $\alpha = \beta = 90^\circ, \gamma = 120^\circ$																																																									
Ideal unit cell formula	$6(5^{12}6^2) \cdot 2(5^{12}) \cdot 46\text{H}_2\text{O}$	$8(5^{12}6^4) \cdot 16(5^{12}) \cdot 136\text{H}_2\text{O}$	$1(5^{12}6^8) \cdot 3(5^{12}) \cdot 2(4^35^66^3) \cdot 34\text{H}_2\text{O}$																																																									
Number of faces ^b :	H = 6 hexagonal (H), pentagonal (P), square (S)	H = 16 P = 144	H = 7 P = 30 S = 3																																																									
Atomic positions: number and symmetry	<table border="0"> <tr> <td>$5^{12}6^2$ (d)</td> <td>$6, \bar{4} 2 \text{ m}$</td> <td>$5^{12}6^4$ (b)</td> <td>$8, \bar{4} 3 \text{ m}$</td> <td>$5^{12}6^8$</td> <td>1, 6/mmm</td> </tr> <tr> <td>5^{12} (a)</td> <td>$2, \text{m}3$</td> <td>5^{12} (c)</td> <td>$16, \bar{3} \text{ m}$</td> <td>5^{12} (g)</td> <td>3, mmm</td> </tr> <tr> <td>O(c)</td> <td>$6, \bar{4} 2 \text{ m}$</td> <td>O(a)</td> <td>$8, \bar{4} 3 \text{ m}$</td> <td>O(o),</td> <td>12, m</td> </tr> <tr> <td>O(i)</td> <td>$16, 3 \text{ m}$</td> <td>O(e)</td> <td>$32, 3 \text{ m}$</td> <td>O(h)</td> <td>4, 3 m</td> </tr> <tr> <td>O(k)</td> <td>$24, \text{m}$</td> <td>O(g)</td> <td>$96, \text{m}$</td> <td>O(n)</td> <td>12, m</td> </tr> <tr> <td>(1/2 H) (i)</td> <td>$16, 3$</td> <td>2(1/2 H) (e)</td> <td>$32, 3 \text{ m}$</td> <td>O(m)</td> <td>6, mm2</td> </tr> <tr> <td>3(1/2 H) (k)</td> <td>$24, \text{m}$</td> <td>3(1/2 H) (g)</td> <td>$96, \text{m}$</td> <td>X(1/2 H)</td> <td></td> </tr> <tr> <td>2(1/2 H) (l)</td> <td>$48, 1$</td> <td>(1/2 H) (i)</td> <td>$192, \text{m}$</td> <td>X(1/2 H)</td> <td></td> </tr> </table>	$5^{12}6^2$ (d)	$6, \bar{4} 2 \text{ m}$	$5^{12}6^4$ (b)	$8, \bar{4} 3 \text{ m}$	$5^{12}6^8$	1, 6/mmm	5^{12} (a)	$2, \text{m}3$	5^{12} (c)	$16, \bar{3} \text{ m}$	5^{12} (g)	3, mmm	O(c)	$6, \bar{4} 2 \text{ m}$	O(a)	$8, \bar{4} 3 \text{ m}$	O(o),	12, m	O(i)	$16, 3 \text{ m}$	O(e)	$32, 3 \text{ m}$	O(h)	4, 3 m	O(k)	$24, \text{m}$	O(g)	$96, \text{m}$	O(n)	12, m	(1/2 H) (i)	$16, 3$	2(1/2 H) (e)	$32, 3 \text{ m}$	O(m)	6, mm2	3(1/2 H) (k)	$24, \text{m}$	3(1/2 H) (g)	$96, \text{m}$	X(1/2 H)		2(1/2 H) (l)	$48, 1$	(1/2 H) (i)	$192, \text{m}$	X(1/2 H)		<table border="0"> <tr> <td>$5^{12}6^3$</td> <td>$2, \bar{6} \text{ m}2$</td> </tr> <tr> <td>O(o),</td> <td>12, m</td> </tr> <tr> <td>O(h)</td> <td>4, 3 m</td> </tr> <tr> <td>O(n)</td> <td>12, m</td> </tr> <tr> <td>X(1/2 H)</td> <td></td> </tr> </table>	$5^{12}6^3$	$2, \bar{6} \text{ m}2$	O(o),	12, m	O(h)	4, 3 m	O(n)	12, m	X(1/2 H)	
$5^{12}6^2$ (d)	$6, \bar{4} 2 \text{ m}$	$5^{12}6^4$ (b)	$8, \bar{4} 3 \text{ m}$	$5^{12}6^8$	1, 6/mmm																																																							
5^{12} (a)	$2, \text{m}3$	5^{12} (c)	$16, \bar{3} \text{ m}$	5^{12} (g)	3, mmm																																																							
O(c)	$6, \bar{4} 2 \text{ m}$	O(a)	$8, \bar{4} 3 \text{ m}$	O(o),	12, m																																																							
O(i)	$16, 3 \text{ m}$	O(e)	$32, 3 \text{ m}$	O(h)	4, 3 m																																																							
O(k)	$24, \text{m}$	O(g)	$96, \text{m}$	O(n)	12, m																																																							
(1/2 H) (i)	$16, 3$	2(1/2 H) (e)	$32, 3 \text{ m}$	O(m)	6, mm2																																																							
3(1/2 H) (k)	$24, \text{m}$	3(1/2 H) (g)	$96, \text{m}$	X(1/2 H)																																																								
2(1/2 H) (l)	$48, 1$	(1/2 H) (i)	$192, \text{m}$	X(1/2 H)																																																								
$5^{12}6^3$	$2, \bar{6} \text{ m}2$																																																											
O(o),	12, m																																																											
O(h)	4, 3 m																																																											
O(n)	12, m																																																											
X(1/2 H)																																																												

^a Lattice parameters are a function of temperature, pressure, and guest composition. Values given are typical average values.

^b Number of faces accounting for face-sharing in the unit cell.

^c Space group reference numbers from the International Tables for Crystallography.

Atomic positions indicate the Wyckoff letter in parentheses.

Table modified from Jeffrey (1984, p. 150).

dodecahedra lead to either fivefold or sixfold coordination of water molecules, except the following two, which yield fourfold hydrogen bonds (1) by linking the vertices of dodecahedra or (2) by sharing common faces of adjacent dodecahedra.

Structure I is an example of vertex-linking of the 5^{12} cavities in three dimensions, while structure II illustrates face-sharing of the 5^{12} cavities in three dimensions (see Figure 2.7). In structures I and II the spaces between the 5^{12} cavities form larger $5^{12}6^2$ or $5^{12}6^4$ cavities, respectively. Structure H illustrates

TABLE 2.2b
Atomic Coordinates and Isotropic Displacement Parameters for sI, sII, and sH Hydrates

sI Hydrate, CH₄ · 5 · 75D₂O^a				Temperature factor (10⁻² Å²)
Atom	x	y	z	
O1	0.1841(2)	0.1841(2)	0.1841(2)	0.92(7)
O2	0.0000	0.3100(2)	0.1154(2)	0.57(5)
O3	0.0000	0.5000	0.2500	0.76(9)
D7	0.2314(3)	0.2314(3)	0.2314(3)	1.7(1)
D8	0.0000	0.4305(5)	0.2007(5)	1.5(2)
D9	0.0000	0.3801(5)	0.1614(5)	1.2(2)
D10	0.0000	0.3157(5)	0.0349(4)	1.8(2)
D11	0.0673(4)	0.2662(4)	0.1373(4)	2.4(2)
D12	0.1177(4)	0.2257(4)	0.1582(4)	1.9(2)
5 ¹² center	0	0	0	
5 ¹² 6 ² center	0	0.25	0.5	
sII Hydrate, C₃H₈ · 17D₂O^b				
Atom	x	y	z	U(eq)
O1	0.1823(4)	0.1823(4)	0.3693(4)	1.52(9)
O2	0.2187(4)	0.2187(4)	0.2187(4)	1.52(9)
O3	1/8	1/8	1/8	1.52(9)
D4	-0.0613(1)	-0.021(1)	0.149(1)	4.2(2)
D5	0.1453(8)	0.1453(8)	0.369(2)	4.2(2)
D6	0.192(1)	0.192(1)	0.316(1)	4.2(2)
D7	0.208(1)	0.208(1)	0.270(1)	4.2(2)
D8	0.160(1)	0.160(1)	0.160(1)	4.2(2)
D9	0.183(1)	0.183(1)	0.183(1)	4.2(2)
5 ¹² center	0	0	0	
5 ¹² 6 ⁴ center	3/8	3/8	3/8	
sH Hydrate, 2,2-dimethylpentane.5(Xe,H₂S).34H₂O^c				
Atom	x	y	z	B_{iso}
O1	0.79099(6)	0.20901	0.27765(13)	2.27(4)
O2	0.66667	0.33333	0.36433(23)	2.17(7)
O3	0.61389(12)	0.61389	0.13726(13)	2.39(5)
O4	0.86798(8)	0.13202	0.50000	2.26(7)
5 ¹² center	0.66667	0.33333	0.00000	1.99(3)
4 ³ 5 ⁶ 6 ³ center	0.50000	0.50000	0.50000	1.99(3)
5 ¹² 6 ⁸ center	0.00000	0.00000	0.00000	

^a Gutt et al. (2000) from Rietveld refinement of high-resolution neutron powder diffraction at 2 K.

^b Rawn et al. (2003) from Rietveld refinement of neutron powder diffraction at 17 K.

^c Udachin et al. (1997b), from single crystal x-ray diffraction at 193 K. B_{iso} is the mean of the principal axes of the thermal ellipsoid.

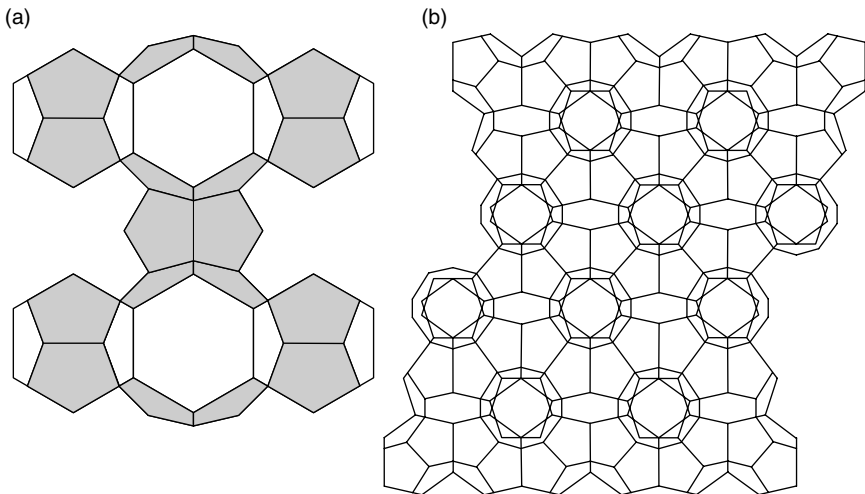


FIGURE 2.7 (a) Linking five 5^{12} polyhedra by two $5^{12}6^2$ polyhedra to form structure I. (b) Two-dimensional view of face-sharing of 5^{12} polyhedra to form $5^{12}6^4$ polyhedra voids for structure II. (Reproduced from Jeffrey, G.A., McMullan, R.K., *Prog. Inorg. Chem.*, 8, 43 (1967), John Wiley & Sons. With permission.)

face-sharing in two dimensions, so that a layer of 5^{12} cavities connects a layer of $5^{12}6^8$ and $4^35^66^3$ cavities.

Davidson and Ripmeester (1984) discuss the mobility of water molecules in the host lattices, on the basis of NMR and dielectric experiments. Water mobility comes from molecular reorientation and diffusion, with the former being substantially faster than the water mobility in ice. Dielectric relaxation data suggest that Bjerrum defects in the hydrate lattice, caused by guest dipoles, may enhance water diffusion rates.

Jeffrey's (1984) list of a series of seven hydrate crystals (structures I–VII) are summarized in Table 2.3. These seven hydrate crystals are formed by polyhedra such as those in the last section. He noted, however, that a “study of all the possible three-dimensional four-connected structures based on polyhedra with twelve or more vertices is a formidable topological problem,” inferring that some structures may have been overlooked. Indeed, structure H is not one of the seven structures listed by Jeffrey. Although only two of these structures (sI and sII) have been identified so far with hydrocarbon gas components, Jeffrey's list of seven hydrate structures for the true clathrate hydrates are given here for completeness. Exploring new and less common hydrate structures is becoming of increasing interest for a range of technological applications of hydrates. Dyadin et al. (1991) have also proposed seven structures, including the three listed in natural gas hydrates (sI, sII, sH); the others have yet to be found with hydrocarbons such as natural gas components.

TABLE 2.3
Jeffrey's (1984) List of a Series of Seven Hydrate Crystal Structures

I	II	III	IV	V	VI	VII
12-Hedra (5^{12})	12-Hedra (5^{12})	12-Hedra (5^{12})	12-Hedra (5^{12})	12-Hedra (5^{12})	8-Hedra (4^45^4)	
14-Hedra ($5^{12}6^2$)	16-Hedra ($5^{12}6^4$)	14-Hedra ($5^{12}6^2$)	14-Hedra ($5^{12}6^2$)	16-Hedra ($5^{12}6^4$)	17-Hedra ($4^35^96^27^3$)	14-Hedra (4^66^8)
		15-Hedra ($5^{12}6^3$)	15-Hedra ($5^{12}6^3$)			
Cubic (sI) Pm3n $a = 12 \text{ \AA}$	Cubic (sII) Fd3m $a = 17.3 \text{ \AA}$	Tetragonal* P4 ₂ /mm $c \sim 12.4,$ $a \sim 23.5 \text{ \AA}$	Hexagonal P6/mmm $c \sim 12.5,$ $a \sim 12.5 \text{ \AA}$	Hexagonal P6 ₃ /mmc $c \sim 19,$ $a \sim 12 \text{ \AA}$	Cubic I43d $a = 18.8(2) \text{ \AA}$	Cubic Im3m $a = 7.7 \text{ \AA}$
6X.2Y. 46H ₂ O	8X.16Y. 136H ₂ O	20X.10Y. 172H ₂ O	8X.6Y. 80H ₂ O	4X.8Y. 68H ₂ O	16X 156H ₂ O	2X.12H ₂ O
Gas hydrates	Gas hydrates	Bromine hydrate	None known	None known	Me ₃ CNH ₂ hydrate	HPF ₆ hydrate

Note: X refers to guest molecules in 14-hedra or larger voids, Y refers to guests in 12-hedra.

2.1.2.2.1 Structure I

Definitive x-ray diffraction data on structure I was obtained by McMullan and Jeffrey (1965) for ethylene oxide (EO) hydrate, as presented in Table 2.2a. The crystal consists of a primitive cubic lattice, with parameters as given in Table 2.2a. The common pictorial view of structure I is presented in Figure 1.5a. In that figure, the front face of a 12 Å cube is shown, with two complete $5^{12}6^2$ (emphasizing hydrogen bonds) connecting four 5^{12} .

An alternative, less frequent view is found in Figure 2.7a, which shows five 5^{12} connected by two $5^{12}6^2$; this is a primary illustration of linking 5^{12} through additional water molecules, which form $5^{12}6^2$. Jeffrey (1984, p. 153) suggests that the structure is defined by the $5^{12}6^2$ hedra, in the following description:

“There is no direct face sharing between the 12-hedra (5^{12}). The structure can be constructed from the vertices of face-sharing 14-hedra ($5^{12}6^2$) arranged in columns with the 14-hedra sharing their opposing hexagonal faces. These columns are then placed in contact so as to share a pentagonal face between each pair of 14-hedra, with the column axes along ($x, 1/2, 0$) a 12 Å cubic cell. The remaining space is then the 12-hedra in a body centered cubic arrangement of their centers.”

While Figure 1.5a appears to contain many water molecules, there are only 46 water molecules inside the structure I cubic cell and there are only eight polyhedra totally within the cube. Each of six cube faces contains two halves of a $5^{12}6^2$, for a total of six $5^{12}6^2$ within the cell. Each of the eight vertices of the

cube contains one-eighth of a 5^{12} , which, when added to the 5^{12} in the center of the cube, gives a total of two 5^{12} per cell.

2.1.2.2.2 Structure II

After crystal structure II was deduced, a definitive x-ray diffraction study of tetrahydrofuran/hydrogen sulfide hydrate was undertaken by Mak and McMullan (1965), two of Jeffrey's colleagues. The crystal consists of a face-centered cubic lattice, which fits within a cube of 17.3 Å on a side, with parameters as given in Table 2.2a and shown in Figure 1.5b. In direct contrast to the properties of structure I, this figure illustrates how a crystal structure may be completely defined by the vertices of the smaller 5^{12} cavities. Because the 5^{12} outnumber the $5^{12}6^4$ cavities in the ratio 16:8, only 5^{12} are clearly visible in Figure 1.5b.

A second view of a layer of structure II is presented in Figure 2.7b, which is a two-dimensional view of the way many face-sharing 5^{12} are arranged so that the residual voids are $5^{12}6^4$ (which share all the hexagonal faces). This is only a partial view of the crystal cell. These layers are stacked in a staggered pattern ABCABC so that the centers of the 16-hedra form a diamond lattice within a cube, with shared hexagonal faces. An alternative view of the packing in structure II is given in Figure 2.8 (in the {111} direction). Layers of face-sharing 5^{12} cavities alternate with layers consisting of $5^{12}6^4$ and 5^{12} cavities.

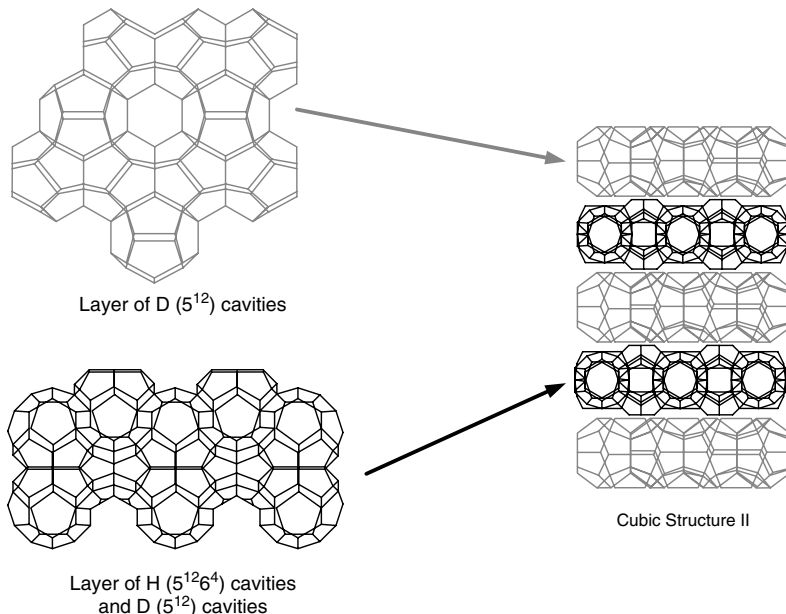


FIGURE 2.8 Schematic diagram showing structure II is built up of layers of 5^{12} cavities alternating with layers of $5^{12}6^4$ and 5^{12} cavities. (Reproduced from Udachin, K., Ripmeester, J.A., in *Proc. Fifth Int. Conf. on Gas Hydrates*, Trondheim, Norway, June 13–16, Paper 2024 (2005). With permission.)

Jeffrey (1984, p. 156) suggests that the voids formed by connecting 16-hedra could accommodate much larger guests (perhaps sharing voids) than those normally found in gas hydrates, but such clathrates have yet to be found. When the layer in [Figure 2.7b](#) forms the pattern ABABA, a hexagonal rather than cubic cell is formed; this structure is not found in natural gas hydrates, but is present with such molecules as isopropylamine, $(\text{CH}_3)_2\text{CHNH}_2 \cdot 8\text{H}_2\text{O}$ (Jeffrey's structure V).

2.1.2.2.3 Structure H

Ripmeester et al. (1987) reported structure H with evidence provided by NMR spectroscopy and x-ray powder diffraction. The structure was found to be isostructural with clathrasil dodecasil-1H, a clathrate formed with SiO_2 replacing H_2O as the host molecule (Gerke and Gies, 1984). It is likely that structure H was first prepared (but unrecognized) by de Forcrand in 1883, more than 100 years earlier than the structure was identified by Ripmeester et al. De Forcrand prepared binary (double) hydrates with iso-butyl chloride or bromide as the large guest, where these guests are similar in size to iso-pentane, now known to be an sH hydrate former.

Similar to Jeffrey's hypothetical structure IV, structure H is a hexagonal crystal of space group P6/mmm. However, in contrast to structure IV, structure H comprises $4^35^66^3$ and $5^{12}6^8$ cavities in addition to 5^{12} cavities. On the basis of size considerations (including the relative size of the guests, the size of the cages in I–VII, and the unit cell parameters for sH), the structure was incompatible with Jeffrey's structures. Therefore, sH is not one of Jeffrey's (1984) known or hypothetical structures. Single crystal diffraction data for structure H have been obtained by Udachin et al. (1997b, 2002) and Kirchner et al. (2004).

The structure H unit cell, has a composition of $3(5^{12}) \cdot 2(4^35^66^3) \cdot 1(5^{12}6^8) \cdot 34\text{H}_2\text{O}$. An orthogonal view is shown in [Figure 1.5c](#). One important aspect of sH is that two sizes of molecules are required to stabilize the structure. Small molecules, such as methane or hydrogen sulfide, enter both small cavities (5^{12} and $4^35^66^3$) and large molecules typically larger than 7.3 Å, such as 2,2-dimethylbutane (neohexane), enter the $5^{12}6^8$ cavity. In contrast to sI and sII, which generally form hydrates readily with single occupants of either the small and/or large cavity, no exception to the requirement of a double hydrate has been found for sH.

[Figures 2.9a,b](#) provide more enlightening perspectives of sH, as top and side views of the unit cell. Figure 2.9a is a top view of the unit cell rhombus (dark lines) with an edge length of 12.26 Å. Four $5^{12}6^8$ cavities (labeled A, B, C, and D) are shown at the vertices of the unit cell; quarters of these cavities within the unit crystal combine to make one complete $5^{12}6^8$ cavity contributing to the unit cell. The two $4^35^66^3$ cavities (labeled 1 and 2, each with three pentagonal faces showing) are within the unit cell connecting the $5^{12}6^8$ cavities. Four other $4^35^66^3$ cavities (labeled 3, 4, 5, and 6—also showing three pentagonal faces each) are connected through square faces to the sides of the rhombus.

Figure 2.9a illustrates (bird's eye view) that on one layer, the $5^{12}6^8$ cavities are connected by $4^35^66^3$ cavities, only by hexagonal faces. The $4^35^66^3$ cavities are connected to other $4^35^66^3$ cavities only by square faces. All pentagonal faces of each type of cavity serve to connect this layer of unusual cavities to layers of

5^{12} cavities (not shown). The figure also illustrates that the $4^3 5^6 6^3$ cavities are both strained and nonspherical in the unit cell, in contrast to the free standing cavities shown in [Figure 2.5](#). No 5^{12} cavities are in this layer.

Figure 2.9b is an end-on, side view of the cell rhombus. In the figure, are outlines of three $5^{12}6^8$ cavities (labeled A, B, and C) are shown with the vertical borders of the rhombus at centroids of each $5^{12}6^8$. The fourth $5^{12}6^8$ of Figure 2.9a is aligned behind the middle $5^{12}6^8$ cavity in Figure 2.9b. This view shows both the nonspherical nature of the $5^{12}6^8$ cavities and their nonplanar, strained hexagonal faces in contrast to the almost planar hexagonal faces in sI and sII.

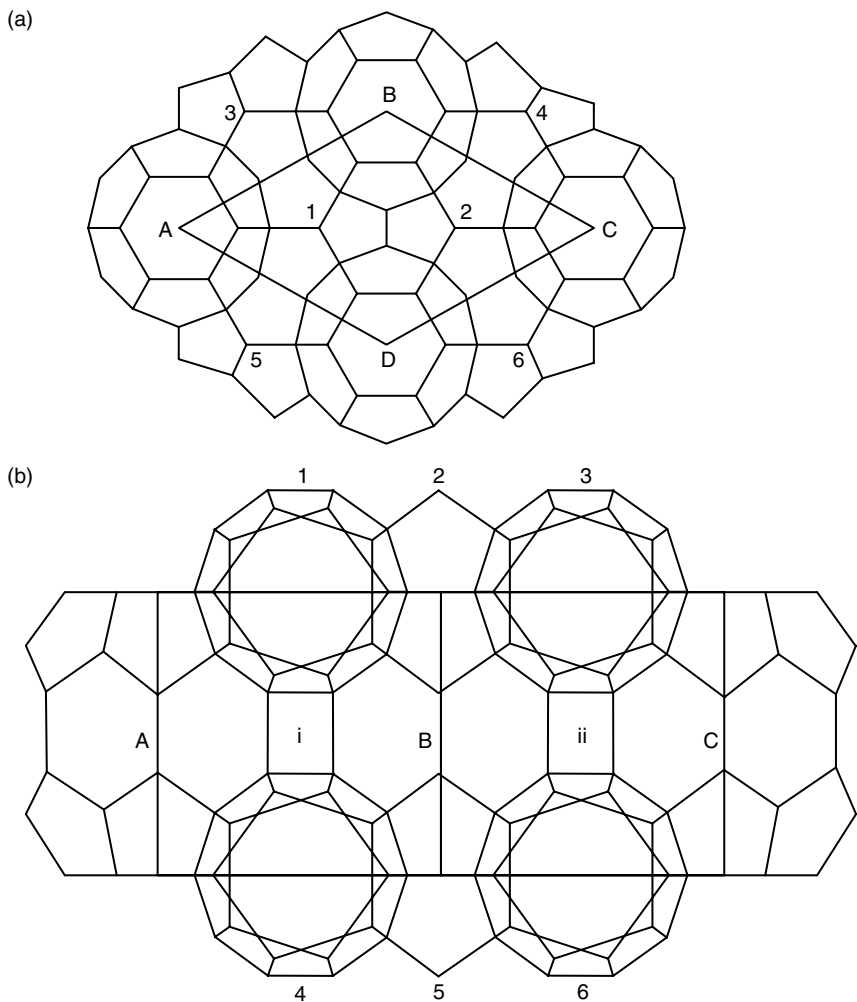


FIGURE 2.9 Top view (a) and side view (b) of a structure *H* hydrate unit cell. (Reproduced from Lederhos et al., *AIChE J.* (1992). With permission.)

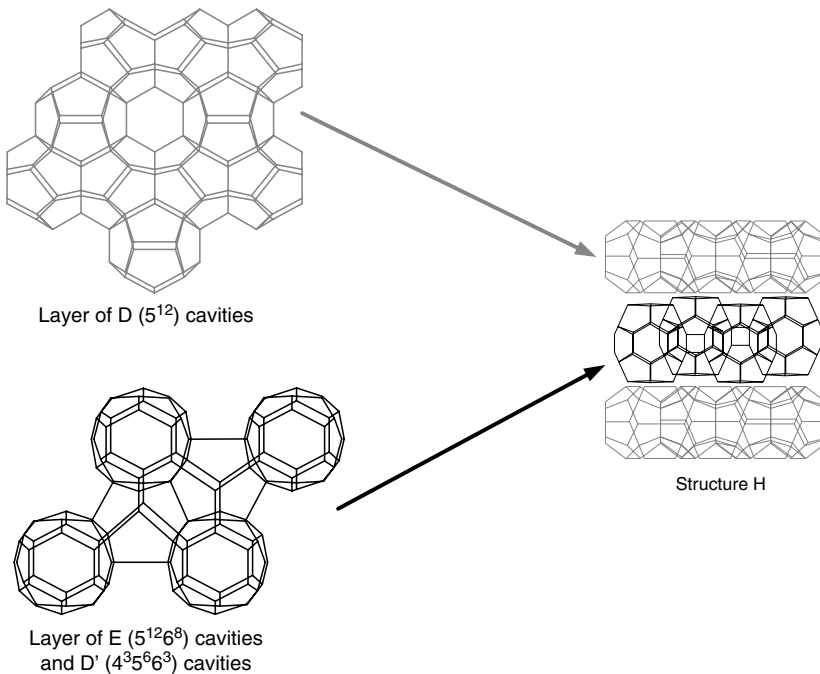


FIGURE 2.10 Schematic diagram showing structure H is built up of layers of 5^{12} (D) cavities and layers of $5^{12}6^8$ (E) and $4^35^66^3$ (D') cavities. (Reproduced from Udachin, K., Ripmeester, J.A., in *Proc. Fifth Int. Conf. on Gas Hydrates*, Trondheim, Norway, June 13–16, Paper 2024 (2005). With permission.)

Also in Figure 2.9b, six 5^{12} cavities (labeled 1 through 6) protrude from the top and bottom edges of the unit crystal, to illustrate the 5^{12} connecting role to layers composed of one $5^{12}6^8$ and two $4^35^66^3$ cavities within the unit crystal. The figure clearly shows one-half of each of six 5^{12} cavities (or three complete 5^{12} cavities) contained in the unit cell.

In Figure 2.9b, two square faces (labeled i and ii, connecting the three $5^{12}6^8$ cavities) each belong to $4^35^66^3$ cavities. Since the $4^35^66^3$ cavities alone possess square faces, these unusual cavities have only square face connections.

Another way of viewing the packing in structure H is shown in Figure 2.10 (in the {001} direction). Layers consisting of 5^{12} cavities alternate with layers consisting of large $5^{12}6^8$ and small $4^35^66^3$ cavities.

2.1.2.2.4 Jeffrey's structures III to VII, and other unusual structures

Jeffrey's structure III (given in Table 2.3) has been observed with Br_2 single guest molecules. Br_2 molecules occupy the larger polyhedra to give a stoichiometry of $20\text{Br}_2 \cdot 172\text{H}_2\text{O}$. This Br_2 hydrate tetragonal structure was revisited by Udachin et al. (1997a). Single crystal x-ray analysis was performed on crystals grown

from $\text{Br}_2\text{:H}_2\text{O}$ solutions of composition 1:20 to 1:5, confirming the space group $\text{P}4_2/\text{mnm}$, where $a = 23.04 \text{ \AA}$, $c = 12.075 \text{ \AA}$. The unit cell is composed of two types of 5^{12} (D) cavities ($2\text{D}_A \cdot 8\text{D}_8$), two distinct $5^{12}6^2$ (T) cavities ($8\text{T}_A \cdot 8\text{T}_B$), and four ($5^{12}6^3$) cavities. Variable filling of large cages can occur, such that the hydration number varies (the minimum hydration number is 8.6). In this structure the large cages need not be full (this can also be the case for other hydrate structures). Guest–guest interactions could play a role in dictating the structure type. Particularly, in this case where the electron-rich bromine molecule has a sizeable molecular quadrupole moment.

Jeffrey's structure types IV and V are composed of known cavities 5^{12} , $5^{12}6^2$, $5^{12}6^3$, and $5^{12}6^4$. However, so far there are no “true” clathrate hydrates known for structures IV or V. These structures were extrapolated from semiclathrate hydrate structures of alkylamines (IV: Me_3N , EtCH_2NH_2 , $(\text{CH}_3)_2\text{CHNH}_2$; V: Me_2CHNH_2). An analogous extrapolation is that for the structure I gas hydrate that forms the same primitive cubic structure as semiclathrate hydrates with EtNH_2 and Me_2NH guests. In semiclathrates, the host lattice consists of hydrogen-bonded water molecules and hydrogen-bonded functional groups of the guest molecules. The polyhedral voids are then occupied by the hydrophobic component of the guest molecules.

Structure IV (and also structures H and II) can be constructed by stacking two-dimensional sheets of 5^{12} cages, which are joined by sharing pentagonal faces (Udachin and Ripmeester, 1999a). Structure IV can be obtained by AA stacking of these two-dimensional sheets of 5^{12} cages.

The unusual cavities in Jeffrey's structure VI ($4^45^4, 4^35^96^27^3$) and structure VII (4^66^8) have been observed only for single *tert*-butylamine guests and hexafluorophosphoric acid ($\text{HPF}_6 \cdot 6\text{H}_2\text{O}$) guests, respectively. *tert*-Butylamine, Me_3CNH_2 (Jeffrey and McMullan, 1967), is unique among amine hydrates since it forms a true clathrate rather than a semiclathrate.

Other unusual structures that are different to Jeffrey's structures III–VII are summarized as follows. Structure T is a trigonal structure (space group = $\text{P}321$, $a = 35$, $c = 12.4 \text{ \AA}$) that is formed from single dimethyl ether guests (Udachin et al., 2001a). Similar to Jeffrey's structure III (bromine hydrate; as mentioned above), structure T consists of $5^{12}6^3$ cavities. In addition to the known $5^{12}6^2$ and $5^{12}6^3$ cavities, structure T also contains some more unusual $4^25^86^1$ small cavities and $4^15^{10}6^3$ large cavities. A striking feature of structure T is the ratio of small/large cages in the unit structure is much smaller than any of the known hydrate structures. Therefore, in the absence of small guests, this structure is most efficient at minimizing vacant void space.

The complex hydrate structure, 1.67 choline hydroxide-tetra-*n*-propylammonium fluoride 30.33 H_2O (space group = R-3, $a = 12.533$, $c = 90.525 \text{ \AA}$) was discovered by Udachin and Ripmeester (1999b). It should be noted that the tetra-*n*-propylammonium salt will not form a hydrate on its own (Dyadin et al., 1988), even though other tetra-alkylammonium salts will form a variety of hydrate structures. Similar to structures II, H, and IV, this complex structure consists of stacked sequences of layers, CABBCAABCCABCABCAB. That is,

alternating layers of structure H and structure II pack together to form this structure. Choline is located in both the large cavities ($5^{12}6^8$ and $5^{12}6^4$) present in the lattice. However, as the choline molecule is too large to fully fit inside the $5^{12}6^4$ cavity, the guest hydroxyl displaces one of the water molecules in the host lattice and forms hydrogen bonds with the framework.

Udachin and Ripmeester (2005) proposed that several hypothetical structures can be formed by stacking layers of cubic structure II and structure H. Simulated x-ray powder diffraction patterns were calculated for these proposed structures, and atomic positions were also determined from these simulated x-ray patterns. For example, a closed cage version of the above complex structure was proposed. In this idealized structure, the guests do not hydrogen bond to the water cavities, and the 5^{12} and $4^35^66^3$ cavities are complete (space group = R $\bar{3}$ m, $a = 5.533$, $c = 90.525$ Å). Also, a hypothetical hexagonal P6m2 structure ($a = 12.16$, $c = 29.77$ Å) can be obtained from two layers of cubic structure II and one layer of structure H. Udachin and Ripmeester suggest this structure (consisting of 5^{12} , $4^35^66^3$, $5^{12}6^4$, and $5^{12}6^8$ cavities) may exist in nature and could accommodate guests such as methane, hydrogen sulfide, propane, butane, and isopentane. The simulated x-ray diffraction pattern for this structure can be indexed as a macroscopic mixture of phases of structure II and H, which the authors warn could result in misinterpretations of diffraction data. Also proposed were structures consisting of intergrowths of structure II, and the new closed cage complex structures, since all of these structures are based on stacking layers of 5^{12} cavities. The occurrence of these new structures would depend on their stability compared to the stability of the simpler hydrate structures.

Other unusual hydrate structures are formed by tetra-*n*-alkylammonium salts. The hydrates of these salts were first identified by Fowler et al. (1940), then later examined using x-ray diffraction by McMullan and Jeffrey (1959) and Dyadin et al. (1988). The tetra-*n*-butylammonium bromide (TBAB) hydrate is a semiclathrate, in which part of the hydrate cage is broken to accommodate the large TBAB molecule. The hydration number in TBAB hydrate ($C_4H_9)_4N^+Br^- \cdot nH_2O$ has been reported to vary from $n = 2.03$ to $n = 36$, which results in a range of crystal cell structures (Lipkowski et al., 2002; Shimada et al., 2005). For example, the hydrate crystal structure consists of a trigonal cell (space group R3c) for $n = 2.03$, or an orthorhombic cell (space group Pmma) for $n = 32$. Other studies have shown that small molecules (such as H_2S , H_2) can be encaged inside the 5^{12} dodecahedral cavities of TBAB hydrate (Oyama et al., 2003; Strobel et al., 2006a).

As this text is primarily concerned with natural gas hydrates, no further discussion will be given to Jeffrey's structures III–VII and the other unusual structures described above, since as stated previously these structures have yet to be found for natural gas components.

2.1.2.2.5 High pressure gas hydrate phases

At very high pressures (in the GPa range), gas hydrates can undergo structural transitions to hydrate phases and filled ice structures. Figure 2.11 illustrates the structural changes that have been reported for gas hydrates at very high pressures at

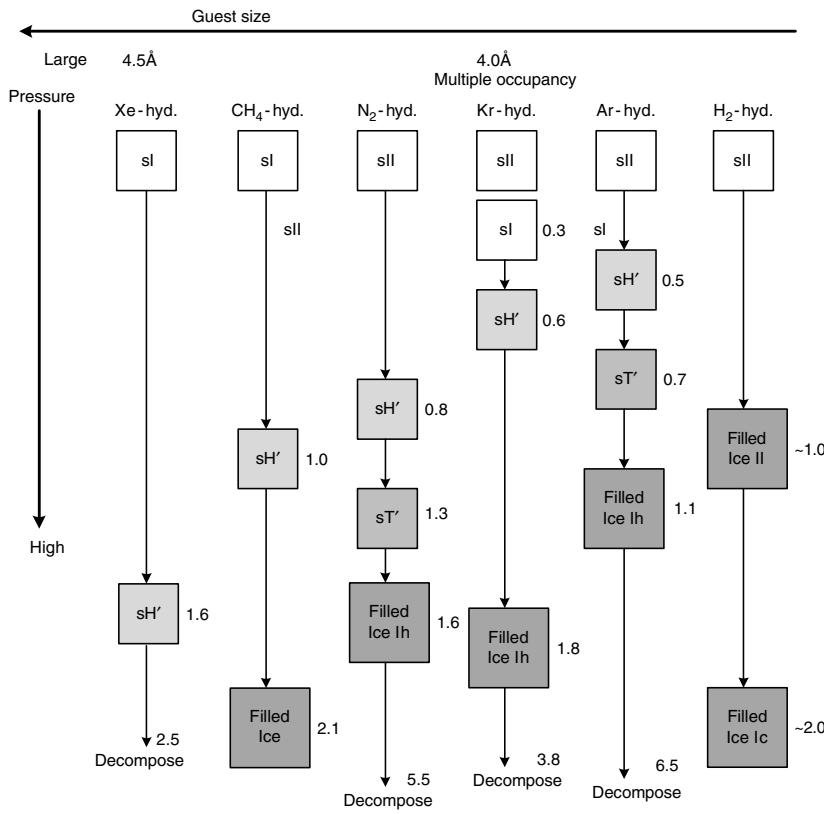


FIGURE 2.11 Very high pressure (0.3–2.1 GPa) structural changes of gas hydrates at room temperature. Numerical values (adjacent to square boxes) indicate transition pressures. Hexagonal (sH') and tetragonal (sT') hydrate phases are distinct from sH and sT hydrate structures found at normal pressures. (Modified and redrawn from Hirai, H., Tanaka, H., Kawamura, K., Yamamoto, Y., Yagi, T., *J. Phys. Chem. Solids*, **65**, 1555 (2004). With permission from Elsevier.)

room temperature (Hirai et al., 2004). The horizontal axis shows the guest size and the vertical axis indicates the pressure. The numerical values indicate the structural transition pressures in GPa. The hexagonal sH' and tetragonal sT' structures indicated in Figure 2.11 are distinct from sH and sT hydrate structures described in Sections 2.1.2.2.3 and 2.1.2.2.4, respectively.

As shown in Figure 2.11, hydrogen sII hydrate (stable at around 220 MPa at 249 K) transforms to a filled ice II structure as the pressure increases to around 1 GPa. On increasing the pressure further to around 2 GPa a filled cubic ice Ic structure forms (Vos et al., 1993). For argon, sII is the initial structure stable at normal pressures (<30 MPa). Increasing the pressure to about 0.5 GPa, a hexagonal hydrate phase is formed. Increasing the pressure further to around 0.7 GPa, a tetragonal hydrate structure is formed, and at even higher pressures,

a filled ice Ih structure is formed (Kurnosov et al., 2001; Hirai et al., 2002; Loveday et al., 2003).

Krypton forms sII hydrate at normal pressures and then transforms to sI hydrate at 0.3 GPa, to a hexagonal hydrate phase at 0.6 GPa, and then to a filled ice Ih structure at 1.8 GPa (Desgreniers et al., 2003). Nitrogen forms sII initially and then transforms to a hexagonal hydrate phase at 0.8 GPa, to a tetragonal hydrate structure at around 1.3 GPa, and finally to a filled ice Ih structure at 1.6 GPa (Loveday et al., 2003a; Sasaki et al., 2003). Methane sI hydrate transforms to a dense hexagonal hydrate phase at around 1.0 GPa, and then at 2.1 GPa to a filled-ice orthorhombic structure that has a H-bond network closely related to ice Ih (Hirai et al., 2001; Loveday et al., 2001a,b). Xenon sI hydrate transforms to a dense hexagonal hydrate phase at 1.6 GPa, and then with further increases in pressure decomposes without forming a filled ice structure (Desgreniers et al., 2003; Loveday et al., 2003).

At normal pressures, typically only one guest molecule is accommodated within each clathrate hydrate cage. However, diffraction measurements and computer calculations demonstrate that at very high pressures, clathrate hydrate structures can consist of water cages containing more than one guest molecule. Specifically, neutron diffraction measurements show that double occupancy of the large cage of sII hydrate can occur for both nitrogen hydrate and oxygen hydrate at higher pressures (Chazallon and Kuhs, 2002). Similar conclusions have been derived from molecular dynamics computer calculations (van Klaveren et al., 2001). Multiple occupancy has also been suggested for argon hydrate (Itoh et al., 2001).

Manakov et al. (2002) were able to fit their x-ray data with structure H hydrate by placing five argon molecules in the large cavities. Similarly, Loveday et al. (2003) were able to reconcile their diffraction data with a structure H hydrate structure containing five methane molecules in the large cavities and five methane molecules in two small cavities, giving a dense hydrate structure with a 3.5:1 methane/water ratio. However, Loveday et al. (2003) suggest that despite obtaining a good fit with structure H hydrate, to dispel “residual doubt” of the structure, confirmation from single crystal diffraction data is needed. Multiple cage occupancy has also been proposed in sI, sII, and sH argon hydrates from first principle and lattice dynamics calculations (Inerbaev et al., 2004).

In the case of pure hydrogen hydrate, sII hydrate is formed with multiple occupancy of the water cages. Initially, Mao et al. (2002, 2004,) suggested that pure hydrogen hydrate consists of double and quadruple occupancy of hydrogen molecules in the small and large cages of sII hydrate, respectively. However, more recently Lokshin et al. (2004) in collaboration with the Mao group reported that D₂ molecules only singly occupy the small cages of D₂ hydrate. The large cage occupancy was found to reversibly vary from two to four D₂ molecules per 5¹²6⁴ cage over the temperature range of around 200 to 40 K (Lokshin et al., 2004; Lokshin, 2005b). Confirmation that H₂ can form a clathrate hydrate is especially noteworthy since it was previously assumed that small molecules such as H₂ and He are too small to stabilize a clathrate hydrate structure.

The pure H₂ hydrate structure is typically formed at very high pressures. However, the addition of a promoter molecule, for example, tetrahydrofuran (THF), to form a binary H₂/THF hydrate will stabilize H₂ within the sII framework (with THF occupying all large cavities) at pressures two orders of magnitude lower than that in pure hydrogen hydrates (Florusse et al., 2004). H₂ singly occupies the small cage of sII H₂/THF hydrate (Hester et al., 2006; Strobel et al., 2006b).

2.1.3 Characteristics of Guest Molecules

A second classification of hydrates is obtained through consideration of the guest molecules. Such a classification is a function of two factors: (1) the chemical nature of the guest molecule and (2) the size and shape (particularly in sH) of the guest. The size of the guest molecule is directly related to the hydration number and, in most cases, to its nonstoichiometric value.

2.1.3.1 Chemical nature of guest molecules

Two classifications of the chemical nature of the guest molecule have been proposed. The first scheme by von Stackelberg (1956) was a combination of both size and chemical nature as discussed in Section 1.2.3. The second scheme by Jeffrey and McMullan (1967) characterized the guest molecules in one of the following four groups: (1) hydrophobic compounds, (2) water-soluble acid gases, (3) water-soluble polar compounds, and (4) water-soluble ternary or quaternary alkylammonium salts.

Jeffrey (1984) clearly summarized chemical nature-based classification schemes by stating that the guest molecule must not contain either a single strong hydrogen-bond group or a number of moderately strong hydrogen-bonding groups. The molecules of natural gas components are not involved in hydrogen bonding, and so their chemical nature is not a delimiter. Most of the natural gas molecules that form hydrates are hydrophobic, with the notable exceptions of hydrogen sulfide and carbon dioxide, so that natural gas guests fall within the first two categories of Jeffrey and McMullan (1967).

In the third category, experimentalists have capitalized on the complete aqueous miscibility of the cyclic ethers, such as ethylene oxide (EO) for structure I and tetrahydrofuran(THF) for structure II, to provide easy access to hydrate crystal structures. With complete miscibility, an aqueous solution of EO or THF may be made at the hydrate composition of 24 wt% and 19 wt%, respectively (i.e., corresponding to stoichiometric amounts of water/EO = 7.7:1 and water/THF = 17:1, where EO and THF are assumed to occupy all the large cages of sI and sII, respectively; although EO will occupy some of the small cages (Huo, 2002)). Cyclic ether hydrates may thus be formed at atmospheric pressure (by cooling below 284.2 K [EO sI] or 277.5 K [THF sII]) without concern for mass transfer effects. However, the oxygen atoms that cause cyclic ethers to be miscible also promote a disproportionate number of Bjerrum defects in the hydrate (Davidson and Ripmeester, 1984) relative to natural gas guests.

Restrictions on Guest Motions. The physicochemical nature of the guest molecule, once enclathrated, has been studied in some detail. Dielectric constant and NMR techniques have been successfully applied by Davidson (1971) and Davidson and Ripmeester (1984). The translational degree of freedom of the guest is limited.

X-ray and neutron diffraction measurements indicate that the size of the guest and type of cage it occupies influences the guest position within a hydrate cage. Single crystal x-ray diffraction studies have shown that the center of ethane is 0.17 Å from the center of the large cage of structure I (Udachin et al., 2002). Likewise, propane occupies an off-center position in the large cage of structure II (Kirchner et al., 2004). For structure II benzene + xenon hydrate, xenon is located at the center of the small cage, while benzene is 0.27 Å from the center of the large cavity. For sH methylcyclohexane + methane hydrate, the carbon of methane is located at the center of both the 5^{12} and $4^35^66^3$ small cages, with methylcyclohexane in the favored chair conformation in the $5^{12}6^8$ cage (Udachin et al., 2002).

Davidson (1971) determined that the most important rotation inhibition interactions between guest molecules (in adjacent cages) were the dipole–dipole interactions, but even they were of minor importance. Within a single cage, both nonpolar and polar guest molecules such as EO, THF, and acetone have only small barriers to rotational freedom, which approximates that in the vapor phase. The rotational freedom is probably due to the fact that the sum of the cage water dipoles effectively cancel near the center of each cage, and even the quadrupolar fields are relatively small.

2.1.3.2 Geometry of the guest molecules

In a review of the motions of guest molecules in hydrates, Davidson (1971) indicated that all molecules between the sizes of argon (3.8 Å) and cyclobutanone (6.5 Å) can form sI and sII hydrates, if the above restrictions of chemical nature are obeyed. Ripmeester and coworkers note that the largest simple structure II former is tetrahydropyran (THP) ($C_5H_{10}O$) with a van der Waals diameter of 6.95 Å (Udachin et al., 2002). Closely following THP are *m*- and *p*-dioxane and carbon tetrachloride, each with a molecular diameter of 6.8 Å (Udachin et al., 2002). Molecules of size between around 7.1 and 9 Å can occupy sH, provided that the below shape restrictions are obeyed and a help gas molecule such as methane is included.

According to the work by von Stackelberg and Jahns (1954), the structure I and II water lattice parameters showed no significant distortion by any guest. However, Udachin et al. (2002) have shown from single crystal x-ray diffraction that there is a general trend of lattice size with guest size (although this trend is not completely regular). For example, trimethylene oxide, chloroform, THP, and benzene (with Xe as the second guest), which have increasing van der Waals diameters of 6.01, 6.50, 6.95, and 7.07 Å, exhibit increasing lattice parameters of 17.182, 17.236, 17.316, and 17.363 Å, respectively, at 263 K. As detailed in Chapter 5, Holder et al. (1994) and Zele et al. (1999) show that lattice stretches of

this order of magnitude can have a significant effect on thermodynamic parameters. Similar systematic studies on sH await single crystal diffraction measurements.

Increases in lattice parameter with guest size, and hence increasing unit cell volume, may have a significant effect on the free energy change (Tse, 1987). In addition, small changes in lattice parameter have been predicted to cause significant changes to the hydrate formation pressure (Kini et al., 2002). For example, a change of only 0.5% in lattice size may cause a change in predicted pressure of up to 15%, and even a 0.1% change in lattice size can change the predicted pressure by about 2%. The program CSMGem, included in the CD accompanying this book, has corrected the older theory of van der Waals and Platteeuw (1959).

The lattice parameter, and hence the average cavity diameter, is a function of temperature, pressure, and guest composition. The dependence of lattice parameter on guest composition and temperature is illustrated in [Figures 2.12a](#) (sI), b (sII).

Ratios of Guest Molecules to Host Cavities. To determine the size upper limit of each cavity available for a guest, Davidson suggested subtracting the van der Waals radius of the water molecule from the “average cage radius” values given in [Table 2.1](#). To determine the upper and lower limits to guest size, it is instructive to consider the diameter ratios of the guest molecule to each cavity for simple (single guest) hydrate formers.

[Table 2.4](#) presents the diameter ratios of natural gas components (and a few other compounds) relative to the diameter of each cavity in both structures. Also presented are two unusual molecules, cyclopropane and trimethylene oxide, which can form simple hydrates of either structure sI or sII; hydrates of these molecules are discussed in Section 2.1.3.3, in the subsection on structural changes in simple hydrates.

In Table 2.4 size ratios of guest diameter/cavity diameter denoted with the superscript “ ζ ” are those occupied by the simple hydrate formers. For example, in methane hydrate, methane occupies both the small and large cages of structure I. In propane hydrate, propane occupies only the large cages of structure II. The values in Table 2.4 demonstrate a size ratio lower bound of about 0.76, below which the molecular attractive forces contribute less to cavity stability. Above the upper bound ratio of about 1.0, the guest molecule cannot fit into a cavity without distortion. Simple hydrate species capable of occupying the 5^{12} cavity of either structure will also enter the large cavity of that structure.

For simple hydrate-forming components of natural gas, nitrogen was determined (Davidson et al., 1986a) to stabilize the 5^{12} cavities of structure II with a size ratio of 0.82 and it also occupies all the large $5^{12}6^4$ cavities. Nitrogen, being the smallest natural gas hydrate former, provides insignificant stability to the large cavity in either structure ($5^{12}6^2$ or $5^{12}6^4$), so nitrogen forms sII with a fractionally higher number of small cavities occupied in the unit cell. In Table 2.4, the size ratio of nitrogen in the 5^{12} cavity of structure II is 0.82; whereas the $5^{12}6^4$ cavity shows a size ratio of 0.62, which is less than the lower bound value of 0.76, hence indicating less significant cavity stability. Since nitrogen is so small, two molecules can occupy the $5^{12}6^4$ cavity at high pressures, as discussed in Section 2.1.2.2.5.

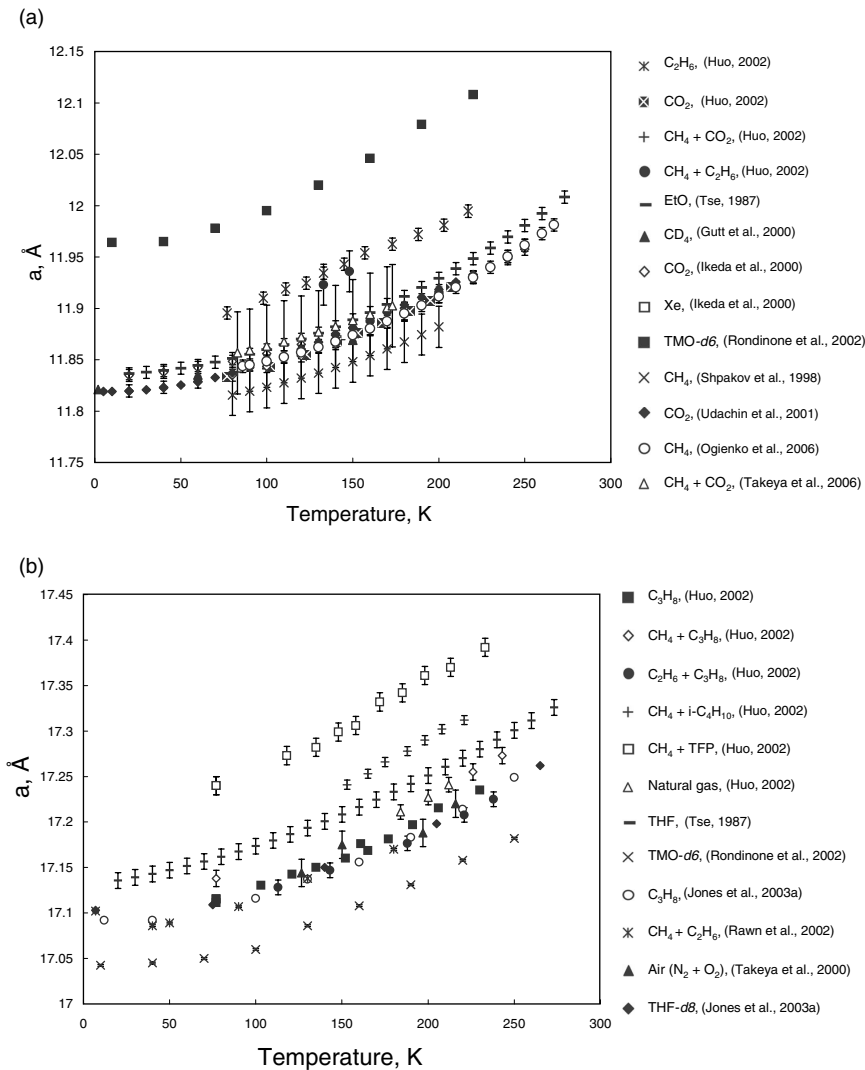


FIGURE 2.12 Lattice parameter vs. temperature plots for sI (a) and sII (b) hydrates.

As simple hydrates, methane, and hydrogen sulfide can stabilize the 5^{12} cavities of structure I (size ratios of 0.86 and 0.90, respectively) and they can occupy all the large $5^{12}6^2$ cavities of sI (size ratios of 0.74 and 0.78, respectively). Ethane occupies the $5^{12}6^2$ cavities of structure I with a ratio of 0.94. Propane and iso-butane each occupy the $5^{12}6^4$ cavities of structure II with a size ratio of 0.94 and 0.98, respectively.

n-Butane does not form a simple hydrate; the ratio of n-butane to the largest cavity of sII is almost 7% larger than the $5^{12}6^4$ free cavity diameter. However,

TABLE 2.4
Ratio of Molecular Diameters^b to Cavity Diameters^c for Natural Gas Hydrate Formers and a Few Others

Guest hydrate former		Molecular diameter/cavity diameter for cavity type			
Molecule	Diameter ^b (Å)	Structure I		Structure II	
		5 ¹²	5 ¹² 6 ²	5 ¹²	5 ¹² 6 ⁴
He	2.28	0.447	0.389	0.454 ^{ζφ}	0.342 ^{ζφ}
H ₂	2.72	0.533	0.464	0.542 ^{ζφ}	0.408 ^{ζφ}
Ne	2.97	0.582	0.507	0.592 ^{ζφ}	0.446 ^{ζφ}
Ar	3.8	0.745	0.648	0.757 ^ζ	0.571 ^ζ
Kr	4.0	0.784	0.683	0.797 ^ζ	0.601 ^ζ
N ₂	4.1	0.804	0.700	0.817 ^ζ	0.616 ^ζ
O ₂	4.2	0.824	0.717	0.837 ^ζ	0.631 ^ζ
CH ₄	4.36	0.855 ^ζ	0.744 ^ζ	0.868	0.655
Xe	4.58	0.898 ^ζ	0.782 ^ζ	0.912	0.687
H ₂ S	4.58	0.898 ^ζ	0.782 ^ζ	0.912	0.687
CO ₂	5.12	1.00 ^ζ	0.834 ^ζ	1.02	0.769
C ₂ H ₆ ^a	5.5	1.08	0.939 ^ζ	1.10	0.826
c-C ₃ H ₆	5.8	1.14	0.990	1.16	0.871 ^ζ
Trimethylene oxide, (CH ₂) ₃ O ^a	6.1	1.20	1.04 ^ζ	1.22	0.916 ^ζ
C ₃ H ₈	6.28	1.23	1.07	1.25	0.943 ^ζ
i-C ₄ H ₁₀	6.5	1.27	1.11	1.29	0.976 ^ζ
n-C ₄ H ₁₀	7.1	1.39	1.21	1.41	1.07

^ζ Indicates the cavity occupied by the simple hydrate former.

^φ Indicates that the simple hydrate is only formed at very high pressure.

^a The structure has been confirmed by single crystal x-ray analysis (Udachin et al., 2002).

^b Molecular diameters obtained from von Stackelberg and Muller (1954), Davidson (1973), Davidson et al. (1984a, 1986a), or Hafemann and Miller (1969).

^c The cavity diameter is obtained from the cavity radius from Table 2.1 minus the diameter of water (2.8 Å).

a hydrate of sII can be formed from n-butane with the help of gases in the small cages, such as methane (Wu et al., 1976), hydrogen sulfide (Davidson et al., 1977a), or xenon (Ripmeester and Ratcliffe, 1990a; Udachin et al., 2002).

Of the natural gas components that form simple hydrates, nitrogen, propane, and iso-butane are known to form structure II. Methane, ethane, carbon dioxide, and hydrogen sulfide all form sI as simple hydrates. Yet, because the larger molecules of propane and iso-butane only fit into the large cavity of structure II, natural gas mixtures containing propane and iso-butane usually form structure II hydrate (see Section 2.1.3.3 in the subsection on structural changes in binary hydrate structure).

In [Table 2.4](#) it is interesting to note that the simple hydrate of methane always occupies the small cavity of structure I (5^{12} diameter ratio is 0.86) while the diameter ratio of methane to the 5^{12} cavity of structure II is 0.87—apparently a very small difference. Ripmeester (1988) suggested that for such small, simple hydrate formers the transition from structure II to structure I is brought about by the additional stability gained by the guest occupying the $5^{12}6^2$ cavity. Yet for smaller molecules, such as nitrogen, sII forms because it has almost three times the number of 5^{12} cages per unit volume ($0.0033/\text{\AA}^3$ in sII vs. $0.0012/\text{\AA}^3$ in sI) that stabilize sII.

Table 2.4 indicates the structures that have been confirmed by single crystal x-ray analysis by Udachin et al. (2002). In this work, Udachin et al. were able to obtain high-quality single crystals on these compounds and therefore obtained the absolute cage occupancies. For ethane sI hydrate, the large cages are filled with a very low fraction (0.058) of the small cages occupied.

[Tables 2.5a,b](#) provide a comprehensive list of guest molecules forming simple sI and sII clathrate hydrates. The type of structure formed and the measured lattice parameter, a , obtained from x-ray or neutron diffraction are listed. Unless indicated by a reference number, the cell dimension is the 0°C value given by von Stackelberg and Jahns (1954). Where no x-ray data exists, assignment of structure I or II is based on composition studies and/or the size of the guest molecule. Tables 2.5a,b also indicate the year the hydrate former was first reported, the temperature ($^\circ\text{C}$) for the stable hydrate structure at 1 atm, and the temperatures ($^\circ\text{C}$) and pressures (atm) of the invariant points (Q_1 and Q_2). Both cyclopropane and trimethylene oxide can form sI or sII hydrates. Much of the contents of these tables have been extracted from the excellent review article by Davidson (1973), with updated information from more recent sources (as indicated in the tables).

A principal theme of this text is the direct relation of macroscopic properties to molecular structure. In concluding the discussion on the sI and sII cavity size ratios, two examples are given of how macroscopic engineering properties (equilibrium pressure and temperature, and heat of dissociation) are determined by the size ratios in [Table 2.4](#).

Example 2.1: Molecular Size Determines Structure and Equilibrium Pressure

When the restriction of a simple hydrate is removed, the addition of a small amount of a second, larger hydrocarbon sometimes has a dramatic effect on the hydrate formation pressure. Consider the hydrate formation pressure effect of adding a small amount of propane (C_3H_8) to methane (CH_4), and how such effects may be interpreted in terms of molecular structure.

In [Chapter 6](#), the data of Deaton and Frost (1946) indicate that at 280.4 K , hydrates form from liquid water with pure CH_4 at 5.35 MPa , yet hydrates are formed at 3.12 MPa with $99\%\text{ CH}_4 + 1\%\text{ C}_3\text{H}_8$. One might wonder

TABLE 2.5a
List of Simple sI and sII Hydrate Formers, and the Hydrate Structure and Properties

Guest molecule	Structure, a value (°C)	Year first reported	T (°C); P (atm) at Q ₁	T (°C); P (atm) at Q ₂	T (°C), P = 1 atm
Ar	II**, 17.07(173°)	1896	-0.8; 87	No Q ₂	-124
Kr	II**, 17.08(173°)	1923	-0.1; 14.3	No Q ₂	-49.8
Xe	I, 12.0	1925	0; 1.5	No Q ₂	-10.4
H ₂	II	1999			
N ₂	II*	1960	-1.3; 141.5	No Q ₂	—
O ₂	II*	1960	-1.0; 109.2	No Q ₂	—
Cl ₂	I, 11.82 ^b (0°)	1811	-0.22; 0.316	28.3; 8.4	9.7
BrCl	I, 12.07	1828	0; 0.165	25, 2.5	18
CO ₂	I, 12.07	1882	0; 12.4	9.9, 44.4	-55
N ₂ O	I, 12.03	1888	0; 9.7	12, 41	—
H ₂ S	I, 12.02	1840	-0.4; 0.918	29.5; 22.1	0.4
H ₂ Se	I, 12.06	1882	0; 0.455	30, 11	8
SO ₂	I, 11.97	1829	-2.6; 0.274	12.1; 2.33	6.8
COS	I, 12.14	1954	—	—	—
CH ₄	I, 11.981 ^c	1888	-0.2; 25.3	No Q ₂	-78.7
C ₂ H ₂	I, 12.00 ^d (-156°)	1878	0; 5.75	15; 33	-40.2
C ₂ H ₄	I	1888	-0.1; 5.44	No Q ₂	-36.9
C ₂ H ₆	I	1888	-0.03; 5.23	14.7; 33.5	-32
Propylene	II	1952	-0.134; 4.60	0.958; 5.93	—
Cyclopropane	I, 12.14	1960		16.21; 5.59	2.8
	II	1969	-0.05; 0.619		
C ₃ H ₈	II, 17.40	1890	0; 1.74	5.7; 5.45	-11.6
iso-butane	II, 17.57	1954	0.00; 1.12	1.88; 1.653	-2.8
Cyclopentene	II	1950	—	3.2	—
Cyclopentane	II	1950	—	7.7	—
CH ₃ F	I	1890	0; 2.1	18.8; 32	—
CH ₂ F ₂	I	1890	—	17.6	—
CHF ₃	I, 12.05	1890	—	21.8	—
CF ₄	I	1969	0; 41.5	—	—
C ₂ H ₃ F	I, 12.11	1954	—	—	—
C ₂ H ₅ F	I	1890	0; 0.7	22.8; 8	3.7
CH ₃ CHF ₂	I, 12.12	1954	0; 0.54	14.9; 4.30	4.3
(CH ₃) ₃ CF	II	1969	—	—	—

* O₂ (Tse et al., 1986) and N₂ (Davidson et al., 1984b) form sII hydrate.

**Ar, Kr (Davidson et al., 1984a) form sII hydrate.

Lattice parameter values determined by ^a(Davidson et al., 1984a), ^b(Pauliing and Marsh, 1952),

^c(Ogienko et al., 2006), ^d(Hou, 2002).

Note: Unless indicated, extracted from Davidson (1973, Table I). Guests requiring an additional small molecule to stabilize the hydrate structure are not included in this table.

TABLE 2.5b
(Continued)

Guest molecule	Structure, a value (°C)	Year 1 st reported	T (°C); P (atm) at Q ₁	T (°C); P (atm) at Q ₂	T (°C), P = 1 atm
CH ₃ Cl	I, 12.00	1856	0; 0.41	20.5; 4.9	7.5
CH ₂ Cl ₂	II, 17.33	1897	0; 0.153	1.7; 0.211	—
CHCl ₃	II, 17.236 ^e	1885	-0.09; 0.065	1.7; 0.090	—
C ₂ H ₃ Cl	II	1897	—	1.15; 1.80	—
C ₂ H ₅ Cl	II, 17.30	1890	0; 0.265	4.8; 0.77	—
CH ₃ CHCl ₂	II	1897	0; 0.072	1.5; 0.092	—
CH ₂ ClF	I	1960	-0.2; 0.222	17.88; 2.825	9.83
CHClF ₂	I, 11.97 (2°)	1947	-0.2; 0.84	16.3; 7.6	0.9
CHCl ₂ F	II	1954	-0.13; 0.145	8.61; 0.998	—
CCl ₂ F ₂	II, 17.37; 17.13 (2°)	1947	-0.1; 0.36	12.1; 4.27	5.2
CCl ₃ F	II, 17.29	1947	-0.1; 0.080	8.5; 0.65	—
CH ₃ CClF ₂	II, 17.29	1954	-0.04; 0.136	13.09; 2.294	9.1
CH ₃ Br	I, 12.09	1856	-0.24; 0.238	14.73; 1.51	11.3
C ₂ H ₅ Br	II	1948	0; 0.2	1.4; 0.22	—
CH ₃ I	II, 17.14	1880	0; 0.097	4.3; 0.23	—
CBrF ₃	II	1961	-0.1; 0.88	11	0.5
CBr ₂ F ₂	II	1960	—	4.9; 0.501	—
CBrClF ₂	II	1960	0.00; 0.189	9.96; 1.673	7.6
CH ₃ SH	I, 12.12	1887	0.00; 0.31	12.0; 1.25	10
Ethylene oxide	I, 12.1 (-10°) 12.03 (-25°)	1863	-2.1	11.1	—
Dimethyl ether	II, 17.47	1954	—	—	—
Propylene oxide	II, 17.124 (-138°)	1952	-4.7	-3.5	—
Trimethylene oxide	II, 17.095 (-138°); I, 12.11 ^f (-52°)	1966	—	-13.1 -20.8	—
1,3-Dioxolane	II, 17.118 (-138°) 17.157 ^a	1966	—	-3	—
Furan	II, 17.3 (-10°)	1950	—	4.6	—
2,5-Dihydrofuran	II, 17.166 (-138°)	1966	-3.3	-1.2	—
Tetrahydrofuran	II, 17.18 (-10°) 17.170 (-138°) 17.194 ^e	1950 1995 ^g	-1 -0.8	4.4 -19.8	4.4
Tetrahydropyran	II, 17.316 ^e (-100°)	1995 ^g	-0.8	—	—
Acetone	II, 17.16 (-38°) 17.181 ^a	1961	—	—	—
Cyclobutanone	II, 17.161 (-138°)	1966	—	0	—

^e Values determined by Udachin et al. (2002), ^f (Rawn et al., 2002), ^g (Dyadin et al., 1995)

Note: Unless indicated extracted from Davidson (1973, Table I). Guests requiring an additional small molecule to stabilize the hydrate structure are not included in this table.

how the addition of only 1% C₃H₈ caused a decrease in pressure by 42%. In Section 5.2, [Figure 5.15](#) (at 277.6 K) shows that such a precipitous pressure decrease is caused by a hydrate crystal change from sI (with 100% CH₄) to sII (with 99% CH₄ + 1% C₃H₈). With a crystal structure change, it seems reasonable that a significantly different thermodynamic state (three-phase temperature and pressure) is required for stability.

We can interpret the 42% decrease in equilibrium pressure, caused by a 1% change in composition, in terms of cavity size ratios shown in [Table 2.4](#). Propane only fits into the 5¹²6⁴ cavity of structure II, C₃H₈ is too large to occupy any other cavity. For CH₄, diameter ratios in the 5¹² cavities of sI (0.86) and sII (0.87) differ by 1.5%.

Pure methane is stabilized in sI only by the additional stability of the molecule in the 5¹²6² cavity. With only a small amount of propane to encourage the stability of sII, the similar size ratios of methane in the 5¹² cavities and large degree of stability propane provides (0.94) to the sII large cage enable a structure transition.

In summary, the concept of guest to cavity size ratios (and hydrate structure change) can provide molecular comprehension of a substantial decrease in equilibrium pressure required for a small composition change. The sII stability by small amounts of propane results in the fact that most natural gases form sII, because most reservoirs contain small amounts of propane.

The second example of microscopic structure reflected in macroscopic properties is almost as important as determining phase equilibria conditions. After establishing that hydrates will form (or dissociate) at certain pressure and temperature conditions, engineers are often interested in the amount of energy required for the phase transition.

Example 2.2: Cavity Size Ratios Determine Heat of Dissociation

In Section 4.6.1 enthalpy evidence for structures I, II, and H is presented to suggest that guest size determines the approximate heat of dissociation by determining the cavity occupied.

The heat of dissociation (ΔH_d) is defined as the enthalpy change to dissociate the hydrate phase to a vapor and aqueous liquid, with values given at temperatures just above the ice point. To a fair engineering approximation ΔH_d is

1. a function not only of the hydrogen bonds in the crystal but also of cavity occupation, and
2. independent of guest components and mixtures of similar size components within a limited size range.

As one illustration, simple hydrates of C_3H_8 and i- C_4H_{10} have similar ΔH_d of 129 and 133 kJ/mol (Handa, 1986) because they both occupy the $5^{12}6^4$ cavity, although their size/cavity ratios are somewhat different (0.94 and 0.98). This similarity of ΔH_d is remarkable, but it is due principally to the occupation of the $5^{12}6^4$ cavity.

Similar statements could be made about the ΔH_d values for other simple hydrate formers that occupy similar size cavities, such as C_2H_6 ($\Delta H_d = 72$ kJ/mol; Handa, 1986) and CO_2 ($\Delta H_d = 73$ kJ/mol; Long, 1994) in the $5^{12}6^2$ cavity, or CH_4 and H_2S (ΔH_d within 3% of each other; Long, 1994) that occupy both 5^{12} and $5^{12}6^2$ as simple hydrates.

As a second illustration, mixtures of $\text{C}_3\text{H}_8 + \text{CH}_4$ have a value of $\Delta H_d = 79$ kJ/mol over a wide range of composition. In such mixtures, C_3H_8 occupies most of the $5^{12}6^4$ cavities while CH_4 occupies only a small number of $5^{12}6^4$ and many 5^{12} . As shown in Section 4.6, most natural gases (which form structure II) have similar values of ΔH_d . Note that mixtures that fill both sII cavities have a lower value of ΔH_d (79 kJ/mol) than components such as C_3H_8 that fill only the $5^{12}6^4$ cavity ($\Delta H_d = 129$ kJ/mol).

Similarly, over a wide range of composition for methane and ethane, ΔH_d values are similar (74 kJ/mol) for components entering both cavities of sI. Identical arguments may be used to explain similar ΔH_d values of 79.5 ± 7 kJ/mol (Mehta and Sloan, 1996) for sH binary mixtures with methane, since all three cavities are occupied.

The second illustration indicates that less energy is required to dissociate structures with both cavities filled, than those with one cavity filled. Tse (1994) suggests that collisions of a guest with the cavity wall weakens interactions between the hydrogen bonds, which is also reflected in a high value of thermal expansion.

Table 2.6 lists the help guests for sII hydrate and includes the works of Ripmeester and Ratcliffe (1990b), Udachin et al. (2002), and Davidson (1973, table VII) of stabilizing effects of help guests. The stabilizing effect of a second encageable component is particularly evident for structure II hydrates, in which the help gas may occupy the otherwise empty cages. In all the cases listed, the large molecule does not form a hydrate on its own and requires a help guest to stabilize the structure. For example, benzene and cyclohexane will not form a hydrate on their own, but are stabilized in structure II hydrate with Xe as the help gas (Ripmeester and Ratcliffe, 1990a). Similarly, cyclohexanone will not form a hydrate on its own, but in the presence of a help gas, such as hydrogen, will form sII hydrate (Strobel et al., 2007).

Pressure reductions have been observed for methane hydrate formation when organic components (that are very insoluble in water) are added to the water + methane system. These organic components include THP, cyclobutanone, methylcyclohexane, CHF_3 , and CF_4 (Mooijer-van den Heuvel et al., 2000;

TABLE 2.6
List of Help Guests for sII Hydrate

Hydrate former	Hydrate structure	Help gas
Cyclohexanone ^a	sII	H ₂
Benzene*	sII	Xe
Cyclohexane*	sII	Xe
Cyclohexene oxide*	sII	Xe
Isobutylene*	sII	Xe
cis-2-Butene*	sII	Xe
Allene*	sII	Xe
n-Butane*	sII	CH ₄ , H ₂ S, Xe
Norbornane*	sII	Xe
Bicycloheptadiene*	sII	Xe
Methyl formate*	sII	Xe
Acetonitrile*	sII	Xe
Neopentane*	sII	Xe
1,4-Dioxane	Assumed sII	CH ₄
1,3-Dioxane	Assumed sII	CH ₄
CCl ₄		CO ₂ , N ₂
C ₂ H ₅ I		N ₂
CS ₂		N ₂ , O ₂
CH ₂ ClCH ₂ Cl		Air

^a Confirmed from neutron diffraction data by Strobel et al. (2007).

* Hydrate structures containing hydrate former + Xe help gas have been confirmed by ¹²⁹Xe NMR spectroscopy by Ripmeester and Ratcliffe (1990a).

Hara et al., 2005). THP, cyclobutanone, and cyclohexane also showed pressure reductions for carbon dioxide hydrate formation (Mooijer-van den Heuvel et al., 2001). THP, cyclobutanone, cyclohexane, and methylcyclohexane all reduced not only the pressure for propane hydrate formation, but also shifted the H-Lw-LC₃H₈ line to lower temperature (Mooijer-van den Heuvel et al., 2002).

Tohidi et al. (2001) also suggested that the stability of simple methane and nitrogen hydrates could be increased by using sH large guest formers. They suggested that the C₆–C₁₀ fraction of real petroleum fluids are potential sH hydrate formers, though no evidence exists so far that real reservoir fluids are more likely to form structure H.

As a complement to Table 2.4, size ratios of sH formers are shown in Table 2.7. Although many large sH formers are known, only alkanes and cycloalkanes are of interest, because alkenes and alkynes do not occur in natural hydrocarbons due to their reactivity. A large number of branched alkanes, including methyl butane, all polymethyl butanes, and a number of polymethyl pentanes form sH hydrates.

TABLE 2.7

Structure H Size Ratios of Molecular Diameters^d to Cavity Diameters^e for Alkanes, Cycloalkanes with Methane, and Other Small Molecules in Both the Small Cavities

Large molecule guest diameter ^d (Å)	Cavity type	Molecular diameter/cavity diameter ^e	
		Small molecule	$5^{12}6^8$
2-Methylbutane ^a	7.98	Xe	0.91
2,2-Dimethylbutane ^a	8.02	CH ₄ , Xe	0.91
2,3-Dimethylbutane ^a	7.44	CH ₄ , N ₂ , Xe	0.85
2,2,3-Trimethylbutane ^a	7.49	CH ₄ , Xe	0.85
2,2-Dimethylpentane ^{a,c}	9.20	CH ₄ , N ₂ , Xe, Xe/H ₂ S	1.05
3,3-Dimethylpentane ^a	9.24	CH ₄ , Xe	1.05
Methylcyclopentane	7.33	CH ₄ , Xe	0.83
Ethylcyclopentane	9.15	CH ₄	1.04
Methylcyclohexane ^{a,b}	8.37	CH ₄ , N ₂ , Xe	0.95
cis-1,2-Dimethyl-cyclohexane ^a	8.38	Xe	0.95
1,1-Dimethyl-cyclohexane	8.33	Xe	0.95
Ethylcyclohexane	9.82	CH ₄	1.12
Cycloheptane	7.60	CH ₄	0.87
Cyclooctane ^a	7.83	Xe	0.89
Adamantane ^{a*}	7.36	Xe	0.84
Hexamethylmethane ^a	7.32	Xe	0.83
Cycloheptene ^a	7.51	Xe	0.85
cis-Cyclooctene ^a	7.75	Xe	0.88
Bicyclo[2.2.2]oct-2-ene ^a	7.17	Xe	0.82
2,3-Dimethyl-2-butene ^a	6.78	Xe	0.77
2,3-Dimethyl-1-butene ^a	7.87	Xe	0.90
3,3-Dimethyl-1-butene ^a	7.66	Xe	0.87
3,3-Dimethyl-1-butyne ^a	7.74	Xe	0.88
2-Adamantanone ^a	7.87	Xe	0.90
Hexachloroethane ^a	6.86	Xe	0.78
Tetramethylsilane ^a	7.32	Xe	0.83
tert-Butylmethylether ^a	7.72	Xe	0.88
Isoamyl alcohol ^a	8.96	Xe	1.02

^a Large guest occupancy in the $5^{12}6^8$ cavity of sH hydrate confirmed by ^{129}Xe NMR spectroscopy (Ripmeester and Ratcliffe, 1990a).

^b sH hydrate structure confirmed by single crystal x-ray data (Udachin et al., 2002).

^c sH confirmed by single crystal x-ray diffraction with Xe, H₂S in small cages (Udachin, 1997b).

^d Longest length of large guest molecules derived from DFT B3LYP computations using SPARTAN, coordinates exported to HyperChem, and H atom van der Waals diameter added.

^e Cavity diameter determined from cavity radii from Table 2.1 (see note d of Table 2.1) minus the molecular diameter of water (2.8 Å).

Table 2.7 contains data for natural gas help gases (methane, hydrogen sulfide, and nitrogen) for sH (Ripmeester et al., 1987, 1991; Tse, 1990; Danesh et al., 1994; Udachin et al., 1997b, 2002). These help gases occupy both small cavities. Xe is also included in the list of help gases since this has been used for structure confirmation of the sH cavity occupancy of many of the large molecules (Ripmeester and Ratcliffe, 1990a).

In Table 2.7, $5^{12}6^8$ cavity size ratios exceed unity for a few of the large guest components. Yet there is a substantial amount of data indicating that the compounds in Table 2.7 form sH hydrates, for example, isoamyl alcohol has a size ratio in the $5^{12}6^8$ cage of 1.02, yet has been confirmed by ^{129}Xe NMR to form sH hydrate. It is uncertain whether ratios exceeding unity are because of the overestimation of the sizes of the large guests or a slight underprediction of the $5^{12}6^8$ cavity, or perhaps the guest shape plays a significant role.

Shape of Guest Molecules. The shape of guest molecules plays a minor part in the hydrate structure and properties for sI and sII; however for structure H, guest shape does play a very significant role. Although spectroscopic evidence exists for the shape effect in sI and sII, most of the sH shape evidence relies upon phase equilibria of compound homologs of similar size, but slightly different shapes.

For sI and sII, Davidson et al. (1977a, 1981) performed NMR spectroscopy and dielectric relaxation measurements where applicable, in order to estimate the barriers to molecular reorientation for simple hydrates of natural gas components, except carbon dioxide. Substantial barriers to rotation should also affect such properties as hydrate heat capacity.

For structure I formers, essentially no barriers were found for methane and hydrogen sulfide, while the average barrier for ethane was 1.2 kcal/mol, indicating a rotational restriction due to its shape in the oblate 14-hedra. The average barriers for structure II formers were 0.6, 1.2, and 1.4 kcal/mol for propane, iso-butane, and n-butane (double hydrate with hydrogen sulfide), respectively (Davidson et al., 1977b). These barriers may be compared to a van der Waals interaction of 0.3 kcal/mol or a hydrogen bond of 5 kcal/mol. For example, using heat capacity measurements, White and MacLean (1985) determined that there was no barrier to rotation for hydrated THF molecules.

Due to shape restrictions, n-butane forms sII (with a small help gas) in the gauche isomer (Davidson et al., 1977b; Subramanian and Sloan, 2002)—rather than the *trans* isomer that is preferred in the gas phase. At most temperatures of interest to the natural gas processor above 100 K, sII guest molecules have only small restrictions to reorientation.

However, the “small rotation inhibition” heuristic for sI and sII may be flawed for guests at the upper size boundary of the large cavity. For guest molecules of intermediate sizes, such as cyclopropane and trimethylene oxide, small changes in size caused by thermal stimulation of rotational and vibrational energies may be sufficient to determine the occupied cavity as discussed in the following section.

For structure H, however, the shape of the large guest molecule is of considerable importance, perhaps because it is important to fill the available large cage efficiently. Ripmeester and Ratcliffe (1990a) indicate that, unlike sI and sII,

in sH size considerations are necessary but not sufficient, stating that *trans*-2-butene and the methyl butenes are of a size to fit into the $5^{12}6^8$, yet they do not form hydrates. Molecules of similar or larger sizes have been demonstrated to be sH guests. Efficient space filling of the available cage space is therefore also an important factor to establish whether a molecule will form sH hydrate. That is, the maximum van der Waals contact between the guest and cage walls is required for a large molecule to form sH hydrate. In contrast, this is not an important factor in sI or sII hydrates, where with very few exceptions all molecules of the correct size will stabilize these hydrate structures.

Recently, n-pentane and n-hexane, both previously thought not to form a hydrate, have been shown to occupy the sH lattice with CH₄ and 2,2-dimethylbutane, a known sH former (Lee et al., 2006).

The specifications for the small help gas molecules that fill the small cages of sH hydrate are less rigorous and all guests that adequately fill the small cages in sI and sII hydrate are thought to be suitable sH help gas molecules, for example, Ar, O₂, Kr, CO, Xe, CH₄, H₂S, and then to a lesser extent SO₂, CO₂, CH₃Cl, and acetylene. CH₄, Xe, H₂S, H₂ have been confirmed to be small sH help gas molecules by structural tools, such as NMR spectroscopy, x-ray, and neutron diffraction.

Molecular simulations (Rodger, 1990a,b; Tanaka and Kiyohara, 1993) and neutron scattering (Tse et al., 1993; Baumert et al., 2002) indicate that repulsions between guest and water molecules in sI and sII help stabilize the hydrate structure. A strained cage such as the $5^{12}6^8$ may require optimal filling to achieve the repulsion necessary to form easily at low pressures. Baumert and colleagues (2002) suggest that the repulsive interaction between the guest and cage could also be responsible for the effective energy transfer between the guest and host vibrations, which may cause the low glasslike thermal conductivity of the hydrates.

2.1.3.3 Filling the hydrate cages

In all three hydrate structures, at usual pressures, each cavity can contain at most one guest molecule. At very high pressures, nitrogen, hydrogen, methane, and argon can multiply occupy the large cavity of structure II. (Further discussion on high-pressure phases and multiple occupancy is given in Section 2.1.2.2.5.) [Figure 2.13](#), a revision of a figure originally by von Stackelberg (1949) presents the sizes of simple gas hydrates relative to the size of each cavity.

Five points should be made about Figure 2.13:

1. At normal pressures (i.e., less than around 30 MPa at about 260–290 K), molecules below 3.5 Å become too small to stabilize any cavity, while above 7.5 Å molecules are too large to fit into any cavity of sI or sII.
2. Some molecules can only stabilize the large cavity of sII (e.g., propane and iso-butane only stabilize the $5^{12}6^4$).
3. When a molecule stabilizes the small cavities of a structure, it will also enter the large cavities of that structure.

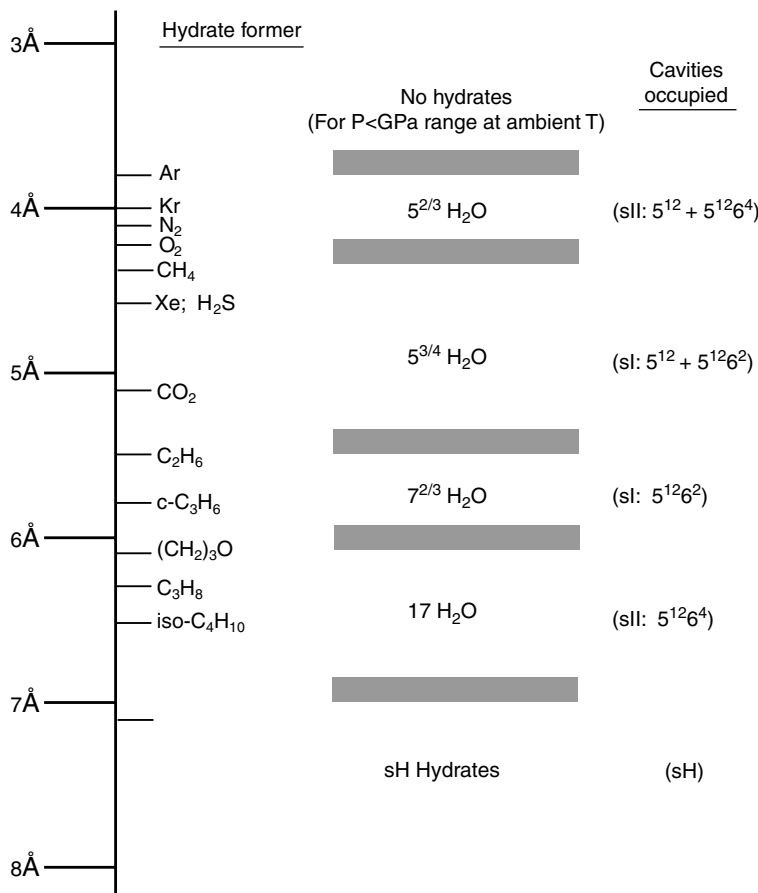


FIGURE 2.13 Comparison of guest molecule sizes and cavities occupied as simple hydrates. (Modified from von Stackelberg, M., *Naturwiss.*, **36**, 359 (1949). With permission from Springer-Verlag.)

4. Since 1983, it has been known that the smallest guests (argon, krypton, nitrogen, and oxygen) form sII rather than sI.
5. Molecules of a size within the shaded boundaries exhibit the most nonstoichiometry.

Ideal Hydration Numbers. In Figure 2.13, x-ray and neutron results by Davidson et al. (1984a, 1986a) for argon, krypton, oxygen, and nitrogen indicate that these simple hydrates not only stabilize the 16 smaller cavities of the sII unit cell but also occupy the 8 larger cavities of that structure, for an ideal guest/water ratio of $24\text{G} \cdot 136\text{H}_2\text{O}$ or $\text{G} \cdot 5 \frac{2}{3}\text{H}_2\text{O}$. If guest molecule G can only fit the $5^{12}6^4$ of structure II, the ideal ratio will be $8\text{G} \cdot 136\text{H}_2\text{O}$ or $\text{G} \cdot 17\text{H}_2\text{O}$.

The ideal guest/water ratio is $G \cdot 5\frac{3}{4}\text{H}_2\text{O}$ for molecules that can occupy both cavities of structure I, and $G \cdot 7(2/3)\text{H}_2\text{O}$ for occupants of only the $5^{12}6^2$ of structure I. As indicated in [Figure 2.13](#) molecules of transitional size (shaded region) such as cyclopropane (Majid et al., 1969) and trimethylene oxide (Hawkins and Davidson, 1966) with diameters of 5.8 and 6.1 Å, respectively, may form either structure.

Simple hydrates of sH do not form (at normal pressures), so the concept of an ideal hydrate number is only applicable to two or more guests. In the simplest case, with type X guests fully occupying the smallest two cavity types (5^{12} and $4^35^66^3$) and molecule Y occupying the $5^{12}6^8$ cavity, the ideal hydrate number is $5\text{X} \cdot 1\text{Y} \cdot 34\text{H}_2\text{O}$.

Ideal hydrate numbers validate the notion that a substantial amount of hydrocarbon is present in the hydrate. For example, if all cavities of structure II are filled, each volume of hydrate may contain 182 volumes of gas at standard temperature and pressure. This ratio shows the hydrated gas density to be equivalent to a highly compressed gas, but somewhat less than the density of a liquid hydrocarbon. The similarity of hydrates to a highly compressed gas suggests their use for storage, or as an unconventional gas resource, where they occur *in situ* in the deep oceans or permafrost.

Because it is impossible for all cavities to be occupied (an analog would be a perfect crystal) simple hydrates always have more water molecules than the ideal composition. Usually the ratios range from $G \cdot 5(3/4)\text{H}_2\text{O}$ to $G \cdot 19\text{H}_2\text{O}$, with typical fractional occupancies of the smaller cavities of 0.3–0.9, based on size restrictions. This variation causes clathrate hydrates to be called “nonstoichiometric hydrates,” to distinguish them from stoichiometric salt hydrates.

Hydrate Nonstoichiometry. The cause of the nonstoichiometric properties of hydrates has been considered. Evidence for the view that only a fraction of the cavities need to be occupied is obtained from both the experimental observations of variation in composition, and the theoretical success of the statistical thermodynamic approach of van der Waals and Platteeuw (1959) in [Chapter 5](#). Typical occupancies of large cavities are greater than 95%, while occupancy of small cavities vary widely depending on the guest composition, temperature, and pressure.

Davidson (1971) indicated that occupancy of the smaller cages is incomplete for molecules less than 5.0 Å in diameter, and that larger cages in each structure seem to be almost completely occupied. Via the use of NMR, Ripmeester and Davidson (1981) have determined that for ^{129}Xe , the occupancy of the small cages of structure I is 0.74 times that of the large cages.

Glew (1959) suggested that the most nonstoichiometric guest molecules are those for which the size of the guest approaches the upper limit of the free volume of a cavity. For two molecules that approach the size limit of cavities, Glew and Rath (1966) presented experimental evidence that hydrate nonstoichiometry for both chlorine and ethylene oxide was due to the composition of the phase in equilibrium with the hydrates.

A systematic determination of both hydration number (Cady, 1983) and relative cage occupancies (Davidson and Ripmeester, 1984) shows that molecules such as CH_3Cl and SO_2 are the most nonstoichiometric. Although theoretical calculations using the van der Waals and Platteeuw model provides some rationale for the nonstoichiometry, experimental quantification of nonstoichiometry as a function of guest/cavity size ratio has yet to be determined.

Structural Changes in Simple Hydrates. Of particular interest to the question of structure are the simple hydrates of cyclopropane and trimethylene oxide because they can form hydrates of either structure I or structure II as a function of formation conditions. These hydrates are unique examples of structural change of single guest species at different conditions of pressure and temperature.

Consider cyclopropane, first determined to form each structure by Hafemann and Miller (1969). Because trimethylene oxide is miscible, it has a very dissimilar phase diagram, confounding a comparable analysis.

Figure 2.14 is a corrected phase diagram by Majid et al. (1969). In Figure 2.14 most of the hydrate area is occupied by structure I, except for a smaller area between 257.1 and 274.6 K where structure II hydrate forms. This provides four quadrupole points:

1. The normal lower point Q_1 ($\text{I}-\text{L}_w-\text{H}_{\text{II}}-\text{V}$) at about the ice point.
2. The normal upper point Q_2 ($\text{L}_w-\text{H}_{\text{I}}-\text{V}-\text{L}_{\text{CP}}$) at 289.4 K.

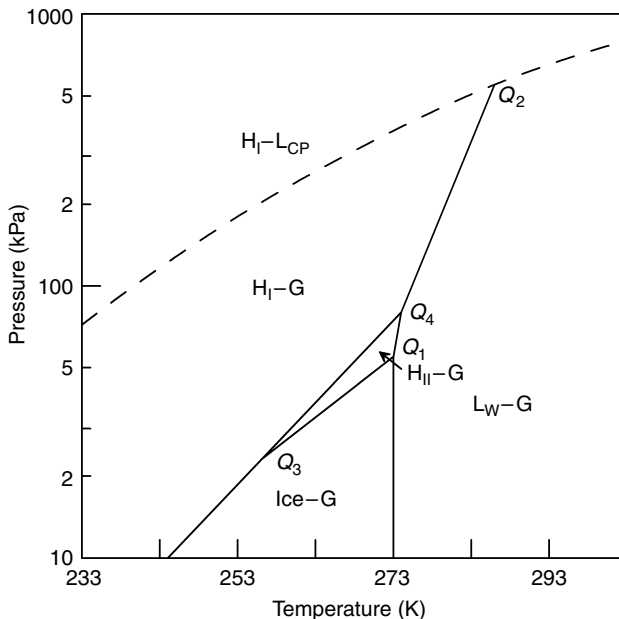


FIGURE 2.14 Pressure–temperature phase diagram for cyclopropane. (Reproduced from Majid, Y.A., Garg, S.K., Davidson, D.W., *Can. J. Chem.*, **47**, 4697 (1969). With permission from the National Research Council of Canada.)

3. The new lowest point Q_3 ($I-H_I-H_{II}-V$) at 257.1 K.
4. A new intermediate point Q_4 ($L_w-H_I-H_{II}-V$) at 274.6 K.

Quadrupole points Q_3 and Q_4 are unusual in that they have two coexisting hydrate phases. Between these two points is a line along which the two hydrate structures coexist with vapor, this line may be a unique example of the way guest size affects the cavity occupied and the pressure and temperature of hydrate formation.

Ohgaki and coworkers (Suzuki, 2001) suggest from Raman spectroscopy measurements that the small 5^{12} cavity of structure I, although vacant at pressures below 200 MPa, is occupied to a small extent by cyclopropane at pressures higher than 200 MPa. The small cage occupancy was also shown to increase with increasing pressures of up to 400 MPa (reaching a small cage/large cage occupancy ratio of around 0.08). The corresponding vibrational energy for cyclopropane in the large cage showed no pressure dependence. Examination of the O–O vibrational modes of the hydrate lattice showed no significant shifts with pressure, unlike that observed for carbon dioxide or methane hydrate. Therefore, these measurements suggest that the cavities of cyclopropane hydrate do not easily contract.

The above findings are analogous to those reported by the same research group for ethane (Morita et al., 2000) and ethylene (Sugahara et al., 2000) hydrates. Based on Raman spectroscopy, ethane or ethylene occupancy of the small cavities of structure I increases with increasing pressure. The low small cage occupancy of ethane in structure I hydrate was also detected from single crystal x-ray diffraction measurements (Udachin et al., 2002).

Structural Changes in Binary (Double) Hydrates. Although CH_4 and C_2H_6 are both sI hydrate formers, Subramanian et al. (2000) showed that a binary CH_4/C_2H_6 mixture can exhibit sI/sII transitions with varying pressure and/or composition. In contrast, a binary CH_4/CO_2 mixture, where again both pure components are sI hydrate formers, forms only sI hydrate.

The sI/sII structural transition of CH_4/C_2H_6 was predicted in 1996 by Hendricks et al. (1996). sI/sII structural transitions were first discovered in the mid-1950s. Von Stackelberg showed from x-ray data that guest combinations of H_2S with CH_3Br , COS, and CH_3CHF_2 form sII hydrates, even though all these guests individually are structure I formers (von Stackelberg and Jahns, 1954). Ripmeester suggested that all small sI guests (occupying the small cavity to a significant extent) when combined with large structure I guests (which do not occupy the small cavity) may form sII hydrate under certain circumstances (Ripmeester, 2000). The formation of sI vs. sII for methane–ethane hydrate has significant effects on the phase equilibria data for this system.

Figure 2.15 (Ripmeester, 2000) correlates the observations of double hydrates and demonstrates the complexity of the structure–size relationship for hydrates containing two types of guest molecules. The combinations of two different types of guests forming sII and sH double hydrates are also listed in [Tables 2.6](#) and [2.7](#), respectively.

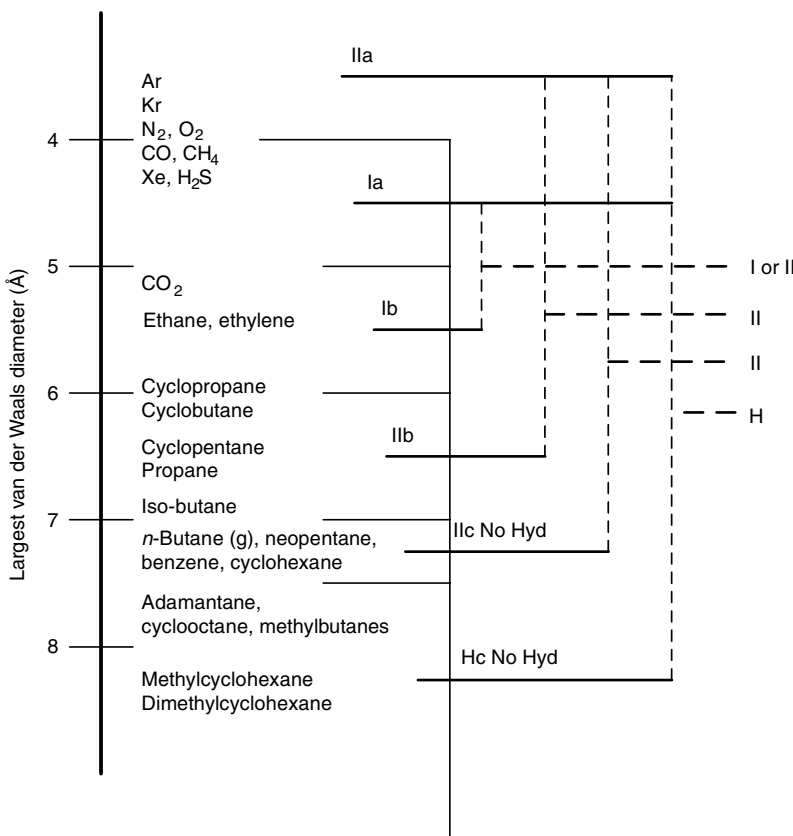


FIGURE 2.15 Correlations of single and double H hydrates. Demonstrating the complexity in guest size–structure correlations for hydrates containing two types of guests. Molecules are classified by how they would behave as single guests. (For example, structure II guests can be divided into three size ranges: [a] occupy 5^{12} cages, [b] only/mostly occupy $5^{12}6^4$ cages, and [c] do not occupy either cage.) The following combinations are known to form double hydrates, although some of the boundaries may not be firmly established: Ia + Ib → structure I or II; IIa or Ia + IIb → structure II; Ia or IIa + IIc → structure II; and Ia or IIa + Hc → structure H. (Redrawn from Ripmeester, J., in *Proc. Third Int. Conf. on Gas Hydrates* (Holder, G.D. and Bishnoi, P.R., eds.), Salt Lake City, UT, Annals of the New York Academy of Sciences, **912**, 1 (2000). With permission.)

Hester and Sloan (2005) extended the size–structure correlations for double hydrates. A simple scheme of guest size–structure boundaries was proposed to predict the sI/sII structural transitions for double hydrates consisting of sI hydrate formers (Figure 2.16). Raman spectroscopy and neutron diffraction measurements were performed to test the limits of these structural transitions.

In agreement with this simple scheme, Ohgaki and coworkers (Makino et al., 2005) used Raman spectroscopy to confirm that a mixture of methane + cyclopropane (one of the largest sI formers) exhibits a sI/sII transition depending

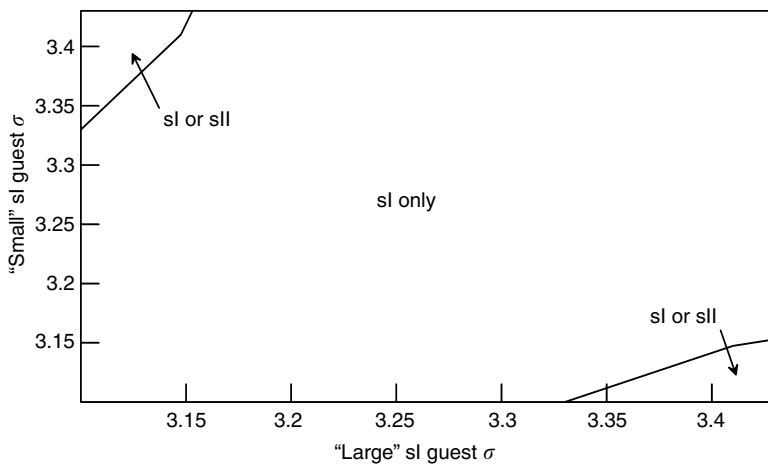


FIGURE 2.16 Qualitative schematic diagram showing predicted sigma (σ) ranges (sigma is effectively the size of the molecule), where a sI to sII transition occurs in a binary system of two sI formers (Hester, 2007).

on the guest composition. Both methane and cyclopropane are sI formers at the experimental conditions of 2.35 MPa, 291.1 K. Conversely, methane + ethylene (a relatively small sI former) mixtures do not undergo a sI/sII structural transition (Makino et al., 2005; Hester, 2007). The relatively small size of ethylene compared to ethane would place it outside of the sI + sII region in Figure 2.16.

2.1.4 Summary Statements for Hydrate Structure

On the basis of the analyses presented in Section 2.1, the following statements represent a summary of hydrate structures:

1. Natural gas clathrate hydrates normally form either in the primitive cubic structure I, in the face-centered cubic structure II, or in the hexagonal structure H.
2. The hydrogen bond is the basis for the interactions of the water molecules bonding in tetrahedral structures similar to that of ice. Pentagonal and hexagonal water clusters formed by hydrogen bonds are frequently found in water, square clusters exist at less frequent intervals.
3. A common cavity to hydrate structures is the pentagonal dodecahedron (5^{12}), which is connected through its vertices to form structure I, through face-sharing in three dimensions to form structure II, or through face-sharing in two dimensions to form connecting layers in structure H.
4. Spaces between the 5^{12} cavities are the larger, oblate $5^{12}6^2$ cavities in structure I, or the spherical $5^{12}6^4$ cavities in structure II. In structure H, both large ($5^{12}6^8$) and small ($4^35^66^3$) cavities form between layers of 5^{12} cavities.

5. Small molecules that occupy the small cavities, also occupy the large cavities. Large molecules can stabilize sI or sII by only occupying the large cavity, leaving the smaller cavity vacant. Structure H requires that both large and small cavities be occupied.
6. Occupation of hydrate cavities and the hydrate structure is determined to a large degree by the guest size in structures I and II. In structure H both size and shape considerations are necessary for a guest molecule. The repulsive interactions between guests and hosts stabilize the hydrate structure.
7. Hydrate nonstoichiometry appears to be related to the ratio of the guest molecule diameter to the free cavity diameter. Nonstoichiometry increases as that ratio approaches unity.
8. The size ratio of the guest to cavity, is a general guide to determining crystal structures and cage occupancy. In turn, crystal structure determines equilibrium pressures and temperatures for the hydrate phase, as shown in Example 2.1.
9. The combination of structure I guests in a binary hydrate can result in a structural transition (sI/sII), when one guest is small (occupying the small cages to a significant extent) and the other guest is large (only occupying the large cages).
10. Heats of dissociation for all three structures are largely determined by hydrogen bonding and the cavity occupation, as shown in Example 2.2. When similar cavities are occupied, the heats of dissociation are similar (regardless of the guest) within the restrictions listed. Detailed evidence for heats of dissociation effects is presented in Chapter 4.6.1.1.
11. At very high pressures (0.3–2.1 GPa), gas hydrates undergo structural transitions to other hydrate phases and filled ice phases. Guests can multiply occupy the large cages of these high-pressure hydrate phases.
12. The less common structures, Jeffrey's structures III–VII, structure T, and complex layer structures have so far only been found for compounds other than natural gas. These compounds form tetragonal (sIII), hexagonal (sIV, sV), cubic (sVI, sVII), trigonal (sT), and alternating sI/sH layer structures.

2.2 COMPARISON OF PROPERTIES OF HYDRATES AND ICE

If all the cavities of structure I or structure II were occupied as a simple hydrate, for example, with xenon or argon, the minimum number of water molecules (5.75 and 5.67, respectively) would be obtained per guest molecule. Both these values yield a structure that is 85 mol.% water. If all three cavity types were completely filled in structure H with two guests, the water mole fraction would be 0.85 as well. As discussed in Section 2.1, due to the nonstoichiometric nature of hydrates, the mole fraction of water is invariably higher than 0.85.

With such high water contents, it is useful as a first approximation to consider some properties of hydrates as variations from those of ice. Davidson (1973)

provides a second microscopic rationale for this comparison by noting that hydrate hydrogen bonds average only 1% longer than those in ice and the O—O—O angles differ from the ice tetrahedral angles by 3.7° and 3.0° in structures I and II, respectively.

Section 2.2.1 summarizes the spectroscopic measurements that have been performed to examine the dynamics of water molecules in hydrate versus ice networks. Sections 2.2.2 and 2.2.3 provide a brief overview of the mechanical and thermal properties, respectively, of hydrates compared to ice. Characterization of these properties will aid in facilitating the accurate interpretation of data obtained from *in situ* detection measurements of natural hydrates. These natural hydrates occur in sediments in permafrost and marine environments. The hydrate mechanical and thermal properties are also important in the evaluation of the location and distribution of natural hydrates in sediments. (Further details are given in Chapter 7—Hydrates in the Earth.)

Table 2.8 is a slight modification of a microscopic and macroscopic property summary by Davidson (1983) for ice and hydrate structures I and II. Although the values in the table were generally measured or estimated for methane or propane hydrates, the contribution of the guest molecule (other than causing the structure to exist) may be considered small for these properties, to a first approximation.

One might anticipate similar results for structures I and II in the absence of measurements. In many of the properties that are derived from structure, the differences between the hydrate crystal structures are not appreciable. One might intuitively expect properties on the basis of the water crystal structure to exhibit less variation between hydrate structures than between hydrate and ice properties, in view of the fact that the 5¹² cavity is common to each hydrate structure.

2.2.1 Spectroscopic Implications

Via NMR and Raman spectroscopy, we can measure the solid hydrate phase. Although an overview of such spectroscopy measurements is provided in Section 6.2, some of the important results for hydrate properties in comparison to ice are provided here.

Proton NMR spectroscopy and dielectric constant measurements provide evidence about the motion of the water molecules in crystal structures, as reviewed by Davidson and Ripmeester (1984). At very low temperatures (<50 K) molecular motion is “frozen in” so that hydrate lattices become rigid. The hydrate proton NMR analysis suggests that the first-order contribution to motion is due to reorientation of water molecules in the structure; the second-order contribution is due to translational diffusion at these low temperatures.

This is one distinguishing feature between hydrates and ice; water molecules diffuse two orders of magnitude slower in hydrates than in ice. As shown in Table 2.8, ice water molecules diffuse almost an order of magnitude faster than they reorient about a fixed position in the crystal structure. In direct contrast, hydrate water molecules reorient 20 times faster than they diffuse. As for all

TABLE 2.8
Comparison of Properties of Ice, sI, and sII Hydrates*

Property	Ice	Structure I	Structure II
Structure and dynamics			
Crystallographic unit cell space group	P6 ₃ /mmc	Pm3n	Fd3m
No. of H ₂ O molecules	4	46	136
Lattice parameters at 273 K (Å)	$a = 4.52, c = 7.36$	12.0	17.3
Dielectric constant at 273 K	94	~58	~58
Far infrared spectrum	Peak at 229.3 cm ⁻¹	Peak at 229.3 cm ⁻¹ with others	
H ₂ O reorientation time at 273 K (μs)	21	~10	~10
H ₂ O diffusion jump time (μs)	2.7	>200	>200
Mechanical properties			
Isothermal Young's modulus at 268 K (10 ⁹ Pa)	9.5	8.4 ^{est}	8.2 ^{est}
Poisson's ratio	0.3301 ^a	0.31403 ^a	0.31119 ^e
Bulk modulus (GPa)	8.8; 9.097 ^a	5.6; 8.762 ^a	8.482 ^a
Shear modulus (GPa)	3.9; 3.488 ^a	2.4; 3.574 ^a	3.6663 ^a
Compressional velocity, V_p (m/s)	3870.1 ^a	3778 ^{a,b}	3821.8 ^a
Shear velocity, V_S (m/s)	1949 ^a	1963.6	2001.14 ^b
Velocity ratio (comp/shear)	1.99	1.92	1.91
Thermal properties			
Linear thermal expansion at 200 K (K ⁻¹)	56×10^{-6}	77×10^{-6}	52×10^{-6}
Thermal conductivity (Wm ⁻¹ K ⁻¹) at 263 K	2.23	0.49 ± 0.02 ;	0.51 ± 0.02
		2.18 ± 0.01^c	0.51 ± 0.01^c
			0.587 ^d
Adiabatic bulk compression at 273 K (GPa)	12	14 ^{est}	14 ^{est}
Heat capacity (Jkg ⁻¹ K ⁻¹)	1700 ± 200^c	2080	2130 ± 40^c
Refractive index (632.8 nm, -3°C)	1.3082 ^e	1.346 ^e	1.350 ^e
Density (g/cm ³)	0.91 ^f	0.94 also see Example 5.2	1.291 ^g

* Note: Unless indicated, values are from Davidson (1983), Davidson et al. (1986b) and Ripmeester et al. (1994).

^a Helgerud et al. (2002) at 253–268 K, 22.4–32.8 MPa (ice, Ih), 258–288 K, 27.6–62.1 MPa (CH₄, sI), 258–288 K, 30.5–91.6 MPa (CH₄–C₂H₆, sII).

^b Helgerud et al. (2003) at 258–288 K, 26.6–62.1 MPa.

^c Waite et al. (2005) at 248–268 K (ice Ih), 253–288 K (CH₄, sI), 248–265.5 K (THF, sII).

^d Huang and Fan (2004) for CH₄, sI.

^e Bylov and Rasmussen (1997).

^f Fractional occupancy (calculated from a theoretical model) in small (S) and large (L) cavities: sI = CH₄: 0.87 (S) and CH₄: 0.973 (L); sII = CH₄: 0.672 (S), 0.057 (L); C₂H₆: 0.096 (L) only; C₃H₈: 0.84 (L) only.

^g Calculated for 2,2-dimethylpentane 5(Xe,H₂S)-34H₂O (Udachin et al., 1997b); est = estimated.

solids, however, water diffusion rates in either solid structure is still several orders of magnitude slower than that of a vapor or liquid.

The dielectric constant values in Table 2.8 also suggest that, while hydrate water molecules reorient rapidly compared to molecules in other solids, reorientation rates are only one-half those in ice. The hydrate value is lower than that of ice due to the lower density of hydrogen-bonded water molecules.

Far infrared spectral data by Bertie et al. (1975) and Bertie and Jacobs (1978) indicate that the strength of the hydrogen bonds in hydrates is very similar to that in ice. The far infrared peak at around 229 cm^{-1} , assigned to the lattice modes (translational vibrations) of water molecules, is not significantly shifted in H_2O ice Ih compared to the hydrates. However, the lattice mode peak is different in the deuterated hydrate compared to D_2O ice (Bertie, 1972). Inelastic neutron scattering studies indicate that the water (D_2O) lattice vibrations are coupled to the guest vibrations (Tse et al., 2001; Gutt et al., 2002). Dielectric and NMR measurements also show that the water lattice dynamics are strongly coupled to the guest motions (Ripmeester et al., 2004).

2.2.2 Mechanical Properties

2.2.2.1 Mechanical strength

Compression deformation measurements at constant applied stress (creep) of methane hydrate (Stern et al., 1996) and of gas-hydrate-bearing sediment (Parameswaran et al., 1989; Cameron et al., 1990) suggested that the strength of hydrate is roughly comparable to that of ice. However, in 2003, Durham and coworkers (2003) suggested that these previous creep measurements may have been influenced by impurities, such as liquid water or ice in the sample, a secondary ice layer formed during compaction/deformation, or by a lack of sufficient confining pressure to suppress fracture. Indeed, in 2003, Durham and coworkers determined from compression deformation experiments (at 260–273 K) that methane hydrate is more than 20 times stronger (creep resistant) than ice Ih. That is, under the same applied stress, ice will deform significantly faster by several orders of magnitude than pure methane hydrate. It is known that ice deforms by the coordinated motion of crystalline defects, which are generally diffusion limited (Poirier, 1985). Therefore, the higher mechanical strength of methane hydrate compared to ice may be related to the rate of diffusion of water in methane hydrate being two orders of magnitude slower than ice (Durham et al., 2003). Hence, hydrate should be more creep resistant than ice.

Winters et al. (2000) showed that the compressive strength of a core containing methane hydrate in the pore space is greater than that without hydrate in the pore space. Ebinuma and coworkers (2005) recently performed compression tests on samples consisting of different saturations (48–52%) of methane hydrate filling the pores of silica sand. Methane hydrate saturation is the ratio of the hydrate volume to pore volume. The mechanical strength of the silica sand was found to increase with increasing methane hydrate saturation. The mechanical strength of hydrate samples prepared from sand/ice/gas was shown to remain

constant until the methane hydrate saturation reached up to 25%. Conversely, the mechanical strength of hydrate samples prepared from water-wet sand/gas increased monotonically with methane hydrate saturation.

Hydrate formation in sediment pores depends on the wettability of the sediment, phase saturations of free water and gas in the pores, the size of the pores, etc. The growth habit of hydrate in sediment pores has been described by Dvorkin et al. (2000) as: (1) hydrate floating in the pore fluid, (2) hydrate as a load-bearing part of the solid phase, (3) hydrate cementing grain contacts, or (4) hydrate acting as a cement forming only at grain contacts. Winters et al. (Winters et al., 2004, Pecher, et al., 2004) suggested that the sediment strength is much lower in the pore filling model than in the cementing model. They showed that laboratory hydrates made from Ottawa sand exhibited strong cementing behavior, while a natural gas hydrate sample from the Mallik 2L-38 well was pore filling.

2.2.2.2 Elastic properties

There is a paucity of reliable, consistent data for hydrate elastic properties. Since these properties depend on crystal structures, many of them can be estimated reliably. However, since 1998, there have been significant efforts to perform accurate measurements of these properties in order to help facilitate correct interpretation of sonic or seismic velocity field data obtained on hydrates in the natural environments.

Whalley (1980) presented a theoretical argument to suggest that both the thermal expansivity and Poisson's ratio should be similar to that of ice. With the above two estimates, Whalley calculated the compressional velocity of sound in hydrates with a value of 3.8 km/s, a value later confirmed by Whiffen et al. (1982) via Brillouin spectroscopy. Kieft et al. (1985) performed similar measurements on simple hydrates to obtain values for methane, propane, and hydrogen sulfide of 3.3, 3.7, and 3.35 km/s, respectively, in substantial agreement with calculations by Pearson et al. (1984).

Pandit and King (1982) and Bathe et al. (1984) presented measurements using transducer techniques, which are somewhat different from the accepted values of Kieft et al. (1985). The reason for the discrepancy of the sonic velocity values from those in [Table 2.8](#) and above is not fully understood. It should be noted that compressional velocity values can vary significantly depending on the hydrate composition and occupancy. This has been demonstrated by lattice-dynamics calculations, which showed that the adiabatic elastic moduli of methane hydrate is larger than that of a hypothetical empty hydrate lattice (Shpakov et al., 1998).

Shimizu et al. (2002) extended the previous Brillouin spectroscopy measurements by performing *in situ* measurements on a single crystal methane hydrate. They examined the effect of pressure on shear (TA) and compressional (LA) velocities, and compared these results to that for ice. The shear velocities of methane hydrate and ice were very similar, showing a slight decrease (about 2 to 1.85 km/s) with increasing pressure (0.02–0.6 GPa). Conversely, the compressional velocities of ice and methane hydrate were different. The

compressional velocity of methane hydrate varied from about 3.76 to about 4 km/s, starting at pressures of 0.02–0.6 GPa. The compressional velocity of ice varied from about 3.9 to 4.0 as the pressure was increased from 0.02 to 0.3 GPa. Similar compressional (3.65 km/s) and shear (1.89 km/s) velocities of methane hydrate were measured by Waite et al. (2000).

Pandit and King (1982) also presented values for the bulk modulus, the shear modulus, and the ratio of compressional to shear velocity, with comparisons to ice values as given in [Table 2.8](#). Shimizu et al. (2002) used Brillouin spectroscopy to determine the elastic anisotropy, bulk modulus, and elastic modulus, based on velocity measurements for methane hydrate at high pressures (0.02–0.6 GPa). Methane hydrate was found to exhibit almost isotropic elasticity. This is in contrast to cubic crystals (e.g., pressure-induced solid CO₂, CH₄, ice VII), which, although they are optically isotropic, generally show substantial anisotropy. The isotropic elasticity of methane hydrate was attributed to its void-rich network of cavities and larger deviations from an ideal tetrahedral geometry. The adiabatic elastic moduli and bulk modulus values for methane hydrate were found to increase almost linearly with pressure. Shimizu (2002) indicated, based on the evaluation of the compressional components of elastic moduli, that methane hydrate is significantly more compressible than ice.

Lee and Collett (2001) measured the compressional (P-wave) and shear (S-wave) velocities of natural hydrates in sediments (33% average total porosity) at the Mallik 2L-38 well. The P-wave velocity of nongas-hydrate-bearing sediment with 33% porosity was found to be about 2.2 km/s. The compressional velocity of gas-hydrate-bearing sediments with 30% gas hydrate concentration (water-filled porosity of 23%) was found to be about 2.7 km/s, and 3.3 km/s at 60% concentration (water-filled porosity of 13%), that is, about a 20% or 50% increase to nongas-hydrate-bearing sediment. The shear velocity was found to increase from 0.81 to 1.23 km/s.

2.2.3 Thermal Properties

2.2.3.1 Thermal conductivity of hydrates

Stoll and Bryan (1979) first measured the thermal conductivity of propane hydrates ($0.393 \text{ W m}^{-1}\text{K}^{-1}$ at $T = 215.15 \text{ K}$) to be a factor of 5 less than that of ice ($2.23 \text{ W m}^{-1}\text{K}^{-1}$). The low thermal conductivity of hydrates, as well as similarities of the values for each structure (shown in [Table 2.8](#)) have been confirmed from numerous studies (Cook and Leaist, 1983 [$0.45 \text{ W m}^{-1}\text{K}^{-1}$ for methane hydrate at 216.2 K]; Cook and Laubitz, 1981; Ross et al., 1981; Ross and Andersson, 1982; Asher et al., 1986; Huang and Fan, 2004; Waite et al., 2005). The thermal conductivity of the solid hydrate ($0.50\text{--}0.58 \text{ W m}^{-1}\text{ K}^{-1}$) more closely resembles that of liquid water ($0.605 \text{ W m}^{-1}\text{ K}^{-1}$).

A pictorial summary of the relative thermal conductivities of water structures (water, ice, and hydrate), including those in sediment is presented in [Figure 2.17](#) (Gupta, 2007). The large variation in composite thermal conductivity for water

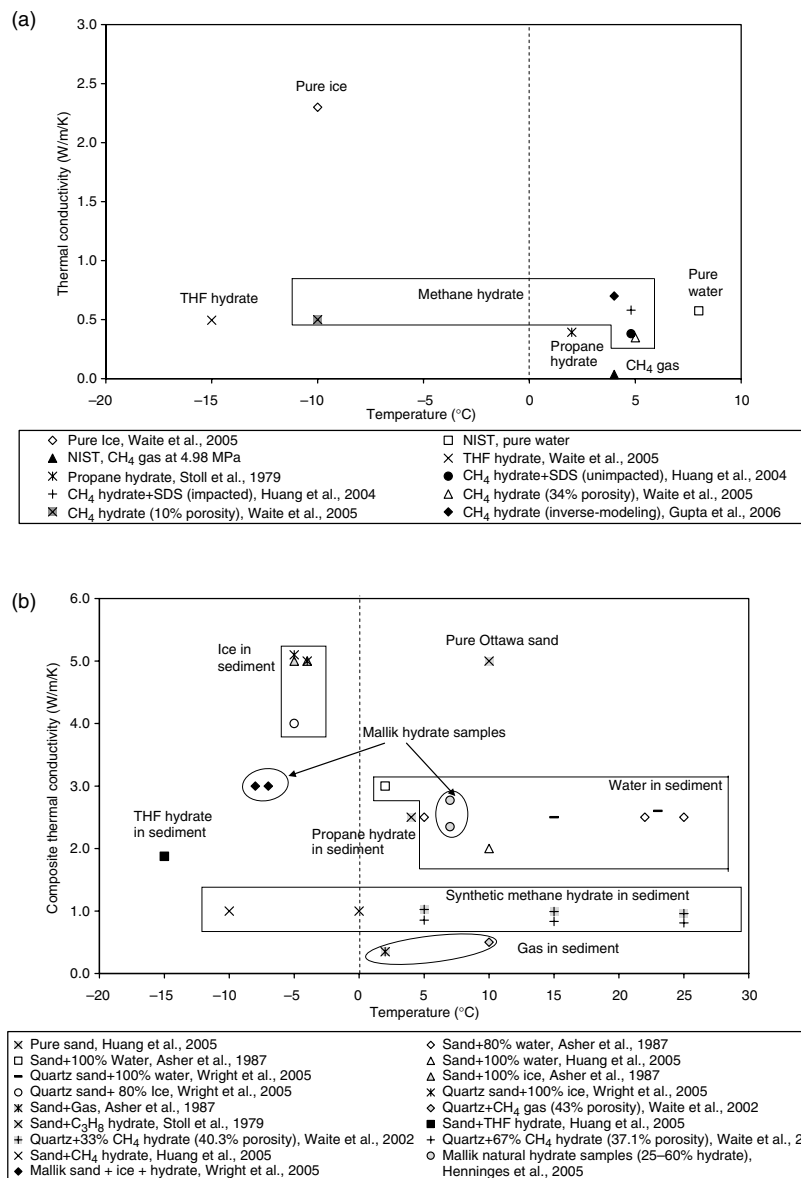


FIGURE 2.17 Thermal conductivity of gas, water, ice, and hydrates: (a) without and (b) with unconsolidated sediment (Gupta, 2007).

structures in sediment can be attributed to different phase saturations and types of sediment.

Ross et al. (1981) also determined that the THF hydrate thermal conductivity was proportionally dependent on temperatures, but had no pressure dependence.

Ross and Andersson (1982) suggested that this behavior, which was never before reported for crystalline organic materials, was associated with the properties of glassy solids. Waite et al. (2005) measured the temperature dependence of porous methane hydrate thermal conductivity. Early work on this anomalous property led to the development of a thermal conductivity needle probe (Asher et al., 1986) as a possible means of *in situ* discrimination of hydrates from ice in the permafrost.

Most of the thermal conductivity measurements have been performed using THF hydrate since this hydrate is fully miscible with water, is stable at atmospheric pressure, and will form a uniform hydrate (with all the large cages occupied by THF). Conversely, methane hydrate samples can contain gas, water, or ice, and hence exhibit variable densities that are interrelated to the thermal conductivity (Waite et al., 2005). Also, unlike THF hydrate, it is difficult to synthesize a non-porous methane hydrate sample in the laboratory. The thermal conductivity of methane hydrate increases from 0.50 to 0.587 on decreasing the sample porosity from 34% to about 5% (by compacting the hydrate sample with an external pressure; Huang and Fan, 2004; Waite et al., 2005). The use of THF hydrate as a model for methane hydrate would at first thought seem reasonable considering that the thermal conductivity has been reported to be independent of hydrate structure and type (Cook and Laubitz, 1981; Ross and Andersson, 1982; Cook and Leaist, 1983). However, there are increasing concerns that THF hydrate may not be a suitable thermal property analog to methane hydrate.

Waite et al. (2005) showed that the thermal conductivity of THF hydrate ($0.50 \text{ W m}^{-1} \text{ K}^{-1}$) is similar to that of methane hydrate (0.50 and $0.51 \text{ W m}^{-1} \text{ K}^{-1}$ for porous and compacted samples, respectively) below -7.5°C . However, above -7.5°C , there are significant discrepancies between the thermal properties of these hydrates. THF hydrate exhibited a sharp increase in thermal conductivity to around $0.7 \text{ W m}^{-1} \text{ K}^{-1}$ when the temperature was changed from -7.5°C to around 3°C . Thereby indicating that THF hydrate is not a suitable thermal property analog of methane hydrate above -7.5°C . Huang and Fan (2005) showed that the thermal conductivity values of THF hydrate measured over the temperature range -10°C to -2°C were similar to that of methane hydrate. (Variations in the temperature dependence range of THF hydrate may be due to THF hydrate + ice being formed.) At higher temperatures, the thermal conductivity of methane hydrate and THF hydrate can differ by about 20% (Huang and Fan, 2004), indicating that the guest molecule can affect the hydrate thermal conductivity.

Several models have been proposed to estimate the thermal conductivity of hydrate/gas/water or hydrate/gas/water/sediment systems. The most common are the classical mixing law models, which assume that the effective properties of multicomponent systems can be determined as the average value of the properties of the components and their saturation (volumetric fraction) of the bulk sample composition. The parallel (arithmetic), series (harmonic), or random (geometric) mixing law models (Beck and Mesiner, 1960) that can be used to calculate the composite thermal conductivity (k_θ) of a sample are given in Equations 2.1 through 2.3.

Parallel model:

$$k_\theta = k_H S_H + k_W S_W + k_G S_G \quad (2.1)$$

Series model:

$$k_\theta = (S_H/k_H + S_W/k_W + S_G/k_G)^{-1} \quad (2.2)$$

Random model:

$$k_\theta = k_H^{SH} * k_W^{SW} * k_G^{SG} \quad (2.3)$$

where S_H , S_W , and S_G are the saturations of hydrate, water, and gas, respectively, and k_H , k_W , and k_G are the thermal conductivities of hydrate, water, and gas, respectively.

Thermal conductivity can also be estimated from thermal response measurements of the test sample. A particularly powerful approach is the application of the inverse model, ITOUGH2 (Finsterle, 1997; Moridis, 2005b), to estimate the thermal conductivity of porous hydrate and hydrate-bearing sediment systems from thermal response data coupled with gas pressure and x-ray computed tomography (x-ray CT) measurements (Finsterle, 1997; Kneafsey et al., 2005; Gupta, 2007). Composite thermal conductivities of 2.380 and $3.145 \text{ W m}^{-1} \text{ K}^{-1}$ were determined for a water/gas/sand system and a water/gas/hydrate/sand system, respectively (Kneafsey et al., 2005; Moridis, 2005a).

Henninges et al. (2005) estimated the composite thermal conductivities of hydrate-bearing sediments during the Mallik 2002 research program in the Mackenzie-Delta in the northwestern part of arctic Canada. Hydrate-bearing sand sediments with k_θ values in the range $2.35\text{--}2.77 \text{ W m}^{-1} \text{ K}^{-1}$ were estimated from well-logging data obtained from fiber optic distributed temperature sensing cables. However, there were considerable uncertainties in the hydrate saturations in the natural sediments due to the heterogeneity of these systems. Therefore, controlled laboratory measurements (similar to the above CT x-ray measurements) as a function of hydrate composition, saturation, and microstructure would be valuable in aiding the interpretation of field data.

In the hydrate lattice structure, the water molecules are largely restricted from translation or rotation, but they do vibrate anharmonically about a fixed position. This anharmonicity provides a mechanism for the scattering of phonons (which normally transmit energy) providing a lower thermal conductivity. Tse et al. (1983, 1984) and Tse and Klein (1987) used molecular dynamics to show that frequencies of the guest molecule translational and rotational energies are similar to those of the low-frequency lattice (acoustic) modes. Tse and White (1988) indicate that a resonant coupling explains the low thermal conductivity.

The above molecular dynamics results have been confirmed by incoherent inelastic neutron scattering (IINS) measurements on xenon hydrate (Tse et al., 2001; Gutt et al., 2002). In earlier measurements on methane hydrate, the dominant

rotational motions of methane obscured any direct information on host–guest coupling. However, in the Xe hydrate measurements, the scattering intensity of xenon is negligible compared to water, and therefore the translational vibrations of the water lattice can be directly studied. It was suggested that thermal resistivity in a real solid is caused by scattering of the lattice phonons. Therefore, the coupling between guest and host vibrations or phonons may cause the anomalous temperature dependence of the thermal conductivity. This coupling between the guest and host lattice does not noticeably affect most structural thermodynamic and mechanical properties, but results in a marked decrease in the transport of heat.

2.2.3.2 Thermal expansion of hydrates and ice

Linear thermal expansion coefficients of hydrate structures I, II, and ice have been determined through dilatometry (Roberts et al., 1984) and through x-ray and neutron powder diffraction (Tse, 1987; Tse et al., 1987; Ikeda et al., 1999, 2000; Udachin et al., 2001b; Circone et al. 2003; Rawn et al., 2003). The values for sH hydrate at 200 K have been measured for hexamethylethane (HME) and 2,2-dimethylbutane (DMB) at 150 and 200 K by Tse (1990) who notes that cubic expansion values are similar to those of sI and sII, but there is a difference in the direction of linear expansion for structure H. At 200 K, linear thermal expansions for sI ($77 \times 10^{-6} \text{ K}^{-1}$), sII ($52 \times 10^{-6} \text{ K}^{-1}$), sH ($a = 67 \times 10^{-6}$, $c = 59 \times 10^{-6} \text{ K}^{-1}$ for DMB), and ice ($a = 56 \times 10^{-6}$, $c = 57 \times 10^{-6} \text{ K}^{-1}$) were listed. Figure 2.18 shows plots of linear thermal expansions vs. temperature for sI, sII, and ice Ih (Hester et al., 2007).

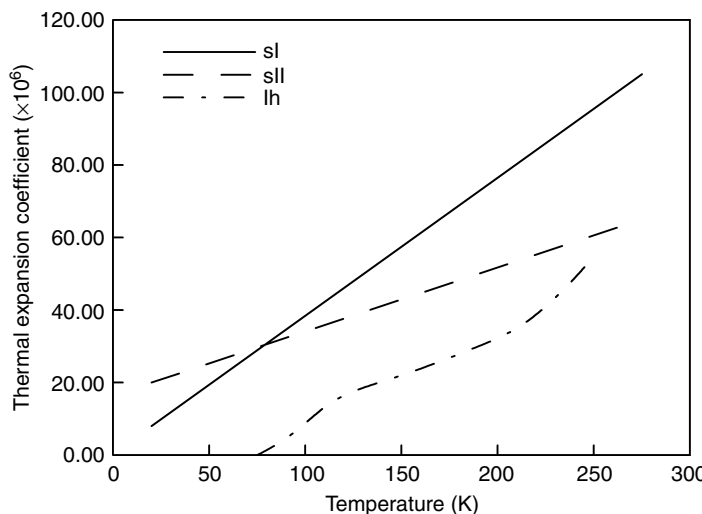


FIGURE 2.18 Linear thermal expansion coefficient vs. temperature for sI and sII hydrates, and ice Ih (Hester et al. 2007).

Through constant pressure molecular dynamics calculations for the thermal expansion of ice and of empty structure I, Tse et al. (1987) determined that the high hydrate thermal expansivity is due to anharmonic behavior in the water lattice. Tse (1994) suggests that this results from collisions of the guest molecule with the cage wall, which exerts an internal pressure to weaken the interaction between the water hydrogen bonds. Free energy calculations of several proton-disordered configurations of structure I hydrate and ice were performed over a wide range of temperatures to evaluate the cause of the high thermal expansion of hydrate compared to ice (Tanaka et al., 1997). In agreement with the work by Tse, the results indicated that the large thermal expansivity of hydrate is caused by the guest molecule, with the different arrangements of oxygen atoms in the hydrate and ice playing only a minor role.

2.3 THE WHAT AND THE HOW OF HYDRATE STRUCTURES

With the conclusion of the present chapter, the reader should have a firm notion of what the molecular structures are and how these structures compare and contrast to that of ice.

If water will normally form ice in the absence of a solute molecule, the question arises about the mechanism for forming a clathrate with an exact structure, when the solubility of hydrocarbon molecules in liquid water is known to be small (or negligible in ice), relative to the amount of hydrocarbon needed for hydrates. Thus, along with the definition of what the hydrate structures are, comes the logical question of how these structures form. During the past two decades, sophisticated experimental and modeling tools have been applied to address this question. The microscopic mechanism and the macroscopic kinetics of hydrate formation are the major considerations of [Chapter 3](#).

REFERENCES

- Allen, K.W., *J. Chem. Phys.*, **41**, 840 (1964).
- Allen, K.W., Jeffrey, G.A., *J. Chem. Phys.*, **38**, 2304 (1963).
- Angell, C.A., *Water: A Comprehensive Treatise*, (Franks, F., ed.) Plenum Press, New York, **7**, 1 (1982).
- Ashbaugh, H.S., Paulaitis, M.E., *J. Am. Chem. Soc.*, **123**, 10721 (2001).
- Asher, G.B., *Development of a Computerized Thermal Conductivity Measurement System Utilizing the Transient Needle Probe Technique: An Application to Hydrates in Porous Media*, Ph.D. Thesis, Colorado School of Mines, Golden, CO (1987).
- Asher, G.B., Sloan, E.D., Graboski, M.S., *Int. J. Thermophys.*, **7**, 285 (1986).
- Ballard, A., *A Non-Ideal Hydrate Solid Solution Model for a Multi-Phase Equilibria Program*, Ph.D. Thesis, Colorado School of Mines, Golden, CO (2002).
- Bathe, M., Vagle, S., Saunders, G.A., Lambson, T.F., *J. Matl. Sci. Lett.*, **3**, 904 (1984).
- Baumert, J., Gutt, C., Press, W., Tse, J.S., Janssen, S., in *Proc. Fourth International Conference on Gas Hydrates*, Yokohama, Japan, May 19–23, 687, (2002).
- Beck, A.E., Mesiner, A.D., in *Methods for Determining Thermal Conductivity and Thermal Diffusivity*, Interscience Publishers Inc., New York, **1**, 49, (1960).

- Benedict, W.S., Gilar, N., Plyler, E.K., *J. Chem. Phys.*, **24**, 1139 (1956).
- Bernal, J.D., Fowler, R.H., *J. Chem. Phys.*, **1**, 515 (1933).
- Bertie, J.A., Bates, F.E., Hendrickson, D.K., *Can. J. Chem.*, **53**, 71 (1975).
- Bertie, J.A., Jacobs, S.M., *J. Chem. Phys.*, **69**, 4105 (1978).
- Bertie, J.A., Othen, D.A., *Can. J. Chem.*, **50**, 3443 (1972).
- Bjerrum, N., *Science*, **115**, 385 (1952).
- Blokzijl, W., Engberts, J.B.F.N., *Angew. Chem., Int. Ed.*, **32**, 1545 (1993).
- Bowron, D.T., Soper, A.K., Finney, J.L., *J. Chem. Phys.*, **114**, 6203 (2001).
- Brownstein, S., Davidson, D.W., Fiat, D., *J. Chem. Phys.*, **46**, 1454 (1967).
- Buchanan, P., Soper, A.K., Westacott, R.E., Creek, J.L., Koh, C.A., *J. Chem. Phys.*, **123**, 164507 (2005).
- Burnham, C.J., Xantheas, S.S., Miller, M.A., Applegate, B.E., Miller, R.E., *J. Chem. Phys.*, **117**, 1109 (2002).
- Bylov, M., Rasmussen, P., *Chem. Eng. Sci.*, **52**, 3295 (1997).
- Cady, G.H., *J. Phys. Chem.*, **85**, 4437 (1983).
- Calvert, L.D., Srivastava, P., *Acta Crystallogr.*, **A25**, S131 (1967).
- Cameron, I., Handa, Y.P., Baker, T.H.W., *Can. Geotechnol. J.*, **27**, 255 (1990).
- Chakoumakos, B.C., Rawn, C.J., Rondinone, A.J., Stern, L.A., Circone, S., Kirby, S.H., Ishii, Y., Jones, C.Y., Toby, B.H., *Can. J. Phys.*, **81**, 183 (2003).
- Chau, P.L., Mancera, R.L., *Mol. Physics*, **96**, 109 (1999).
- Chazallon, B., Kuhs, W.F., *J. Chem. Phys.*, **117**, 308 (2002).
- Chen, T.S., *A Molecular Dynamics Study of the Stability of Small Prenucleation Water Clusters*, Dissertation, U. Missouri-Rolla, Univ. Microfilms No. 8108116, Ann Arbor, MI (1980).
- Chou, I.M., Sharma, A., Burruss, R.C., Shu, J.F., Mao, H.K., Hemley, R.J., Goncharov, A.F., Stern, L.A., Kirby, S.H., in *Proc. National Academic Science USA*, **97**, 13484 (2000).
- Circone, S., Stern, L.A., Kirby, S.H., Durham, W.B., Chakoumakos, B.C., Rawn, C.J., Rondinone, A.J., Ishii, Y., *J. Phys. Chem. B*, **107**, 5529 (2003).
- Cook, J.G., Laubitz, M.J., in *17th Intl. Thermal Conductivity Conf.*, Gathersburg, Maryland, 13 pp (1981).
- Cook, J.G., Leaist, D.G., *Geophys. Res. Lett.*, **10**, 397 (1983).
- Cottrell, T.L., *The Strengths of Chemical Bonds*, Butterworths, London (1958).
- Curl, R.F., Smalley, R.E., *Scientific American*, 54 (1991).
- Danesh, A., Tohidi, B., Burgass, R.W., Todd, A.C., *Trans. I. Chem. E*, **7(A)**, 197 (1994).
- Davidson, D.W., *Can. J. Chem.*, **49**, 1224 (1971).
- Davidson, D.W., *Water: A Comprehensive Treatise*, Plenum, New York, (1973).
- Davidson, D.W., *Natural Gas Hydrates* (Cox, J.L., ed.) Butterworths, Boston, 1 (1983).
- Davidson, D.W., Garg, S.K., Gough, S.R., Hawkins, R.E., Ripmeester, J.A., *Can. J. Chem.*, **55**, 3641 (1977a).
- Davidson, D.W., Gough, S.R., Lee, F., Ripmeester, J.A., *Revue de Chimie Minerale*, **14**, 447 (1977b).
- Davidson, D.W., Gough, S.R., Ripmeester, J.A., Nakayama, H., *Can. J. Chem.*, **59**, 2587 (1981).
- Davidson, D.W., Handa, Y.P., Ratcliffe, C.I., Tse, J.S., Powell, B.M., *Nature*, **311**, 142 (1984a).
- Davidson, D.W., Garg, S.K., Gough, S.R., Handa, Y.P., Ratcliffe, C.I., Tse, J.S., Ripmeester, J.A., *J. Inclusion Phenom.*, **2**, 231 (1984b).

- Davidson, D.A., Handa, Y.P., Ratcliffe, C.I., Ripmeester, J.A., Tse, J.S., Dahn, J.R., Lee, F., Calert, L.D., *Mol. Cryst. Liq. Cryst.*, **141**, 141 (1986a).
- Davidson, D.W., Handa, Y.P., Ripmeester, J.A., *J. Phys. Chem.*, **90**, 6549 (1986b).
- Davidson, D.W., Ripmeester, J.A., *J. Glaciology*, **21**, 33 (1978).
- Davidson, D.W., Ripmeester, J.A., *Inclusion Compounds*, (Atwood, J.L., Davies, J.E.D., MacNichol, D.D., eds.), Academic Press, **3**, Chapter 3, 69 (1984).
- Deaton, W.M., Frost, E.M., Jr., *Oil Gas J.*, **36**, 75 (1937).
- Deaton, W.M., Frost, E.M., Jr., *Gas Hydrates and Their Relation to the Operation of Natural Gas Pipe Lines*, 101 pp. U.S. Bureau of Mines Monograph, **8** (1946).
- De Forcrand, R., *Ann. Chim. Phys.*, **28**, 5 (1883).
- Debenedetti, P.G., *Metastable Liquids, Concepts and Principles*, Princeton University Press, NJ (1996).
- Debenedetti, P.G., *J. Phys.: Condens. Matter*, **15**, R1669 (2003).
- Dec, S.F., Bowler, K.E., Stadterman, L.L., Koh, C.A., Sloan, E.D., *J. Am. Chem. Soc.*, **128**, 414 (2006).
- Desgreniers, S., Flacau, R., Klug, D.D., Tse, J.S. in *Proc. Int. Conf. of CeSMEC*, Miami, FL (2003).
- Dixit, S., Soper, A.K., Finney, J.L., Crain, J., *Europhys. Lett.*, **59**, 377 (2002).
- Durham, W.B., Stern, L.A., Kirby, S.H., *Can. J. Phys.*, **81**, 373 (2003).
- Durrant, P.J., Durrant, B., *Introduction to Advanced Inorganic Chemistry*, John Wiley and Sons, Inc., New York (1962).
- Dvorkin, J., Helgerud, M.B., Waite, W.F., Kirby, S.H., Nur, A., Introduction to physical properties and elasticity models. *Natural Gas Hydrates in Oceanic and Permafrost Environments* (Max, M., ed.), 245 (2000).
- Dyadin, Y.A., Aladko, E.Y., Larionov, E.G., *Mendeleev Commun.*, **7**, 34 (1997).
- Dyadin, Y.A., Bondaryuk, I.V., Shurko, F.V., *Inclusion Compounds*, V5, Edited by Atwood, Davies, MacNichol, Oxford University Press, **5**, 213 (1991).
- Dyadin, Y., Bondaryuk, I.V., Zhurko, F.V., *Inorganics and Physical Aspects of Inclusion*, Oxford University Press, 213 (1991).
- Dyadin, T., Larionov, E., Aladko, E., Yu, A., Manakov, F., *J. Structural Chem.*, **40**, 790 (1999).
- Dyadin, Y., Mikina, T., Zhurko, F., Mironov, Y., Msanuilov, A., Skripko, G., *Mendeleev Commun.*, **5**, 62 (1995).
- Dyadin, Y.A., Udashin, K.A., Bogatyryova, S.V., Zhurko, F.V., *J. Inclusion Phenom.*, **6**, 565 (1988).
- Dyadin, Y.A., Zhurko, F.V., Bondaryuk, I.V., Zhurko, G.O., *J. Inclusion Phenom. Mol. Recognition Chem.*, **10**, 39 (1991).
- Ebinuma, T., Kamata, Y., Minagawa, H., Ohmura, R., Nagao, J., Narita, H., in *Proc. Fifth International Conference on Gas Hydrates*, Trondheim, Norway, June 13–16, Paper 3037 (2005).
- Fan, S., *J. Chem. Eng. Data*, **49**, 1479 (2004).
- Finsterle, S., *Laurence Berkeley National Laboratory Report* LBNL-40400 (1997).
- Florusse, L.J., Peters, C.J., Schoonman, J., Hester, K.C., Koh, C.A., Dec, S.F., Marsh, K.N., Sloan, E.D., *Science*, **306**, 469 (2004).
- Fowler, D.L., Loebenstein, W.A., Pall, D.B., Kraus, C.A., *J. Am. Chem. Soc.*, **62**, 15 (1940).
- Frank, H.S., *Science*, **169**, 635 (1970).
- Frank, H.S., Evans, M.W., *J. Chem. Phys.*, **13**, 507 (1945).
- Franks, F., *Water: A Comprehensive Treatise*, Plenum Press, New York, (1972–1982).
- Franks, F., *Water: A Comprehensive Treatise*, Plenum Press, New York, **4** (1975).

- Franks, F., *Water Science Reviews*, Cambridge University Press, New York (1985–1990).
- Franks, F., Reid, D.S., *Water: A Comprehensive Treatise*, (Franks, F., ed.) Plenum Press, New York **1**, Chapter 5 (1973).
- Geil, B., Kirschgen, T.M., Fujara, F., *Phys. Rev. B.*, **72**, 014304 (2005).
- Gerke, H., Gies, H., Z. *Kristallographie*, **166**, 11 (1984).
- Glew, D.W., *Nature*, **184**, 545 (1959).
- Glew, D.W., Rath, N.S., *J. Chem. Phys.*, **44**, 1710 (1966).
- Gough, S.R., Garg, S.K., Ripmeester, J.A., Davidson, D.W., *Can. J. Chem.*, **52**, 3193 (1974).
- Gough, S.R., Ripmeester, J.A., Davidson, D.W., *Can. J. Chem.*, **53**, 2215 (1975).
- Gupta, A., *Methane Hydrate Dissociation Measurements and Modeling: The Role of Heat Transfer and Reaction Kinetics*, Ph.D. Thesis, Colorado School of Mines, Golden, CO (2007).
- Gupta, A., Sloan, E.D., Kneafsey, T.J., Tomutsa, L., Moridis, G., in *Proc. Fifth International Conference on Gas Hydrates*, Trondheim, Norway, June 13–16, Paper 2005 (2005).
- Gutt, C., Asmussen, B., Press, W., Johnson, M.R., Handa, Y.P., Tse, J.S., *J. Chem. Phys.*, **113**, 4713 (2000).
- Gutt, C., Baumert, J., Press, W., Tse, J.S., Janssen, S., *J. Chem. Phys.*, **116**, 3795 (2002).
- Hafemann, D.R., Miller, S.L., *J. Phys. Chem.*, **73**, 1392 (1969).
- Handa, Y.P., *J. Phys. Chem.*, **90**, 5497 (1986).
- Haenel, R., Stegema, L., Rybach, (eds.) *Handbook of Terrestrial Heat-Flow Density Determination*, Kluwer Academic Publishers, Dordrecht, Netherlands, 87 (1988).
- Hara, T., Hashimoto, S., Sugahara, T., Ohgaki, K., *Chem. Eng. Sci.*, **60**, 3117 (2005).
- Harker, H.A., Viant, M.R., Keutsch, F.N., Michael, E.A., McLaughlin, R.P., Saykally, R.J., *J. Phys. Chem. A*, **109**, 6483 (2005).
- Hawkins, R.E., Davidson, D.W., *J. Phys. Chem.*, **70**, 1889 (1966).
- Head-Gordon, T., in *Proc. National Academic Science U.S.A.*, **92**, 8308 (1995).
- Helgerud, M.B., Circone, S., Stern, L., Kirby, S., Lorenson, T.D., in *Proc. Fourth International Conference on Gas Hydrates*, Yokohama May 19–23, 2002, 716 (2002).
- Helgerud, M.B., Waite, W.F., Kirby, S.H., Nur, A., *Can. J. Phys.*, **81**, 47 (2003).
- Hendricks, E.M., Edmonds, B., Moorwood, R.A.S., Szcepanski, R., *Fluid Phase Equilib.*, **117**, 193 (1996).
- Henninges, J., Heunges, E., Buirkhardt, H., in *Proc. Fifth International Conference on Gas Hydrates*, Trondheim, Norway, June 13–16, Paper 3034 (2005).
- Hester, K.C., *Probing Hydrate Stability and Structural Characterization of Both Natural and Synthetic Clathrate Hydrates*, Ph.D. Thesis, Colorado School of Mines, Golden, CO (2007).
- Hester, K.C., Huo, Z., Ballard, A.L., Miller, K.T., Koh, C.A., Sloan, E.D., *J. Phys. Chem. B*, in press (2007).
- Hester, K.C., Koh, C.A., Sloan, E.D., Schultz, A.J., in *Proc. Fifth International Conference on Gas Hydrates*, Trondheim, Norway, June 13–16, Paper 5038 (2005).
- Hester, K.C., Sloan, E.D., *Intl. J. Thermophysics*, **26**, 95 (2005).
- Hester, K.C., Strobel, T.A., Huq, A., Schultz, A.J., Sloan, E.D., Koh, C.A., *J. Phys. Chem. B*, **110**, 14024 (2006).
- Hirai, H., Nishimura, Y., Kawamura, T., Yamamoto, Y., Yagi, T., *J. Phys. Chem. B*, **106**, 11089 (2002).
- Hirai, H., Tanaka, H., Kawamura, K., Yamamoto, Y., Yagi, T., *J. Phys. Chem. Solids*, **65**, 1555 (2004).

- Hirai, H.H., Uchihara, Y., Fujihisa, H., Sakashita, M., Katoh, E., Aoki, K., Nagashima, K., Yamamoto, Y., Yagi, T., *J. Chem. Phys.*, **115**, 7066 (2001).
- Holder, G.D., Manganello, D.J., *Chem. Eng. Sci.*, **37**, 9 (1982).
- Holder, G.D., Zele, S., Enick, R., LeBlond, C., in *Proc. First International Conference on Natural Gas Hydrates*, (Sloan, E.D., Happel, J., Hnatow, M.A., eds.), Annals of the New York Academy of Sciences, **715**, 344 (1994).
- Holland, P.M., Castleman, A.W., *J. Chem. Phys.*, **72**, 5984 (1980).
- Huo, Z., *Hydrate Phase Equilibria Measurements by X-Ray Diffraction and Raman Spectroscopy*, Ph.D. Thesis, Colorado School of Mines, Golden, CO (2002).
- Huang, D., Fan, S., *J. Chem. Eng. Data*, **49**, 1479 (2004).
- Huang, D., Fan, S., *J. Geophysical Research-Solid Earth*, **110**, B01311 (2005)
- Huang, D.Z., Fan, S.S., *J. Chem. Eng. Data*, **49**, 1479 (2004).
- Huang, D.Z., Fan, S.S., *J. Geophysical Research-Solid Earth*, **110**, B01311 (2005).
- Hummer, G., Garde, S., Garcia, A.E., Pohorille, A., Pratt, L.R., in *Proc. National Academic Science U.S.A.*, **93**, 8951 (1996).
- Ikeda, T., Mae, S., Yamamuro, O., Matsuo, T., Ikeda, S., Ibberson, R.M., *J. Phys. Chem. A*, **104**, 10623 (2000).
- Ikeda, T., Yamamuro, O., Matsuo, T., Mori, K., Torii, M.S., *J. Phys. Chem. Solids*, **60**, 1527 (1999).
- Inerbaev, T.M., Belosludov, V.R., Belosludov, R.V., Sluiter, M., Kawazoe, Y., Kudoh, J.I., *J. Inclusion Phenom. Macrocyclic Chem.*, **48**, 55 (2004).
- Itoh, H., Tse, J.S., Kawamura, K., *J. Chem. Phys.*, **115**, 9414 (2001).
- Jeffrey, G.A., *Inclusion Compounds*, (Atwood, J.L. Davies, J.E.D., MacNichol, D.D., eds.) Academic Press, pp. 135 (1984).
- Jeffrey, G.A., McMullan, R.K., *Prog. Inorg. Chem.*, **8**, 43 (1967).
- Jones, C.Y., Marshall, S.L., Chakoumakos, B.C., Rawn, C.J., Ishii, Y., *J. Phys. Chem. B*, **107**, 6026 (2003).
- Jones, C.A., Rondonone, A.J., Chakoumakos, B.C., Circone, S., Stern, L.A., Kirby, S.H., Ishii, Y., *Can. J. Phys.*, **81**, 431 (2000).
- Kieft, H., Clouter, M.J., Gagnon, R.E., *J. Phys. Chem.*, **89**, 3103 (1985).
- Kini, R.A., Huo, Z., Jager, M.D., Bollavararam, P., Ballad, A.L., Dec, S.F., Sloan, E.D., in *Proc. Fourth International Conference on Gas Hydrates*, Yokohama, Japan, May 19–23, 867 (2002).
- Kirchner, M.T., Boese, R., Billups, W.E., Norman, L.R., *J. Am. Chem. Soc.*, **126**, 9407 (2004).
- Kirschgen, T.M., Zeidler, M.D., Geil, B., Fujara, F., *Phys. Chem. Chem. Phys.*, **5**, 5247 (2003).
- Kneafsey, T.J., Tomutsa, L., Moridis, G.J., Seol, Y., Freifeld, B., Taylor, C.E., Gupta, A., in *Proc. Fifth International Conference on Gas Hydrates*, Trondheim, Norway, June 13–16, Paper 1033 (2005).
- Kollman, P., *J. Am. Chem. Soc.*, **99**, 4875 (1977).
- Kurnosov, A.V., Manakov, A.Y., Komarov, V.Y., Voronin, V.I., Teplykh, A.E., Dyadin, Y.A., *Doklady Phys. Chem.*, **381**, 303 (2001).
- Kursonov, A.V., Komarov, V.Y., Voronin, V.I., Teplykh, A.E., Manakov, A.Y., *Angew. Chem. Int'l. Ed.*, **43**, 2922 (2004).
- Latimer, W.M., Rodebush, W.H., *J. Am. Chem. Soc.*, **42**, 1419 (1920).
- Lederhos, J.P., Mehta, A.P., Nyberg, G.B., Warn, K.J., Sloan, E.D., *AICHE J.*, **38**, 1045 (1992).
- Lee, J-W, Lu, H., Moudrakovski, I.L., Ratcliffe, C.I., Ripmeester, J.A., *Angew. Chem. Int. Ed.*, **118**, 2516 (2006).

- Lee, M.W., Collett, T.S., *Geophysics*, **66**, 763 (2001).
- Lipkowski, J., Yu, V., Rodionova, T.V., *J. Supramol. Chem.*, **2**, 435 (2002).
- Liu, S., Welch, M., Klinowski, J., *J. Phys. Chem.*, **101**, 2811 (1997).
- Lokshin, K.A., Zhao, Y.S., He, D.W., Mao, W.L., Mao, H.K., Hemley, R.J., Lobanov, M.V., Greenblatt, M., *Phys. Rev. Lett.*, **93**, 125503 (2004).
- Lokshin, K.A., Zhao, Y., Lobanov, M.V., Greenblatt, M., in *Proc. Fifth International Conference on Gas Hydrates*, Trondheim, Norway, June 13–16, Paper 2005 (2005a).
- Lokshin, K.A., Zhao, Y., Mao, W.L., Mao, H., Hemley, R.J., Lobanov, M.V., Greenblatt, M., in *Proc. Fifth International Conference on Gas Hydrates*, Trondheim, Norway, June 13–16, Paper 5024 (2005b).
- Long, J.P., *Gas Hydrate Formation Mechanism and Kinetic Inhibition*, Ph.D. Thesis, Colorado School of Mines, Golden, CO (1994).
- Lonsdale, H.K., in *Proc. Roy. Soc. Series A*, **247**, 424 (1958).
- Lotz, H.T., Schouten, J.A., *J. Chem. Phys.*, **111**, 10242 (1999).
- Loveday, J.S., Nelmes, R.J., Guthrie, M., Belmonte, S.A., Allan, D.R., Klug, D.D., Tse, J.S., Handa, Y.P., *Nature*, **410**, 661 (2001a).
- Loveday, J.S., Nelmes, R.J., Guthrie, M., Klug, D.D., Tse, J.S., *Phys. Rev. Lett.*, **87**21, 215501 (2001b).
- Loveday, J.S., Nelmes, R.J., Klug, D.D., Tse, J.S., Desgreniers, S., *Can. J. Phys.*, **81**, 539 (2003).
- Luck, W.A.P., in *Water a Comprehensive Treatise*, (Franks, F., ed.) Plenum Press, New York, **2**, Chapter 4 (1973).
- Lynden-Bell, R.M., Debenedetti, P.G., *J. Phys. Chem. B*, **109**, 6527 (2005).
- Lyusternik, L.A., *Convex Figures and Polyhedra*, Dover, New York (1963).
- Majid, Y.A., Garg, S.K., Davidson, D.W., *Can. J. Chem.*, **47**, 4697 (1969).
- Mak, C.W., McMullan, R.K., *J. Chem. Phys.*, **42**(8), 2732 (1965).
- Makino, T., Sugahara, S., Ohgaki, K., in *Proc. Fifth International Conference on Gas Hydrates*, Trondheim, Norway, June 13–16, Paper 5026 (2005).
- Makogon, Y.F., *Hydrates of Natural Gas*, Moscow, Nedra, Izadatelstro, p. 208 (1974 in Russian) Trans. W.J. Cieslesicz, PennWell Books, Tulsa, Oklahoma, pp. 237 (1981 in English).
- Manakov, A.Y., Voronin, V.I., Teplykh, A.E., Kurnosov, A.V., Goryainov, S.V., Anchakov, A.I., Likhacheva, A.Y., in *Proc. Fourth International Conference on Gas Hydrates*, Yokohama, Japan, May 19–23, 630 (2002).
- Mao, H.K., Mao, W.L., *PNAS*, **101**, 708 (2004).
- Mao, W.L., Mao, H.K., Goncharov, A.F., Struzhkin, V.V., Guo, Q.Z., Hu, J.Z., Shu, J.F., Hemley, R.J., Somayazulu, M., Zhao, Y.S., *Science*, **297**, 2247 (2002).
- Matsumoto, M., Saito, S., Ohmine, I., *Nature*, **416**, 409 (2002).
- McCelland, A.L., *Dipole Moments*, W.H. Freeman & Co., San Francisco, CA (1963).
- McMullan, R., Jeffrey, G.A., *J. Chem. Phys.*, **31**, 1231 (1959).
- McMullan, R.K., Jeffrey, G.A., *J. Chem. Phys.*, **42**, 2725 (1965).
- Mehta, A.P., *A Thermodynamic Investigation of Structure-H-Type Clathrate Hydrates*, Ph.D. Thesis Colorado School of Mines, Golden, CO (1996).
- Mehta, A.P., Sloan, E.D., *AIChE J.*, **40**, 312 (1994).
- Mehta, A.P., Sloan, E.D., in *Proc. Second International Conference on Gas Hydrates*, (Monfort, J.P., ed.) Toulouse, France, June 2–6, 1 (1996).
- Mooijer-van den Heuvel, M.M., Peters, C.J., Arons, J.D., *Fluid Phase Equilib.*, **172**, 73 (2000).

- Mooijer-van den Heuvel, M.M., Peters, C.J., Arons, J.D., *Fluid Phase Equilib.*, **193**, 245 (2002).
- Mooijer-van den Heuvel, M.M., Witteman, R., Peters, C.J., *Fluid Phase Equilib.*, **182**, 97 (2001).
- Moridis, G.J., *Lawrence Berkeley National Laboratory Report*, (2005b).
- Moridis, G.J., Seol, Y., Kneafsey, T.J., in *Proc. Fifth International Conference on Gas Hydrates*, Trondheim, Norway, June 13–16, Paper 1004 (2005a).
- Morita, K., Nakano, S., Ohgaki, K., *Fluid Phase Equilib.*, **169**, 167 (2000).
- Nagashima, U., Shinohara, H., Nishi, N., Tanaka, H., *J. Chem. Phys.*, **84**, 209 (1986).
- Ogienko, A.G., Kurnosov, A.V., Manakov, A.Y., Larionov, E.G., Anchakov, A.I., Sheromov, M.A., Nesterov, A.N., *J. Phys. Chem. B*, **110**, 2840 (2006).
- Ohmine, I., *J. Phys. Chem.*, **99**, 6767 (1995).
- Onsager, L., Runnels, L.K., *J. Chem. Phys.*, **50**, 1089 (1969).
- Oyama, H., Ebinuma, T., Shimada, W., Takeya, S., Nagao, J., Uchida, T., Narita, H., *Can. J. Phys.*, **81**, 485 (2003).
- Pandit, B.I., King, M.S., *Fourth Canadian Permafrost Conference* (French, H.M., ed.), Khangai Mountains, Mongolia, 335 (1982).
- Parameswaran, V.R., Paradis, M., Handa, Y.P., *Can. Geotechnical J.*, **26**, 479 (1989).
- Paul, J.B., Provencal, R.A., Chapo, C., Roth, K., Caseas, R., Saykally, R.J., *J. Phys. Chem.*, **103**, 2972 (1999).
- Pauling, L., *J. Am. Chem. Soc.*, **57**, 2680 (1935).
- Pauling, L., *The Nature of the Chemical Bond*, Cornell University Press, Ithaca, New York (1945).
- Pauling, L., *The Structure of Water*, Pergamon Press, New York 1 (1959).
- Pauling, L., Marsh, R.E., *Proc. Nat. Acad. Sci.*, **38**, 112 (1952).
- Pearson, C., Murphy, J.R., Mermes, R.E., Halleck, P.M., *Los Alamos Scientific Laboratory Report*, LA-9972 MS, **9** (1984).
- Pecher, I.A., Waite, W.F., Winters, W.J., Mason, D.H., Physical properties and rock physics models of sediment containing natural and laboratory-formed methane gas hydrate. *Am. Mineral.*, **89**, 1221 (2004).
- Plummer, P.L.M., Chen, T.S., *J. Chem. Phys.*, **86**, 7149 (1987).
- Poirier, J.P., *Creep of Crystals*, Cambridge University Press, New York (1985).
- Pople, J.A., in *Proc. Royal Society*, **205**, 163 (1951).
- Prielmeier, F.X., Zang, E.W., Speedy, R.J., Ludemann, H-D., *Phys. Rev. Lett.*, **59**, 1128 (1987).
- Privalov, P.L., Gill, S.J., *Adv. Protein Chem.*, **39**, 191 (1988).
- Rawn, C.J., Rondinone, A.J., Chakoumakos, B.C., Circone, S., Stern, L.A., Kirby, S.H., Ishii, Y., *Can. J. Phys.*, **81**, 431 (2003).
- Rawn, C.J., Rondinone, A.J., Chakoumakos, B.C., Marshall, S.L., Stern, L.A., Circone, S., Kirby, S., Jones, C.Y., Toby, B.H., Ishii, Y., in *Proc. Fourth International Conference on Gas Hydrates*, Yokohama, Japan, May 19–23, **595** (2002).
- Ripmeester, J., in *Proc. Third International Conference on Gas Hydrates*, (Holder, G.D., Bishnoi, P.R., eds.), Salt Lake City, UT, Annals of the New York Academy of Sciences, **912**, 1 (2000).
- Ripmeester, J.A., in *Proc. Fifth International Conference on Gas Hydrates*, Trondheim, Norway, June 13–16, Paper 2008 (2005).
- Ripmeester, J.A., Davidson, D.W., *J. Mol. Struct.*, **75**, 67 (1981).
- Ripmeester, J.A., Ratcliffe, C.I., *J. Phys. Chem.*, **94**, 8773 (1990a).
- Ripmeester, J.A., Ratcliffe, C.I., *J. Phys. Chem.*, **94**, 7652 (1990b).

- Ripmeester, J.A., Ratcliffe, C.I., Cameron, I.G., *J. Phys. Chem. B*, **208**, 929 (2004).
- Ripmeester, J.A., Ratcliffe, C.I., Klug, D.D., Tse, J.S., in *Proc. First International Conference on Natural Gas Hydrates*, (Sloan, E.D., Happel, J., Hnatow, M.A., eds.) Annals of the New York Academy of Sciences, **715**, 161 (1994).
- Ripmeester, J.A., Ratcliffe, C.I., McLaurin, G.E., *AICHE Meeting in Houston Texas*, April 10 (1991).
- Ripmeester, J.A., Ratcliffe, C.I., Tse, J.S., *J. Chem. Soc. Faraday Trans. I*, **84**, 3731 (1988).
- Ripmeester, J.A., Tse, J.S., Ratcliffe, C.I., Powell, B.M., *Nature*, **325**, 135 (1987).
- Roberts, R.B., Andrikidis, C., Tainish, R.J., White, G.K., in *Proc. Tenth International Cryogenic Engineering Conference*, Helsinki, 499 (1984).
- Rodger, P.M., *J. Phys. Chem.*, **94**, 6080 (1990a).
- Rodger, P.M., *Mol. Simulation*, **5**, 315 (1990b).
- Rondinone, A.J., Chakoumakos, B.C., Rawn, C.J., Ishii, Y., in *Proc. Fourth International Conference on Gas Hydrates*, Yokohama, Japan, May 19–23, 625 (2002).
- Ross, R.G., Andersson, P., *Can. J. Chem.*, **60**, 881 (1982).
- Ross, R.G., Andersson, P., Backstrom, G., *Nature*, **290**, 322 (1981).
- Sasaki, S., Hori, S., Kume, T., Shimizu, H., *J. Chem. Phys.*, **118**, 7892 (2003).
- Satana, L.F., Brown, M.G., Richmond, G.L., *Science*, **292**, 908 (2001).
- Shimada, W., Shiro, M., Kondo, H., Takeya, S., Oyama, H., Ebinuma, T., Marita, H., *Acta Crystallographica Section C, Crystal Structure Commun.*, **C61**, 065 (2005).
- Shimizu, H., Kumazaki, T., Kume, T., Sasaki, S., *Phys. Rev. B: Condens. Matt. Mater. Phys.*, **65**, 212102/1 (2002).
- Shpakov, V.P., Tse, J.S., Tulk, C.A., Kvamme, B., Belosludov, V.R., *Chem. Phys. Lett.*, **282**, 107 (1998).
- Sluiter, M., Inerbaev, T.M., Belosludov, R.V., Kawazoe, Y., Subbotin, O.S., Belosludov, V.R., in *Proc. Fifth International Conference on Gas Hydrates*, Trondheim, Norway, June 13–16, Paper 5003 (2005).
- Sorensen, C.M., “Clathrate Structures and the Anomalies of Supercooled Water,” in *Proc. 12th Int. Conf. on Prop. of Water and Steam*, Orlando, FL, September (1994).
- Speedy, R.J., Angell, C.A., *J. Chem. Phys.*, **65**, 851 (1976).
- Stern, L.A., Kirby, S.H., Durham, W.B., *Science*, **273**, 1843 (1996).
- Stillinger, F.H., in *Water in Polymers*, (Rowland, S.P., ed.) Washington DC, **1**, 11 (1980).
- Stillinger, F.H., Rahman, A., *J. Chem. Phys.*, **60**, 1545 (1974).
- Stoll, R.D., Bryan, G.M., *J. Geophys. Res.*, **84**, 1629 (1979).
- Strobel, T., Hester, K.C., Koh, C.A., Dec, S.F., Miller, K.T., Sloan, E.D., *Hydrogen in Hydrates Workshop*, Kauai, Hawaii, March 5–9 (2006a).
- Strobel, T.A., Hester, K.C., Sloan, E.D., Koh, C.A., *J. Am. Chem. Soc.*, in press (2007).
- Strobel, T.A., Taylor, C.J., Hester, K.C., Dec, S.F., Koh, C.A., Miller, K.T., Sloan, E.D., *J. Phys. Chem. B*, **110**, 17121 (2006b).
- Subramanian, S., Kini, R., Dec, S., Sloan, E., in *Proc. Gas hydrates, Challenges for the Future*, Annals of the New York Academy of Sciences, **912**, 873 (2000).
- Subramanian, S., Sloan, E.D., *J. Phys. Chem. B*, **106**, 4348 (2002).
- Sugahara, T., Morita, K., Ohgaki, K., *Chem. Eng. Sci.*, **55**, 6015 (2000).
- Suzuki, M., Tanaka, Y., Sugahara, T., Ohgaki, K., *Chem. Eng. Sci.*, **56**, 2063 (2001).
- Tabushi, I., Kiyosuke, Y., Yamamura, K., *Bull. Chem. Soc. of Japan*, **54**, 2260 (1981).
- Takeya, S., Kida, M., Minami, H., Sakagami, H., Hachikubo, A., Takahashi, N., Shoji, H., Soloviev, V., Wallmann, K., Biebow, N., Obzhirov, A., Saloatin, A., Poort, J., *Chem. Eng. Sci.*, **61**, 2670 (2006).
- Takeya, S., Nagaya, H., Matsuyama, T., Hondoh, T., Lipenkov, V. Y., *J. Phys. Chem. B*, **104**, 668 (2000).

- Tanaka, H., Kiyohara, K., *J. Chem. Phys.*, **98**, 4098 (1993).
- Tanaka, H., Tamai, Y., Koga, K., *J. Phys. Chem. B*, **101**, 6560 (1997).
- Tanford, C., *The Hydrophobic Effect: Formation of Micelles and Biological Membranes*, Wiley, New York, (1973).
- Tohidi, B., Østergaard, K.K., Danesh, A., Todd, A.C., Burgass, R.W., *Can. J. Chem. Eng.*, **79**, 384 (2001).
- Tse, J.S., *J. De Physique*, **48**, 543 (1987).
- Tse, J.S., *J. Inclusion Phenom. Mol. Recognition Chem.*, **8**, 25 (1990).
- Tse, J.S., in *Proc. First International Conference on Natural Gas Hydrates* (Sloan, E.D., Happel, J., Hnatow, M.A., eds.) Annals of the New York Academy of Sciences, **715**, 187 (1994).
- Tse, J.S., Handa, Y.P., Ratcliffe, C.I., Powell, B.M., *J. Inclusion Phenom.*, **4**, 235 (1986).
- Tse, J.S., Klein, M.L., *J. Phys. Chem.*, **91**, 5789 (1987).
- Tse, J.S., Klein, M.L., McDonald, I.R., *J. Phys. Chem.*, **87**, 4198 (1983).
- Tse, J.S., Klein, M.L., McDonald, I.R., *J. Chem. Phys.*, **81**(12), 6146 (1984).
- Tse, J.S., McKinnon, W.R., Marchi, M., *J. Phys. Chem.*, **91**, 4188 (1987).
- Tse, J.S., Powell, B.M., Sears, V.F., Handa, Y.P., *Chem. Phys. Lett.*, **215**, 383 (1993).
- Tse, J.S., Shpakov, V.P., Belosludov, V.R., Trouw, F., Handa, Y.P., Press, W., *Europhys. Lett.*, **54**, 354 (2001).
- Tse, J.S., White, M.A., *J. Phys. Chem.*, **92**, 5006 (1988).
- Udachin, K., Lipkowski, J., *Supramol. Chem.*, **8**, 181 (1996).
- Udachin, K., Ripmeester, J., *Nature*, **397**, 420 (1999).
- Udachin, K., Ripmeester, J.A., in *Proc. Fifth International Conference on Gas Hydrates*, Trondheim, Norway, June 13–16, Paper 2024 (2005).
- Udachin, K.A., Enright, G.D., Ratcliffe, C.I., Ripmeester, J.A., *J. Am. Chem. Soc.*, **119**, 11481 (1997a).
- Udachin, K.A., Ratcliffe, C.I., Enright, G.D., Ripmeester, J.A., *Supramol. Chem.*, **8**, 173 (1997b).
- Udachin, K.A., Ratcliffe, C.I., Ripmeester, J.A., *Angew. Chem. Int. Ed.*, **40**, 1303 (2001a).
- Udachin, K.A., Ratcliffe, C.I., Ripmeester, J.A., *J. Phys. Chem. B*, **105**, 4200 (2001b).
- Udachin, K.A., Ratcliffe, C.I., Ripmeester, J.A., in *Proc. Fourth International Conference on Gas Hydrates*, Yokohama, Japan, May 19–23, 604 (2002).
- van der Waals, J.H., Platteeuw, J.C., *Adv. Chem. Phys.*, **2**, 1 (1959).
- van Klaveren, E.P., Michels, J.P.J., Schouten, J.A., Klug, D.D., Tse, J.S., *J. Chem. Phys.*, **114**, 5745 (2001).
- von Stackelberg, M., *Naturwiss.*, **36**, 359 (1949).
- von Stackelberg, M., *Rec. Trav. Chim. Pays-Bas*, **75**, 902 (1956).
- von Stackelberg, M., Jahns, W., *Z. Elektrochem.*, **58**, 162 (1954).
- von Stackelberg, M., Müller, H.R., *Z. Electrochem.*, **58**, 25 (1954).
- Vos, W.L., Finger, L.W., Hemley, R.J., Mao, H.K., *Phys. Rev. Lett.*, **71**, 3150 (1993).
- Waite, W., Helgerud, M., Nur, A., Pinkston, J., Stern, L., Kirby, S., in *Proc. Gas Hydrates, Challenges for the Future*, Annals of the New York Academy of Sciences, **912**, 1003 (2000).
- Waite, W.F., Gilbert, L.Y., Winters, W.J., Mason, D.H., in *Proc. Fifth International Conference on Gas Hydrates*, Trondheim, Norway, June 13–16, Paper 5042 (2005).
- Wales, D.J., Hodges, M.P., *Chem. Phys. Lett.*, **286**, 65 (1998).
- Walrafen, G.E., Chu, Y.C., *J. Phys. Chem.*, **99**, 10635 (1995).
- Wei, S., Shi, Z., Castleman, A.W., *J. Chem. Phys.*, **94**, 3268 (1991).

- Whalley, E., *J. Geophys. Res.*, **85**, 2539 (1980).
- Whiffen, B.L., Kieft, H., Clouter, M.J., *Geophys. Res. Lett.*, **9**, 645 (1982).
- White, M.A., MacLean, M.T., *J. Phys. Chem.*, **89**, 1380 (1985).
- Winters, W., Dallimore, S., Collett, J.K., Katsube, J., Cranston, in *Proc. Gas Hydrates: Challenges for the Future*, **912**, 94 (2000).
- Winters, W.J., Mason, D.H., Waite, W.F., Methane hydrate formation in partially-water saturated Ottawa sand. *Am. Mineral.*, **89**, 1202 (2004).
- Wooldridge, P.J., Richardson, H.H., Devlin, J.P., *J. Chem. Phys.*, **87**, 4126 (1987).
- Wright, J.F., Nixon, F.M., Dallimore, S.R., Henninges, J., Cote, M.M., *Geological Survey of Canada Bulletin*, **585**, 129 (2005).
- Wu, B.J., Robinson, D.B., Ng, H.J., *J. Chem. Thermodyn.*, **8**, 461 (1976).
- Zele, S.R., Lee, S.Y., Holder, G.D., *J. Phys. Chem. B*, **103**, 10250 (1999).